

Continuous upstream processing for cell culture-derived virus production

Dissertation zur Erlangung des akademischen Grades

Doktoringenieur

(Dr.-Ing.)

von: Felipe Ignacio Tapia Delgado, M.Sc.(hons)

geboren am: 10. Februar 1984 in Puerto Montt, Chile

genehmigt durch die Fakultät für Verfahrens- und Systemtechnik der
Otto-von-Guericke-Universität Magdeburg

Promotionskommission:

Prof. Dr.-Ing. Andreas Seidel-Morgenstern	(Vorsitz)
Prof. Dr.-Ing. Udo Reichl	(Gutachter)
Prof. Dr. James Piret	(Gutachter)
Prof. Dr.-Ing. Richard Biener	(Gutachter)

eingereicht am: 21. Juni 2019

Promotionskolloquium am: 11. November 2019

*“What we usually consider as impossible
are simply engineering problems.”*

— Dr. Michio Kaku, physicist and writer.

Abstract

Viral vaccines are one of the most successful medical developments in human history. Since their introduction in the global health system, the average human life span and the worldwide population have increased dramatically. The most common method for viral vaccine manufacturing is the propagation in different substrates of the target virus in a high concentration. In a next step, the virus particles are inactivated (if needed) and purified to its final presentation. The substrates used for propagation of viruses could vary according to the application and amounts needed, but living tissues, embryonated chicken eggs or animal cell cultures have been the most common substrates.

Most vaccine production processes are currently operated in batch mode meaning that large scale production requires the repetition of several batch cycles. Batch operation is efficient for production of defined and relatively small volumes, but several limitations arise when scale-up to large volumes is required. Moving from batch to continuous-flow processing can increase efficiency because reactor sizes are reduced, short seed trains are possible, and the manufacturing footprint can be reduced. However, aspects such as the stability of suspension cell lines after weeks of continuous cultivation, the genetic stability of the virus after many days of propagation, or the low virus yields that might arise due to the accumulation of defective interfering particles (DIP) need further investigation.

In this work, continuous production of Modified Vaccinia Ankara (MVA) and influenza viruses were investigated. MVA virus is a candidate for production of recombinant viral vaccines and viral vectors production, for which the use of cascades of continuous stirred tank bioreactors (CSTRs) was investigated. On the other hand, influenza virus is responsible of global seasonal outbreaks and its production in cascades of CSTRs has shown low yields due to the presence of DIPs. Hence, a novel bioreactor system based in a plug-flow tubular bioreactor (PFBR) that allows stable influenza virus production avoiding DIPs-induced low yields was developed.

The continuous system for MVA virus production consisted of a cascade of CSTRs, also referred as a two-stage stirred tank bioreactor (TSB). In the TSB, the avian cell line AGE1.CR.pIX was successfully maintained for 30 days and the virus was propagated for 18 days. The system allowed stable production of MVA virus with a total production of 7.1 L and an average TCID₅₀ titer of 9.0×10^7 virions/mL. Similarly, a small-scale semi-continuous two-stage cultivation system (small-scale cultivation or SSC) consisting of two shaker flasks in series was established as a scale down model of the TSB system. Cells and MVA virus were propagated in the SSC system between 8-18 days and the impact that process parameters such as residence times and other

process parameters might have on virus yields were evaluated. A total of 1 L was produced per SSC experiment with MVA virus titers of up to $0.1-1 \times 10^9$ virions/mL. A genetic stability analysis of a recombinant MVA virus containing a green-fluorescent-protein (GFP) revealed that the virus is stable at least over 16 days of cultivation. The SSC system worked well as a fast and efficient tool for design and optimization of the TSB system.

Influenza virus was continuously produced using a continuous tubular bioreactor system, newly established within the scope of this study. The system consisted of a 500 mL CSTR connected to a 211 mL PFBR with a nominal flow rate of 12 mL/h. The canine suspension cell line MDCK and the avian cell line AGE1.CR.pIX (AGE1, ProBioGen) were continuously produced in the CSTR and transferred to the PFBR with the aid of a peristaltic pump. The MDCK- or AGE1-adapted influenza virus strain A/PR/8/34 (Robert Koch Institute) was used to prepare a virus stock for infection. The virus seed was continuously pumped to the PFBR to infect the cells. Air was injected immediately after infection generating segments of medium and bubbles. Uninterrupted operation without cell sedimentation was possible for up to two months. The residence time in the PFBR was maintained stable at around 20 h. The tubular bioreactor system enabled stable production of cells, with virus titers ranging between 1.5 and 2.5 \log_{10} (HA Units/100 μ L) for AGE1 and MDCK cells, respectively, overcoming the DIPs-induced oscillations observed for influenza virus propagation in cascades of CSTRs. Analysis of DIP accumulation using Polymerase Chain Reaction showed a stable ratio of influenza virus segments S1, S2 and S3 to DIPs over three weeks of production compared to control experiments using batch and the SSC system.

Overall, MVA virus was stable and efficiently produced in continuous and semi-continuous cultivations, which demonstrates that the TSB system is a promising platform that can be considered for industrial production of MVA-derived recombinant vaccines and viral vectors. Stable continuous influenza virus production without DIPs-induced oscillations was possible in a PFBR. The PFBR is an innovation that can be considered for commercial production of influenza vaccines.

Finally, the experimental work presented here provided valuable results into virus production in continuous mode. In particular, the development of a novel continuous bioreactor based in a PFBR represents a significant step forward in continuous production of cell culture-derived viruses. This technology contributes to the production of cost-effective viral vaccines against influenza outbreaks that affect human populations worldwide. This development offers an alternative for safe and stable continuous production of cell culture-derived viruses.

Zusammenfassung

Virusimpfstoffe sind eine der erfolgreichsten medizinischen Entwicklungen in der Geschichte der Menschheit. Seit ihrer Einführung im globalen Gesundheitssystem haben die durchschnittliche Lebenserwartung des Menschen und die Weltbevölkerung deutlich zugenommen. Die gebräuchlichste Methode zur Herstellung viraler Impfstoffe ist die Vermehrung des Zielvirus in hoher Konzentration in verschiedenen Substraten. In einem nächsten Schritt werden die Viruspartikel (falls erforderlich) inaktiviert und bis zu ihrer endgültigen Nutzung gereinigt. Die Substrate, die zur Vermehrung von Viren verwendet werden, können je nach Anwendung und benötigten Mengen variieren. Lebende Gewebe, embryonierte Hühnereier oder tierische Zellkulturen waren die häufigsten Substrate.

Die meisten Impfstoffproduktionsprozesse werden derzeit im Batch-Modus betrieben, was bedeutet, dass die Produktion in großem Maßstab die Wiederholung mehrerer Batch-Zyklen erfordert. Der Batch-Betrieb ist für die Produktion definierter und relativ kleiner Volumina effizient, es ergeben sich jedoch mehrere Einschränkungen, wenn große Volumina produziert werden sollen. Der Übergang von der Chargen- zur kontinuierlichen Durchlaufverarbeitung kann die Effizienz steigern, da die Reaktorgrößen reduziert werden, kurze Serienvermehrungen möglich sind und die Fertigungsfläche reduziert werden kann. Jedoch müssen Aspekte wie die Stabilität der Suspensionszelllinien nach wochenlangem kontinuierlicher Kultivierung, die genetische Stabilität des Virus, oder auch die geringen Virusausbeuten, durch mögliche Anhäufung fehlerhafter interferierender Partikel (DIP) weiter berücksichtigt werden.

In dieser Arbeit wurde die kontinuierliche Produktion von Modified Vaccinia Ankara (MVA)- und Influenza-Viren untersucht. Das MVA-Virus ist ein Kandidat für die Herstellung von rekombinanten viralen Impfstoffen und viralen Vektoren. Für diese wurde die Herstellung in Kaskaden in kontinuierlichen Rührkessel-Bioreaktoren (CSTRs) untersucht. Andererseits ist das Influenzavirus für weltweite saisonale Ausbrüche verantwortlich, und seine Produktion in Kaskaden von CSTRs hat aufgrund des Vorhandenseins von DIPs geringe Erträge gezeigt. Daher wurde ein neuartiges Bioreaktorsystem entwickelt, das auf einem Plug-Flow-Röhren-Bioreaktor (PFBR) basiert und eine stabile Influenzavirus-Produktion unter Vermeidung von DIPs-induzierten niedrigen Ausbeuten ermöglicht.

Das kontinuierliche System zur Herstellung von MVA-Viren bestand aus einer Kaskade von CSTRs, auch als zweistufiger Rührkessel-Bioreaktor (TSB) bezeichnet. In der TSB wurde die Vogelzelllinie AGE1.CR.pIX 30 Tage erfolgreich aufrechterhalten und das Virus 18 Tage vermehrt. Das System ermöglichte eine stabile Produktion des MVA-Virus mit einer

Gesamtproduktion von 7,1 liter und einem durchschnittlichen TCID₅₀-Titer von $9,0 \times 10^7$ Virionen/ml. In ähnlicher Weise wurde ein halbkontinuierliches zweistufiges Kultivierungssystem im kleinen Maßstab (Small Scale Cultivation oder SSC), das aus zwei in Reihe geschalteten Schüttelkolben besteht, als ein verkleinertes Modell des TSB-Systems etabliert. Zellen und MVA-Viren wurden zwischen 8 und 18 Tagen im SSC-System vermehrt. Dabei wurde die Auswirkung der Verweilzeiten und andere Prozessparameter auf die Virusausbeute bewertet. Pro SSC-Experiment wurde insgesamt 1 liter mit MVA-Virustitern von bis zu $0,1-1,0 \times 10^9$ Virionen/ml erzeugt. Eine genetische Stabilitätsanalyse eines rekombinanten MVA-Virus, das ein grün fluoreszierendes Protein (GFP) enthält, ergab, dass das Virus mindestens über 16 Kultivierungstage stabil ist. Das SSC-System hat sich als schnelles und effizientes Werkzeug für die Gestaltung und Optimierung des TSB-Systems bewährt.

Das Influenzavirus wurde kontinuierlich unter Verwendung eines kontinuierlichen röhrenförmigen Bioreaktorsystems hergestellt, welches im Rahmen dieser Studie neu etabliert wurde. Das System bestand aus einem 500-ml-CSTR, der mit einem 211-ml Pfropfenströmung-Bioreaktor (oder Plug-Flow-Bioreaktor, PFBR) mit einer Nenndurchflussrate von 12 ml/h verbunden war. Die Hundesuspensionszelllinie MDCK und die Vogelzelllinie AGE1.CR.pIX (AGE1, ProBioGen) wurden kontinuierlich im CSTR hergestellt und mit Hilfe einer Peristaltikpumpe in den PFBR überführt. Der MDCK- oder pIX-adaptierte Influenza-Virusstamm A/PR/8/34 (Robert Koch Institute) wurde verwendet, um einen Virusstamm für die Infektion herzustellen. Die Virussaat wurde kontinuierlich in den PFBR gepumpt, um die Zellen zu infizieren. Unmittelbar nach der Infektion wurde Luft injiziert, wodurch Segmente von Medium und Blasen erzeugt wurden. Ein unterbrechungsfreier Betrieb ohne Zellsedimentation war für bis zu zwei Monate möglich. Die Verweilzeit im PFBR wurde bei ca. 20 Stunden stabil gehalten. Das tubuläre Bioreaktorsystem ermöglichte eine stabile Produktion von Zellen mit Virustitern zwischen $1,5$ und $2,5 \log_{10}$ (HA-Einheiten/100 μ l) für AGE1- bzw. MDCK-Zellen, um die DIPs-induzierten Oszillationen zu überwinden, die für die Influenzavirus-Vermehrung in Kaskaden von CSTRs beobachtet wurden. Die Analyse der DIP-Akkumulation unter Verwendung der Polymerasekettenreaktion (PCR) zeigte ein stabiles Verhältnis der Influenzavirus-Segmente S1, S2 und S3 zu den DIPs über einen Produktionszeitraum von drei Wochen, im Vergleich zu Kontrollexperimenten unter Verwendung von Chargen- und SSC-System.

Insgesamt war das MVA-Virus bei kontinuierlichen und halbkontinuierlichen Kultivierungen stabil und effizient. Dies zeigt, dass das TSB-System eine vielversprechende Plattform für die industrielle Produktion von MVA-abgeleiteten rekombinanten Impfstoffen und viralen Vektoren sein kann. In einem PFBR war eine stabile kontinuierliche Influenza-Virus-Produktion, ohne

DIPs-induzierte Oszillationen, möglich. Die PFBR ist eine Innovation, die für die kommerzielle Herstellung von Influenza-Impfstoffen in Betracht gezogen werden kann.

Schließlich lieferten die hier vorgestellten experimentellen Arbeiten wertvolle Ergebnisse für die Virusproduktion im kontinuierlichen Modus. Insbesondere die Entwicklung eines neuen kontinuierlichen Bioreaktors auf der Basis eines PFBR stellt einen bedeutenden Fortschritt bei der kontinuierlichen Produktion von, aus Zellkulturen stammenden, Viren dar. Diese Technologie trägt zur Herstellung kostengünstiger Virusimpfstoffe gegen Influenza-Ausbrüche bei, die die Weltbevölkerung betreffen. Zudem bietet diese Entwicklung eine Alternative für die sichere und stabile kontinuierliche Produktion von, aus Zellkulturen stammenden, Viren.

This page was intentionally left blank for the online version.

Erklärung

Ich erkläre hiermit, dass ich die vorliegende Arbeit ohne unzulässige Hilfe Dritter und ohne Benutzung anderer als der angegebenen Hilfsmittel angefertigt habe. Die aus fremden Quellen direkt oder indirekt übernommenen Gedanken sind als solche kenntlich gemacht.

Insbesondere habe ich nicht die Hilfe einer kommerziellen Promotionsberatung in Anspruch genommen. Dritte haben von mir weder unmittelbar noch mittelbar geld-werte Leistungen für Arbeiten erhalten, die im Zusammenhang mit dem Inhalt der vorgelegten Dissertation stehen. Die Arbeit wurde bisher weder im Inland noch im Ausland in gleicher oder ähnlicher Form als Dissertation eingereicht und ist als Ganzes auch noch nicht veröffentlicht.

Magdeburg, am 21.6.2019

Felipe Tapia

Table of Contents

Abstract	iii
Zusammenfassung	v
List of Abbreviations	xiii
List of Symbols	xv
Introduction	1
Background and Theory	6
2.1 Modified vaccinia Ankara virus	6
2.2 Influenza virus.....	8
2.3 The role of defective interfering particles in virus infection and propagation	11
2.3.1 Defective interfering particles in modified vaccinia Ankara virus population	12
2.3.2 Defective interfering particles in influenza virus population	12
2.4 Upstream processing of virus production – an overview	13
2.4.1 Egg-based production.....	13
2.4.2 Cell culture-based batch production.....	14
2.4.3 Semi-continuous virus production.....	16
2.5 Continuous upstream processing of cell culture-derived viruses	17
2.5.1 Cascades of CSTRs	17
2.5.2 Tubular bioreactors	22
Materials and Methods	25
3.1 Cell lines and culture media	25
3.2 MVA and influenza viruses.....	25
3.3 Batch cultivations	25
3.3.1 Modified vaccinia Ankara production in batch mode	25
3.3.2 Influenza virus production in batch mode	26
3.4 Semi-continuous cultivations	26
3.4.1 Modified vaccinia Ankara production in semi-continuous cultures.....	27
3.4.2 Influenza virus production in semi-continuous cultures	27
3.5 Continuous cultivations.....	28
3.5.1 Cascade of stirred tank bioreactors	28
3.5.2 Cascade of stirred tank bioreactors with recirculation	30
3.5.3 Continuous tubular bioreactor system.....	32
3.6 Process productivity estimations	36
3.7 Analytics	37
3.7.1 Influenza virus.....	37
Hemagglutinin assay	37
Tissue culture infectious dose 50 titration assays	37
3.7.2 Modified vaccinia Ankara virus	37

Tissue culture infectious dose 50 assay	37
Green fluorescent-derived TCID ₅₀	37
3.7.3 Cell concentration and viability	38
3.7.4 Extracellular metabolites	38
3.7.5 Stability of modified vaccinia Ankara virus.....	38
3.7.6 Polymerase chain reaction for evaluation of modified vaccinia Ankara virus stability	39
3.7.7 Segment-specific PCR for determination of defective interfering influenza virus particles	39
3.7.8 Software for data analysis	39
Results & Discussion	40
4.1 Virus production in batch mode	40
4.1.1 Batch production of modified vaccinia Ankara virus in AGE1.CR.pIX cells	41
4.1.2 Batch production of influenza A virus in AGE1.CR.pIX cells	42
4.2 Virus production in semi-continuous mode	44
4.2.1 Semi-continuous production of modified vaccinia Ankara virus in AGE1.CR.pIX cells	44
4.2.2 Semi-continuous production of influenza A virus in MDCK.SUS2 cells and in AGE1.CR.pIX cells.....	48
4.3 Virus production in continuous mode	50
4.3.1 Continuous production of modified vaccinia Ankara virus in AGE1.CR.pIX cells in a two-stage stirred tank bioreactor system	50
4.3.2 Genetic stability of MVA virus in long-term cultures.....	54
4.3.3 Continuous production of influenza A virus in AGE1.CR.pIX cells in a cascade of CSTRs with recirculation	56
4.3.4 Development of a continuous tubular bioreactor system for influenza A virus production	57
4.3.5 Continuous production of influenza A virus in MDCK cells in a continuous tubular bioreactor system.....	59
4.3.6 Continuous production of influenza A virus in AGE1.CR.pIX cells in a continuous tubular bioreactor system	65
4.3.7 Genetic stability of influenza A virus produced in long-term continuous tubular bioreactor cultures – comparison with batch and semi-continuous cultures	70
4.4 Productivity of continuous processes versus batch cultivations.....	76
4.4.1 MVA virus productivity in a continuous two-stage bioreactor system	76
4.4.2 IAV productivity in the tubular bioreactor system.....	80
Conclusions	81
Outlook.....	83
List of Figures	86
List of Tables	88
List of Publications.....	89

References	92
Appendices	107
7.1 Oxygen consumption.....	107
7.2 Pressure drop in the tubular plug flow bioreactor	108

List of Abbreviations

Abbreviation	Description
A/PR/8/34	A/Puerto Rico/8/1934
bp	Base pairs
CB	Cell Bioreactor
CDC	Centers for disease control and prevention
CHO	Chinese Hamster Ovary
CSTR	Continuous stirred tank bioreactor
CVA	Chorioallantois vaccinia virus Ankara
CVV	Candidate vaccine virus
DIP	Defective interfering particle
DP	Defective particle
DNA	Deoxyribonucleic acid
DS	Defective segment
EMA	European Medicines Agency
FDA	Food and Drug Administration
FM	Fresh medium
FL	Full length
GD1a	Ganglioside molecule GD1a
GFP	Green fluorescent protein
HA	Haemagglutinin
HEK 293	Human embryonic kidney 293
Hela	Henrietta Lacks
IAV	Influenza A virus
IVP	Infectious virus population
KB	Keratin-forming
MDCK	Madyn Darbin canine kidney
MVA	Modified Vaccinia Ankara
MVA-CR19	MVA virus strain passage 19 in CR cells
MVA-CR19.GFP	MVA-CR19 virus strain with GFP insertion
NA	Neuraminidase

Abbreviation	Description
NIH 3T3	National Institute of Health 3-day transfer, inoculum $3 \cdot 10^5$ cells
NOV	Non occluded virus
PBS	Phosphate buffer saline
PCR	Polymerase chain reaction
PEIVP	Protein-expressing infectious virus population
PFBR	Plug flow bioreactor
p.i.	Post infection
POI	Point of infection
RNA	Ribonucleic acid
SCB	Small cell bioreactor
SSC	Small scale semi continuous culture
STR	Stirred tank bioreactor
STV	Standard virus
SVB	Small virus bioreactor
TSB	Two-stage bioreactor
VB	Virus Bioreactor
Vero	Verda reno
VP	Virus particle
VS	Virus Stock
WHO	World Health Organization
WR	Western reserve
WV	Working volume

List of Symbols

Description	Symbol	[Unit]
Days ¹	d	[h]
Darcy factor ²	fc	[1]
Density	ρ	[kg/m ³]
Dilution rate	D	[h ⁻¹]
Dynamic viscosity	ν	[kg/(m·s)]
Friction (f) head (H) loss	H _f	[bar]
Flow rate	F	[mL/min]
Hydraulic diameter of the tube	ϕ	[m]
Specific cell growth rate	μ	[h ⁻¹]
Length	Le	[m]
Liters	L	[mL]
Maximum specific cell growth rate	μ_{\max}	[h ⁻¹]
Mean fluid velocity	V _T	[m/h]
Multiplicity of infection	MOI	[virus/cell]
Time at event "n"	t _n	[h]
Pressure	P	[Pa]
Plaque forming unit	PFU	[PFU/mL]
Reynolds number ²	Re	[1]
Residence time	RT	[h]
Revolutions per minute	RPM	[min ⁻¹]
Space time yield	STY	[virions/(L h)]
Time yield	TY	[virions/h]
50% tissue culture infective dose	TCID ₅₀	[virions/mL]
Volume	V	[mL]

¹ days are used within this work, as alternative to hours, especially when discussing the results of continuous cultures.

² dimensionless quantities such as Darcy factor and Reynolds number are the result of quantities whose units cancel out, hence the symbol is 1. However, the unit 1 is generally omitted and not specified when referring to these dimensionless quantities.

Chapter 1

Introduction

Viral vaccines are one of the most successful medical developments in human history. Their development is closely linked to smallpox, a human disease caused by vaccinia virus [1]. Smallpox has been present from ancient times and experts estimated that during the last century the virus was responsible for 300-500 million deaths, a mortality rate larger than both World Wars combined [2]. The term *vaccine* was introduced in 1798 by Edward Jenner, who described the use of skin material extracted from cowpox-infected cattle as a protecting agent against smallpox in humans [3]. However, the correlation that microorganisms are the cause of diseases was not known until the contributions of Luis Pasteur and Robert Koch one century later. Viruses were too small to be seen under the light microscope, and their existence was not probed until the early 19th hundreds by a joint effort of scientists such as Adolf Mayer, Dmitry Ivanovsky and Charles Chamberland. In parallel, the Spanish influenza flu killed more people than any other outbreak in a period of just sixteen weeks between 1918-1919 [4]. The human influenza virus, however, was not isolated until 1933 [5]. Since then, significant advances towards vaccine development have been achieved resulting in the control and elimination of important infectious diseases, such as smallpox in 1979, and contributing to increase the human life expectancy worldwide. Nevertheless, still in the 21st century, there is a constant threat from old and emerging diseases that could affect human populations at any time and in any place. Hence, the development of more efficient upstream and downstream vaccine production platforms will play a major role in the fight against viral diseases of the upcoming decades. This work will only focus on establishment of upstream processes for production of viruses that can be used for manufacturing of vaccines.

Modified Vaccinia Ankara (MVA) is a host-range restricted, highly attenuated DNA virus strain that was developed by performing over 500 serial tissue culture passages of the vaccinia virus strain Ankara in primary chicken cells [6]. MVA virus lost about 15% of its parental genome and, as a result, MVA virus replication in most mammalian cells is abortive [7]. MVA virus has a great potential for expression of recombinant antigens or as a viral vaccine vector in humans and animals. However, the relative high doses per patient required for full efficacy (close to 1×10^8 infectious viruses per vaccination) make the MVA virus difficult to produce [8]. One challenge in MVA virus production is the property that a large fraction of infectious units remains cell-associated which requires three freeze-thaw cycles for virus release and harvest. Because cultivation in a single-cell format interferes with the spread of MVA, processes have been developed where the virus is propagated in suspended aggregates of 20-100 cells [8]. Recently, a

novel MVA virus isolate, named MVA-CR19, has been generated that can be produced at high yields in non-aggregated avian suspension cells in chemically defined media [9], which makes MVA an interesting candidate for exploring process options towards vaccine manufacturing.

Influenza viruses can circulate within individual species but occasionally cross-species infection can occur causing influenza outbreaks around the globe. Moreover, the global prevention and control of the disease is increasingly challenged by the interconnectedness of nations. With an increasing population of humans and breeding animals, the chances for virus adaptation and cross species transmission it increases as well. The World Health Organization (WHO) estimated that each year about one billion cases of influenza infection occur, with approximately 3-5 million cases of severe illness [10], and 291.243-645.832 deaths [11]. The total cost of the disease for different governments is difficult to estimate, however, some estimations indicated that only in the United States about \$10.4 billion per year for direct medical costs, and \$87.1 billion for the total economic burden of annual influenza epidemics need to be considered [12] [13]. The main technology platform for influenza virus production is based on the infection of embryonated-chicken eggs. It requires the infection of individual eggs with the strain of interest and subsequent harvest. Despite the need for millions of eggs and a complex logistic needed to fulfill annual demands, this technology is still efficient for production of seasonal influenza vaccines [14]. However, limitations regarding response time and scalability in case of a pandemic is a main public concern [15]. Over the last two decades, animal cell culture and bioreactor technology has been introduced for influenza vaccine production in Europe and the United States [16]. Typically, cells are grown to high concentrations in batch mode ($2-6 \times 10^6$ cells/mL) and, once the desired cell concentration is reached, the culture is infected and harvested after about 2-3 days. More recently, a recombinant influenza vaccine using the baculovirus expression system in insect cells has been approved for commercialization [17].

Despite small differences in process operation and parameters among these manufacturing platforms, all MVA and influenza virus production processes are basically operated in batch mode. A classical batch upstream process can be separated in two steps – cell growth and virus production. Typically, cells are grown up to $5-10 \times 10^6$ cells/ mL in a stirred tank bioreactor (STR) over a period of 2-6 days depending on the cell line [18, 19]. Subsequently, to supply nutrients or mitigate the accumulation of DNA and host cell proteins in the viral harvest [20], the infection can be initiated with a medium exchange [21], to then add the virus to the STR. The virus is added at a ratio of virus per cell [virus/cell] known as multiplicity of infection (MOI). After the harvest, the process continues with different downstream operations such as clarification, concentration, inactivation, nuclease treatment, purification, polishing and sterile filtration [22].

Moving from batch to continuous production could significantly improve productivity and reduce the manufacturing footprint [23] of cell culture-derived viral vaccines. Continuous production is currently promoted by various manufacturers of recombinant proteins and also by regulatory agencies [24]. From an upstream perspective, the most basic setup for continuous cell culture is the use of a “chemostat” [25] which consist of a STR where cells are grown in a fixed volume of culture with continuous addition of fresh medium and simultaneous removal of cells and consumed medium. An important operational parameter is the so called “dilution rate” (D), which is the fraction between the flow rate in the outlet, and the working volume (WV) of the continuous STR (CSTR). In theory, and if there is no nutrient limitation, a stable cell concentration over cultivation time can be achieved when D has a value less than or equal to the maximum specific cell growth rate (μ_{\max}), which can be obtained from a batch culture. When the value of D exceeds μ_{\max} , a washout of cells and metabolic products takes place in the bioreactor. A numerical conditions with D equal μ_{\max} is difficult to achieve in the laboratory and, therefore, a D less than μ_{\max} is preferred [26]. Interestingly, steady-state populations of cells at different growth rates with different conditions of nutrient limitations are possible to achieve in chemostats by varying D [27], which make chemostat suitable for adaptive evolution studies [28]. Chemostats are suitable for production of proteins or other metabolic products, however, its continuous operation can fail when the cell growth is inhibited by the product, e.g., when lytic viruses are propagated in the vessel. For such cases, the use of cascades of CSTRs is the preferred platform because they provide a separation between the cell growth phase and the product-release phase.

Cascades of CSTRs for continuous virus production are characterized by one CSTR for cell growth and at least one CSTR in series for virus infection and propagation [26]. In order to achieve stable operation, the first CSTR must operate as a chemostat with a D less than μ_{\max} while the subsequent vessels can operate at D values less or greater than μ_{\max} [29]. Cascades of CSTRs have been used since the 1960’s for production of viruses in continuous mode [30]. This included adenovirus, polio virus, baculovirus, picornavirus [31], and, in recent years, influenza virus [26]. These research works have successfully reported stable bioreactor operation with high virus titers for several days. However, one main drawback of this system, the possibility of virus drift after several days of propagation, has so far not been addressed. Moreover, after several days of continuous propagation, a low virus productivity level has been observed in cascades of CSTRs when unstable viruses such as influenza virus and baculoviruses are propagated [26] [32]. These viruses show oscillations in virus concentration over cultivation time that can be explained by the accumulation of defective interfering particles (DIPs) in the virus population. DIPs have deletions in genes required for replication. Due to that, they depend on co-infections with standard virus (STV) with full length (FL) genome for successful propagation [33]. At high DIP concentrations, the replication of the STV is reduced, and the viruses are washed out of the CSTR. This generates

oscillations in the virus titers which is known as “von Magnus effect” [34]. Despite these challenges, one hypothesis that motivates this work is that the use of a cascade of CSTRs might be a good option for production of MVA virus because of the relatively high stability of its genome and the fact that the presence of DIPs in MVA virus populations has not been reported so far.

Continuous tubular bioreactors are a type of system widely used in biotechnology but without applications in viral vaccine production [35]. This bioreactor type is characterized by a long tube with a predefined internal diameter and open at both ends. This configuration provides a large area-to-volume ratio with efficient mass and heat transfer. Compared to STRs, tubular bioreactors have usually simple construction and are easier to scale up because fewer number of parameters are required [35]. The use of a continuous tubular bioreactor can, in theory, overcome the “von Magnus effect” observed in cascades of CSTRs. This would be possible if continuous cell infection at the entry of the tube with a defined virus stock is carried out. That configuration would avoid DIPs accumulation within the bioreactor volume due to low passage spreading in the axial direction of the tube. The infected cells, non-infected cells and free virions can be pumped throughout the tube with a residence time (RT) long enough for virus release and further virus infection and propagation. If a close-to-ideal plug-flow condition is achieved inside the tube, the absence of back-mixing and no accumulation of progeny virions and DIPs within the tube would result in a stable virus harvest. Further reduction of virus spread in the axial direction can be possible via compartmentalization of the fluid, e.g., via addition of air bubbles. Hence, an important hypothesis of this work is that the use of a tubular bioreactor would result in continuous influenza virus production with stable viral titers and stable genetic profile over cultivation time.

Accordingly, the aim of this work was to explore options for continuous production of cell culture-derived viruses. With the establishment of continuous cultures, the identification of conditions that allow efficient and stable virus production over weeks of operation was intended. That is to say, the use of stable DNA viruses such as MVA, and changes in process parameters such as RT and multiplicity of infection (MOI) to positively impact process efficiency. Moreover, the implementation of continuous cultures is a demanding experimental task that lacks small-scale approaches to simplify and accelerate the analysis of such systems. Also, overcoming the bottlenecks that DIPs represent in continuous virus production is a major challenge that can be solved with modifications in the infection conditions via the design of tubular bioreactors. Hence, the milestones of this work were the following: 1) the implementation of batch cultures of MVA virus and influenza A virus (IAV) as control experiments for the continuous cultures, 2) the establishment of a small scale approach of a cascade of CSTRs comprising two shake flasks operated in semi-continuous mode to produce MVA virus and IAV, 3) the establishment of a

cascade of two CSTRs, named two-stage bioreactor (TSB), for production of MVA virus over several weeks, 4) the development of a novel continuous tubular bioreactor system for IAV production, which can overcome the “von Magnus effect” and provide a new technology for stable continuous production of viral vaccines.

This doctoral thesis starts with a background and theory chapter describing basic definitions of MVA and influenza viruses, their life cycle, the presence of DIPs in the virus population, and also an overview of current virus production systems. A literature revision for virus production with cascades of CSTRs, and basic concepts about the TSB systems and tubular bioreactors are finally addressed in that chapter. Then, in the materials and methods chapter, the different platforms used in this work and their mode of operation is presented, including batch cultures, small scale semi-continuous cultures, and continuous cultures using TSB and tubular bioreactors. Then, in the following chapter, the results combined with a discussion for the different modes of culture implemented in this work is presented. The results and discussion chapter starts with batch cultures, followed by semi-continuous cultures that are needed for the evaluation of the performance of continuous cultures. Then, the results and discussions of continuous MVA virus production with a TSB system, and of continuous IAV production with a PFBR system are presented. The results and discussion chapter closes with a summary of process productivities obtained with continuous cultures and a comparison with batch and semi-continuous experiments. Finally, this work finishes with a general conclusion, and an outlook for future developments.

Chapter 2

Background and Theory

2.1 Modified Vaccinia Ankara virus

MVA virus was derived from over 500 passages in eggs of chorioallantois vaccinia virus Ankara (CVA) [36], a member of the *Poxviridae* family. CVA was obtained from vaccinia virus and was used as a smallpox vaccine at the Turkish vaccine institute in Ankara. A sample of the Ankara CVA strain was received in Germany in 1953, where it was passaged in chicken-derived cells as substrate [37]. MVA was the term used to name the plaque-purified isolate of passage 516 that was then shown to have lost approximately 15% of its genome at multiple sites in the course of this adaptation [38]. Due to this adaptation, the virus lost its ability to replicate to newly infectious particles in human cells and kept only the ability for binding, entry and presentation of viral antigens in human cells [36]. Poxvirus particles are enveloped, and possess a spherical to ellipsoidal shape with dimensions that range between 260-380 nm in the axial dimension [17] [39] and their replication takes place in the cytoplasm. They possess a double stranded DNA with a size that ranges between 139 kbp and 307 kbp and contains 178–334 open reading frames [40]. Vaccinia viruses can be genetically engineered by homologous recombination and can support inserts of at least 25,000 bp [41].

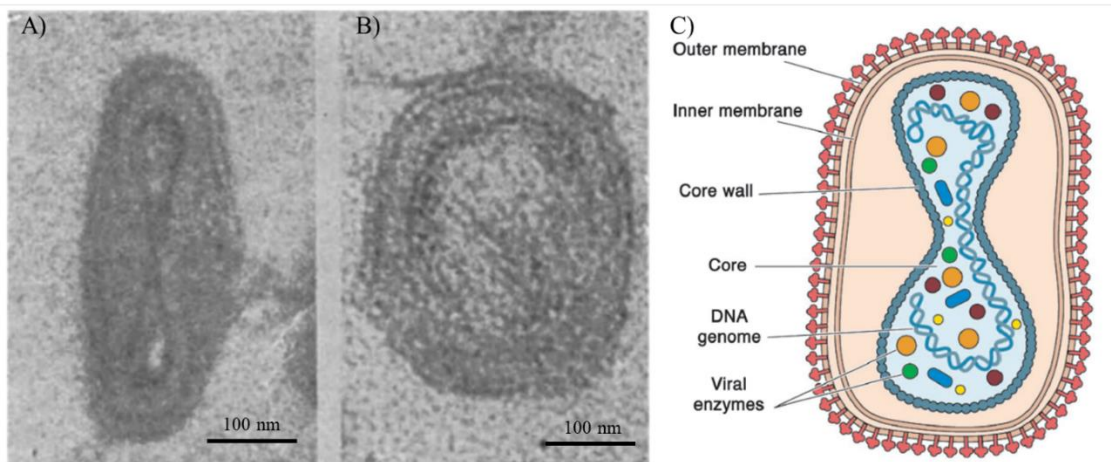


Figure 2.1. Electron photographs and scheme of vaccinia virus structure. A) Vertical section and B) horizontal section of virions. C) Virion structure (Copyright 2004 National Academy of Sciences). Figures modified with permission of [42] and [43].

MVA virus was used in humans during the smallpox eradication campaign of the WHO and also in several clinical trials [44] [45] showing to be safe for clinical applications. However, the high doses for optimal stimulation of the immune system represents a technical challenge for

large-scale manufacture of MVA-based treatments [46]. Large scale production of poxviruses depends on avian host cells and, since the 1950s, the main avian substrates for vaccine manufacturing have been embryonated chicken eggs and primary cells obtained from embryonated chicken eggs [47] [48]. Such material has a limited life span which renders scale-up in bioreactors impossible.

MVA virus has a high potential for expression of recombinant antigens or as a viral vaccine vector because it can accommodate large recombinant inserts and is described to be safe for humans and animals [36]. Recombinant vector vaccines based on MVA against influenza virus [49], Ebola virus [50, 51], HIV [52], tuberculosis [53], chikungunya virus [54], smallpox virus [55], respiratory syncytial virus [56], malaria [57, 58], bluetongue virus [59], and West Nile virus [60] have been described. One challenge in MVA production with modern cell culture technologies is the fact that a large fraction of infectious units is not released and cell-associated conditions is needed for optimal virus spread. Because that, processes have been developed where the virus is propagated in suspended aggregates of 20-100 cells [8]. Recently, a novel MVA virus isolate, named MVA-CR19, has been generated that can be produced at high yields in non-aggregated avian suspension cells in chemically defined media [24], which makes MVA-CR19 an interesting candidate for exploring process options towards continuous vaccine manufacturing.

MVA-CR19 is a strain of MVA virus that was adapted through 19 passages in suspension avian cells AGE1.CR in chemically defined medium [9]. Surprisingly, it was found that 75% of infectious units were in the supernatant, while only 4% of infectious units were obtained in the supernatant with the parental virus seed. A single amino acid mutation in three different proteins was found after a 135 kb gene sequence analysis. Additional experiments with MVA-CR19 virus showed that does not replicate in Vero and HEK 293 cells which suggests that MVA-CR19 can be a safe viral vector. The MVA-CR19 strain may facilitate the supply of recombinant MVA virus vaccines since its production in single cell suspension is less challenging in bioreactors, and the extraction from the supernatant without cell disruption can help to increase the yield of MVA virus purification.

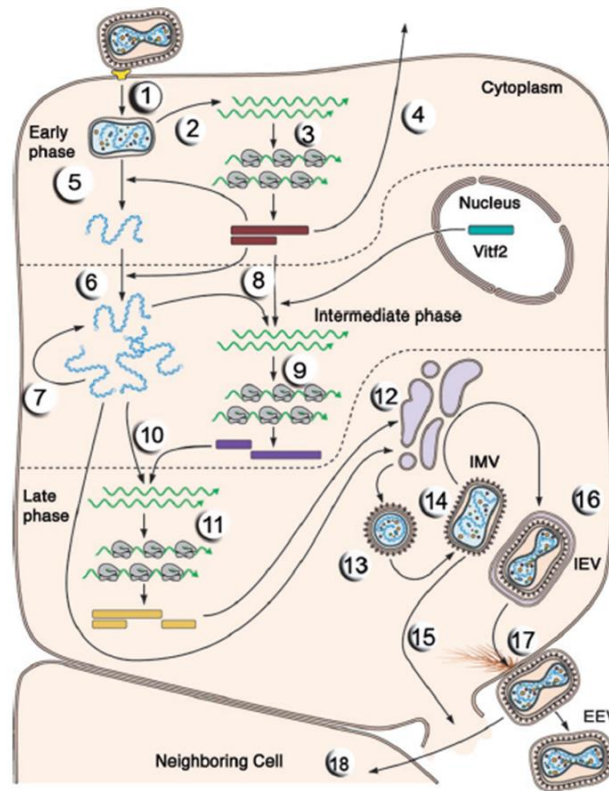


Figure 2.2. Reproductive cycle of vaccinia virus. The figure illustrates the entry and replication of an extracellular enveloped virus (EEV). Step 1: entry of EEV. Step 2: synthesis of viral mRNAs. Step 3: translation by the cellular protein-synthesizing machinery. Step 4: secretion of early proteins. Step 5: genome is released from the core. Step 6: replication of the viral DNA genome. Step 7: additional cycle of genome replication. Step 8: transcription of intermediate-phase genes. Step 9: proteins encoded by intermediate viral mRNAs. Step 10: transcription of late-phase genes. Step 11: synthesis of proteins from step 10. Step 12: early stages of assembly. Step 13: formation of immature virions (IMV). Step 14: formation of brick shaped IMV. Step 15: release of IMV by cell lysis. Step 16: formation of intracellular enveloped virus (IEV) with double membrane. Step 17: fusion of IEV with plasma membrane to form cell associated virions (CEV). Step 18: CEV can be transferred directly to neighbor cells. CEV can also be dissociated from the membrane as EEV. RNA molecules are shown in green. Copyright 2004 National Academy of Sciences [43].

2.2 Influenza virus

Influenza virus is a RNA-virus with an approximate diameter between 80 to 120 nm [61]. Most laboratory-adapted IAV strains have a spherical shape, while wild-type IAV, found in the respiratory tract of fatal infection cases, have mostly a filamentous shape [62] [63]. Its filamentous shape is believed to be essential for virus survival in nature. Influenza viruses can be classified in type A, B or C, according to their nucleoprotein (NP) and matrix protein (M1), which are represented in Figure 2.3. The type A influenza can be found in animals and humans, while influenza B and C can be found only in humans [64]. Type A influenza is naturally found in wild aquatic birds, particularly in wild ducks, geese, swans, gulls, shorebirds and terns, and can infect

people, birds, pigs, horses, dogs, among other animals. Multiple variants of two subtypes of IAV are currently known to be circulating among humans: H1N1, and H3N2 [65, 66].

The subtyping of influenza type A is based according to the antigenicity of two *glycoproteins* on the surface of the virus: haemagglutinin (HA) and neuraminidase (NA) (Figure 2.3 D), for which 16 HA (H1 – H16) and 9 NA (N1-N9) variants have been identified [67] and resulting in many possible combinations. For example, a “H1N1 virus” designates an IAV subtype that has an HA 1 protein and an NA 1 protein. These two surface glycoproteins can recognize carbohydrates such as the sialic acid N-acetylneuramic acid in humans, which is found in the upper respiratory tract and in lung-associated glycoconjugates [68]. Another protein embedded in the surface of the virus is the M2 ion-channel which transports protons through the membrane and is essential for transmembrane pH regulation during the cell entry process [69].

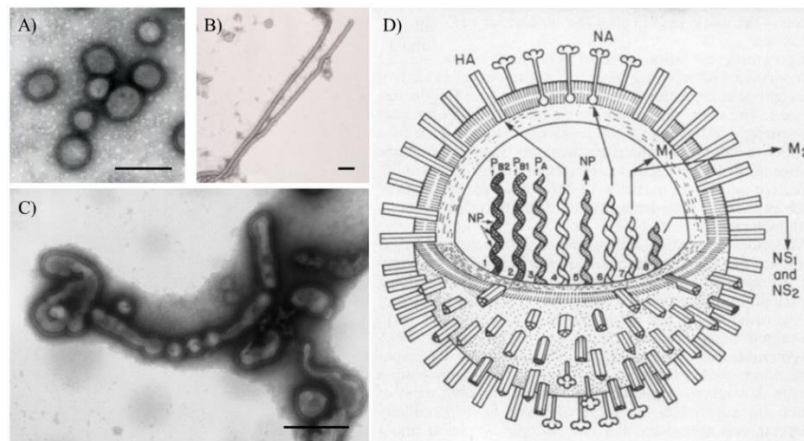


Figure 2.3. Electron micrograph and structure of influenza virus. A) Spherical virions of A/WSN/33 (H1N1). B) Filamentous virions of A/Udorn/307/72 (H3N2). C) irregular-shaped virions of A/Puerto Rico/8/1934 (H1N1) strain. D) Diagram of influenza A virus structure. *NS* means non-structural proteins. PA, PB1 and PB2 are polymerase proteins. HA Hemagglutinin, NP nucleoprotein, NA neuraminidase, M1 matrix protein, and M2 ion channel protein (Copyright 1992 American Society for Microbiology). Scale of figures A, B and C is approx. 100 nm. Figures adapted with permission of [62] and [70].

For establishing the nomenclature of a new isolated influenza virus specific information is required [64]. First, the type of the influenza virus (animal or human, type A, B or C) has to be identified. If the virus has animal origin, the species and the subtype of the influenza virus (for human influenza virus, the specie is not specified) has to be determined. In addition, the location of the virus, the sequence number of the isolate, the year of the isolation, and the formula of the surface antigens (H = Haemagglutinin; N = Neuraminidase (eg, H3N2) are also required. For example, the first IAV subtype H3N2 isolated in Berlin in the year 1989 has the nomenclature of A/Berlin/1/89 (H3N2) [64].

The influenza virus infection cycle can be divided in five steps: 1) entry into the host cell, 2) entry of vRNPs into the nucleus, 3) transcription and replication of the viral genome, 4) export of the vRNPs from the nucleus, and 5) assembly and budding at the host cell plasma membrane [71]. This process can be seen more in detail in Figure 2.4.

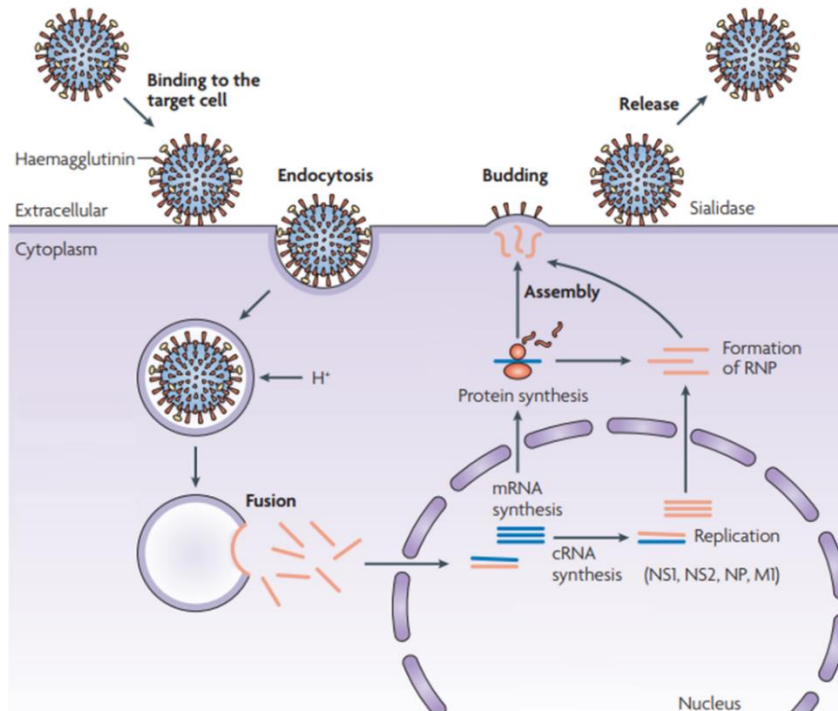


Figure 2.4. Replication cycle of influenza A virus (IAV). Three proteins form part of the IAV surface: an M2 ion channel protein, the haemagglutinin and the enzyme sialidase (or neuraminidase). The cycle starts with an influenza virus particle binding to the target host cell by using its surface glycoprotein haemagglutinin to recognize glycoconjugates that display a terminal α -linked N-acetylneuraminic acid residues such as GD1a. Then, the virus is endocytosed, membrane fusion takes place and the necessary viral components are produced by the host cell machinery. Viral protein synthesis and particle assembly in the host cell prepares the progeny virus to exit the cell via the budding process. Finally, the enzyme sialidase cleaves the terminal α -Neu5Ac residues from both the host cell surface and the progeny virion glycoproteins. This last action enables the host-cell-surface aggregated virion progeny to move away from the cell to infect new host cells. Figure adapted with permission of [68].

Hemagglutinin acts as initial point of contact for the virus to the cell-surface glycoconjugates, and is involved in the internalization process of the virus via the fusion of the virus envelope with the cell [68, 72]. The function of the neuraminidase is to assist in the movement of the virus through the upper respiratory tract, and with the release of the newly formed virions from the cell. The ribonucleoprotein complex consists of a viral RNA segment associated with the nucleoprotein (NP) and three polymerase proteins (PA, PB1 and PB2). The matrix (M1) protein is associated with both the ribonucleoprotein and the viral envelope [67]. Moreover, the IAV genome has eight genes encoding for at least 11 proteins. These proteins include three RNA polymerases that help the virus to replicate its genome. These polymerases have high error rates

which lead to high mutation rates of the virus (nucleotide substitutions). This is the reason for the influenza virus genetic diversity [73].

2.3 The role of defective interfering particles in virus infection and propagation

As mentioned previously, DIPs are virus mutants that are naturally and randomly produced during the virus infection cycle. DIPs are characterized by large deletions in the virus genome [74] [75] [76]. Preben von Magnus discovered them in 1951 after serial passaging of undiluted influenza virus in embryonated chicken eggs [77]. Since then, DIPs have been found in nearly every virus family not only *in vitro* but also *in vivo*. Patients infected with DIPs have been found, for example, in medical cases involving IAV [78], dengue virus [79] and hepatitis C virus [80] (reviewed in [81] and [82]). DIPs lack the ability to replicate by themselves, unless a co-infection with STV particles is carried out, which provides the missing functions *in trans*. DIPs tend to compete with the STV, because they replicate using the machinery of the STV and their replication is relatively faster than the STV. The competition involves molecular mechanisms in virus replication and packaging, and processes as viral protein and polynucleotide synthesis can be slowed down [83] [74]. As a consequence, the cell produces mostly DIPs, and their abundance can fluctuate dramatically under certain conditions. The increase in the ratio of DIPs to STVs and subsequent drop in virus yields that comes out after several viral passages at high MOI is called “von Magnus effect” [74]. In addition, it has been shown that DIPs multiplicity can affect virus replication *in vivo* [84] making DIPs potential antiviral candidates [85]. Another aspect is that DIPs could trigger mutations *in vitro* of the STV by making them more resistant to the interference effect [86] .

Three general aspects are relevant regarding DIP and STV population dynamics [87]:

- 1) The relative DIPs and STV abundance after several passages *in vitro* has unpredictable fluctuations [74].
- 2) Cells that are highly infected by DIPs (high MOI conditions) are producing more DIPs than STV, leading to a decrease in the production of STV.
- 3) It has been suggested that DIPs particles play a role in maintaining persistent infections, because of the reduction in lytic effects which allow DIP-only infected cells to continue growing and be infected at later times [74].

As addressed above, DIPs play an important role in virus replication by interfering in the virus cycle and competing with the STV. Hence, and assuming that infection with pure DIP seeds is harmless, they can be potentially used as therapeutic agents by decreasing the STV-induced

damage in the host tissue in vivo [85]. However, their replication mechanism is still not fully understood. Finally, understanding DIP replication dynamics could be useful to improve current vaccine production and is a key aspect to establish continuous virus production processes.

2.3.1 Defective interfering particles in Modified Vaccinia Ankara virus population

Little is known about the existence and nature of DIPs in poxvirus populations, the mechanisms by which they might interfere and how they would replicate. If DIPs are present, the virus yield following infection and serial passaging in a host cell would be reduced. Such results have been rarely described and only few observations include variations in the yields of virions per cell, changes in ratios of virions plaque-forming units for virus stocks or even complete virus replication failure in serial passage [88].

Previous studies have shown that the vaccinia virus strain Western Reserve (WR) rapidly evolved altered genomes as detected by restriction enzyme analysis in serial passage experiments [89]. The DNA sequence was altered within inverted repetitions near the ends of the genome in a region which does not appear to code for virus proteins. These modification in the DNA sequence were also accompanied by gene deletions adjacent to the left-hand terminal repeat region of the genome, which is known to encode certain early viral functions [89]. Similar DNA deletions were found in a mutant rabbitpox virus that had lost functions required for replication in one host cell line (pig kidney cells), but not in other host cell (chick embryo fibroblasts) [90]. Hence, a possible interpretation is that the ability of DIPs to interfere in poxviruses is host cell dependent [88]. Whether this is true or not, potential DIPs presence in virus stocks should be considered, and conditions which can mitigate DIP generation, such as low MOI conditions and low virus passage number, should be adopted. Finally, this doctoral thesis will explore production of MVA virus in two-stage stirred tank bioreactors, where a continuous passaging of the virus at high MOI conditions takes place in the infected vessel [26]. That system enables MVA evolution studies and might help to elucidate whether DIPs co-evolve with STV in long term cultivations.

2.3.2 Defective interfering particles in influenza virus population

It was already mentioned that the formation of an “incomplete form of influenza virus” was observed in 1951 [68] after serial passaging of undiluted influenza virus in embryonated chicken eggs. Over decades, the progress in understanding influenza DIPs has been limited by difficulties to resolve the viral genome, lack of appropriate cell-virus systems for growing high titer influenza DIPs in controlled conditions, inability to separate influenza DIPs from STV, and lack of suitable assays to quantify influenza DIPs [91]. Many of these limitations still apply to a variety of viruses [82], however, major advances have been made for influenza virus with the development of better

producer cell lines [92], development of assays for IAV DIP quantification [93], and replication of pure IAV DIP seeds in absence of STV [94]. Several terms have been used in literature to refer to these “incomplete forms of influenza virus”, such as “noninfectious virus”, “defective virus”, “deleted virus”, “incomplete virus”, “immature particles”, “defective interfering virus”, and “von Magnus virus”. Among these, the term DIP describes the properties of the virus described by von Magnus, while the others might be misleading. For example, if one or more viral RNA segments are missing, one can be in presence of a noninfectious, deleted or incomplete influenza virus. However, these virus particles will not be interfering and therefore they cannot be referred to as DIPs [91]. For such cases, the term used in this doctoral thesis is defective particle (DP).

DIPs of influenza virus are deficient in at least one of the essential viral gene segments due to large internal deletions in the gene. Typically, the DIP keeps genomic sections that are critical for replication and packaging, such as the 3' and 5' promoters, the adjacent non-coding regions, and also sections of the coding region [95]. Only truncated forms of the protein are encoded by the defective gene segment. The size of the deletion can vary and defects in the polymerase genes on segment 1-3 are most common [96] [97]. On average 100–300 nt of sequence from each end of the vRNA can be retained by these polymerase DI RNAs and can, therefore, lack more than 80% of their original length [95] [98] [96].

2.4 Upstream processing of virus production – an overview

2.4.1 Egg-based production

The most common method for viral vaccine production is the use of embryonated chicken eggs. This method has been used since the 1950's for production of yellow fever [99] and influenza virus [100]. In this process, embryonated eggs are infected with the virus of interest and then harvested a few days later. The embryo is typically destroyed, the virus-containing harvest solution is centrifuged, sterile-filtered, and the supernatant is stored for further processing and vaccine blending.

In the case of influenza vaccines, the egg-based technology is used to produce inactivated or “killed” vaccines, and also live attenuated or “weakened” vaccines. Before production starts, authorized laboratories, such as the Global Influenza Surveillance and the Response System of the WHO, provide to the private sector candidate vaccine virus (CVVs) grown in eggs [100]. CVVs used for IAV vaccines are typically reassortant viruses with genes encoding the surface glycoproteins of HA and NA derived from the wild-type virus of interest. The other six gene segments of the CVV are derived from a high-growth donor virus that can propagate well in the vaccine production substrate (typically eggs) [101] [102]. One high-growth donor is the influenza

A/Puerto Rico/8/34 virus strain. High growth-reassortant viruses are commonly produced infecting eggs with two viruses, however, reverse genetic technology might be used for viruses with pandemic potential [103].

The CVVs are injected in fertilized eggs and incubated for 2-3 days. The fluid that contains the virus is harvested, inactivated (killed) and then the antigen purified. Further testing of the final preparation by local authorities is done before release and shipment. Most manufacturers still use this technology to produce influenza vaccines. For the 2018-2019 season this technology represents 85% of the flu vaccines supplied to the United States [104]. The list of companies using this technology include Seqirus, GlaxoSmithKline, AstraZeneca, MedImmune and Sanofi Pasteur [105, 106, 107].

2.4.2 Cell culture-based batch production

The use of cell culture has been a common approach to grow viruses since the 1930s. However, only over the last two decades, the use of cell culture for commercial influenza vaccine manufacturing has been recommended by regulatory agencies to complement the egg-based technology. In this approach, immortalized animal cells are propagated in tissue culture flasks, roller bottles or bioreactors to cell concentrations of up to 1×10^7 cells/ml and then the virus is added to the vessel. The virus particles replicate within 2-3 days and finally a harvest is taken. This technology was approved in 2001 in Europe and in 2012 in the United States [108] [109]. Egg grown CVVs were used to produce cell culture-based vaccines, however, since 2012 Seqirus in Australia received approval from United States authorities to use cell grown CVVs [110].

Cell culture-based virus production in batch mode and in a bioreactor is typically carried out in a biphasic process - cell growth phase followed by a virus production phase. The production of MVA virus in bioreactors follows a protocol that is representative of the production of cell culture-derived viruses and can be used as an example. An MVA virus production process using avian cells has been recently established and leads to high virus yields [18]. In such a process, in the cell growth phase, the avian cells are inoculated in the bioreactor at concentrations of $0.1-1 \times 10^6$ cells/mL. If the conditions of temperature, agitation, metabolites, oxygenation and pH are optimal, the cells grow in batch mode to concentrations up to $0.1-1 \times 10^6$ cells/mL with or without an exchange of culture medium. The infection is typically carried out in the late phase of cell growth and begins with inoculation by seed virus [111]. Once the genome of the virus replicates within a cell and the viral proteins are produced, the virions are assembled and then virus particles are released. This leads to a growth in the viral titer during the first 48 h post infection (p.i.), followed by a titer peak and finally a virus inactivation phase, as depicted in Figure 2.5. During

the virus production phase, the cells can grow due to the addition of fresh medium at the time of infection, and then end in cell death by virus-induced lysis.

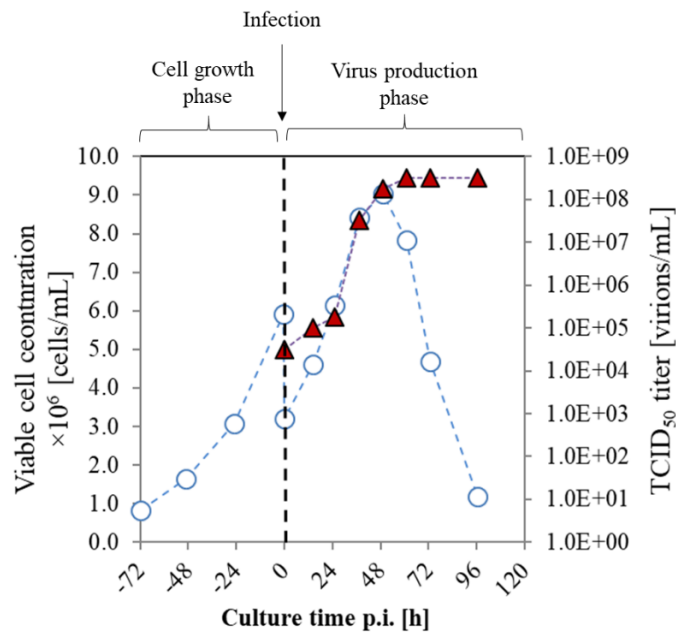


Figure 2.5. Scheme of a batch process for production of Modified Vaccinia Ankara (MVA) virus in avian suspension cells. The process consists of two phases: cell growth phase followed by MVA virus production. First, avian cells are inoculated in the bioreactor for growth to viable cell concentrations (blue circles) close to 5×10^6 cells/mL. Subsequently, and after a dilution step with fresh medium, the cells are infected with MVA virus (infection time represented with a dashed line). The harvest is obtained between 48 and 72 hours post infection, with infectious virus (TCID₅₀, red triangles) titers between 0.1 - 1.0×10^9 virions/mL. After the harvest, the bioreactor is cleaned, sterilized (if it is made of stainless steel) and a new batch production cycle can be started. Note: some MVA strains need cell agglomeration at time of infection. To enable that, a special culture medium has to be used at the dilution step.

While still challenging regarding the manufacturing costs, there are several advantages of using cell culture technology compared to eggs. First, cell lines can be extensively characterized and stored for future use without the need of repeating the whole range testing. This extensive characterization is also beneficial to provide cell seeds of identical characteristics over time, which allows to reduce batch-to-batch variations. Also, certain viruses propagate better in cells, which avoids the down-time required to obtain high growth reassortants. Also, if needed, high growth reassortants can be more easily generated in cells. Cell cultures allow vaccine production in bioreactors, hence, a more standardized and controlled process is possible. In addition, scalability is facilitated with cell culture and use of bioreactors. Other advantages are that allergies to egg proteins are avoided and, in addition, viral antigens propagated in mammalian cells have a similar or identical glycosylation with the wild type virus that infects humans. Moreover, recent studies have shown that the immune response elicited by mammalian cell culture-derived vaccines could be advantageous compared to egg-based vaccines [112].

Recombinant technology is a third production strategy for vaccines where no eggs are needed and no whole virus is produced. Instead, a gene segment capable of eliciting an immune response is isolated from the wild type virus and inserted in bacteria or animal cells with recombinant DNA technology. This recombinant antigen is then produced and purified from bioreactors. In 2013 an influenza vaccine was approved using recombinant baculovirus technology in insect cells [17]. In that particular case, manufacturers isolate the influenza hemagglutinin or “HA” gene from a wild type vaccine candidate virus. Then, a combination of this HA gene with gene portions of another virus that grows to high titers in insect cells is performed. The HA-containing recombinant virus is then used to infect insect cells and allowed to replicate in these cells to high HA protein levels. The HA protein is then harvested and purified from a bioreactor. The HA protein is finally packaged and released for seasonal vaccination. Another example is the use of MVA virus as a recombinant vaccine platform. This approach is different because the expression of the antigen is carried out directly by infection of the patient with a dose of recombinant MVA virus. MVA is a replication-deficient viral vector and therefore it is considered to be safe for use in humans [36]. MVA can encode one or more foreign antigens and therefore can work as a multivalent vaccine. Here, the gene expressing the antigen is inserted into the MVA genome. The resultant recombinant MVA virus is used to infect either animals or humans [113]. Currently, most MVA-based recombinant vaccines are under research and, to the far of the author’s knowledge, no commercial recombinant product is available.

2.4.3 Semi-continuous virus production

Semi-continuous virus propagation has been also carried out in cultures using adherent cells in tissue culture flasks [114] or in cultivation systems involving hollow fiber units [115, 116]. Semi-continuous cultures are carried out when a fixed volume sample is removed from the culture at regular time intervals (e.g., twice a day) to harvest products or components of the culture, followed by the addition of an equal volume of fresh medium to the culture. This leads to a periodic dilution of both the cell and product concentration that has a saw-toothed appearance when plotted against culture time. Growth rates (from cells or products) are estimated from the apparent growth curve obtained by connecting the peaks of the saw-toothed curve [117]. One example of semi-continuous virus production is the use of multiple harvest strategies for retroviral production in a NIH 3T3 fibroblast-derived adherent amphotropic murine cell line (pMFG/ΨCRIP) for efficient retroviral production [118]. More recently, IAV was successfully produced for up to 12 days in a multiple harvest strategy using laboratory scale hollow fiber bioreactors [119]. These options involve only one single vessel where the cell growth phase and the virus propagation phase are taking place in the same compartment (e.g., in the extra-capillary space of the hollow fiber bioreactor). The multi harvest strategy is typically carried out via

collection of the supernatant while keeping the cells in the culture system. Alternative options for semi-continuous viral vaccine production exist for processes using persistently infected cells, as reported for herpes simplex virus growth in lymphoblastoids [120] [121]. In such systems comprising one vessel for cell and virus propagation, however, their long-term cell propagation can be compromised and would not be suitable for virus production at large scale.

2.5 Continuous upstream processing of cell culture-derived viruses

Continuous culture of microorganisms was initiated in the 1950s [25], where it raised many questions and challenges for the production of biologicals such as single-cell proteins, bioethanol and amino acids [122]. However, due to their simplicity of operation and process robustness, the focus over the following decades was on the establishment of batch cultivations. Also, fast advances in genetic engineering were made that led to a significant increase in process productivity [122]. With the large number of biologicals introduced recently into the market, the interest in more efficient production platforms is back and solving technical challenges such as the integration of upstream and downstream in end-to-end continuous operation is being considered [123]. Compared to batch production, continuous processing has several advantages such as steady-state operation, lower plant turndown, and high volumetric efficiency. Continuous production of many biologicals has been possible with the use of CSTRs operated in single (chemostat) or cascades of CSTRs configurations. The use of chemostats [25] is suitable for processes where cells are cultivated on a defined substrate, to obtain large biomass volumes and/or high product yields such as in molecular biology research [29]. Nevertheless, there are cases when the operation of chemostats can result in unstable operation, for example when the product is produced in small amounts [124], when the product inhibits cell growth or even leads to cell lysis, e.g., with lytic viruses.

Since the 1960's, continuous virus production has been realized with the use of CSTRs. The most common approach has been the combination of several CSTRs in cascades which allowed virus production over several weeks. However, another approach to be considered is the use of continuous tubular bioreactors. In the following, both approaches are presented in relation to their use for the continuous production of viruses.

2.5.1 Cascades of CSTRs

One potential platform for continuous production of viruses is a cascade of two CSTRs, also known as TSB system. A TSB system consists of one vessel for continuous propagation of cells connected in series with a second vessel, where the desired product is obtained, as shown in Figure 2.6 A [125]. The physical separation of the cell growth vessel from the production bioreactor

allows stable cell propagation of processes involving lytic viruses. TSB systems have been used for the production of recombinant proteins using baculovirus [126], and for continuous production of influenza A/Puerto Rico/8/1934 (A/PR/8/34) virus using AGE1.CR cells [26].

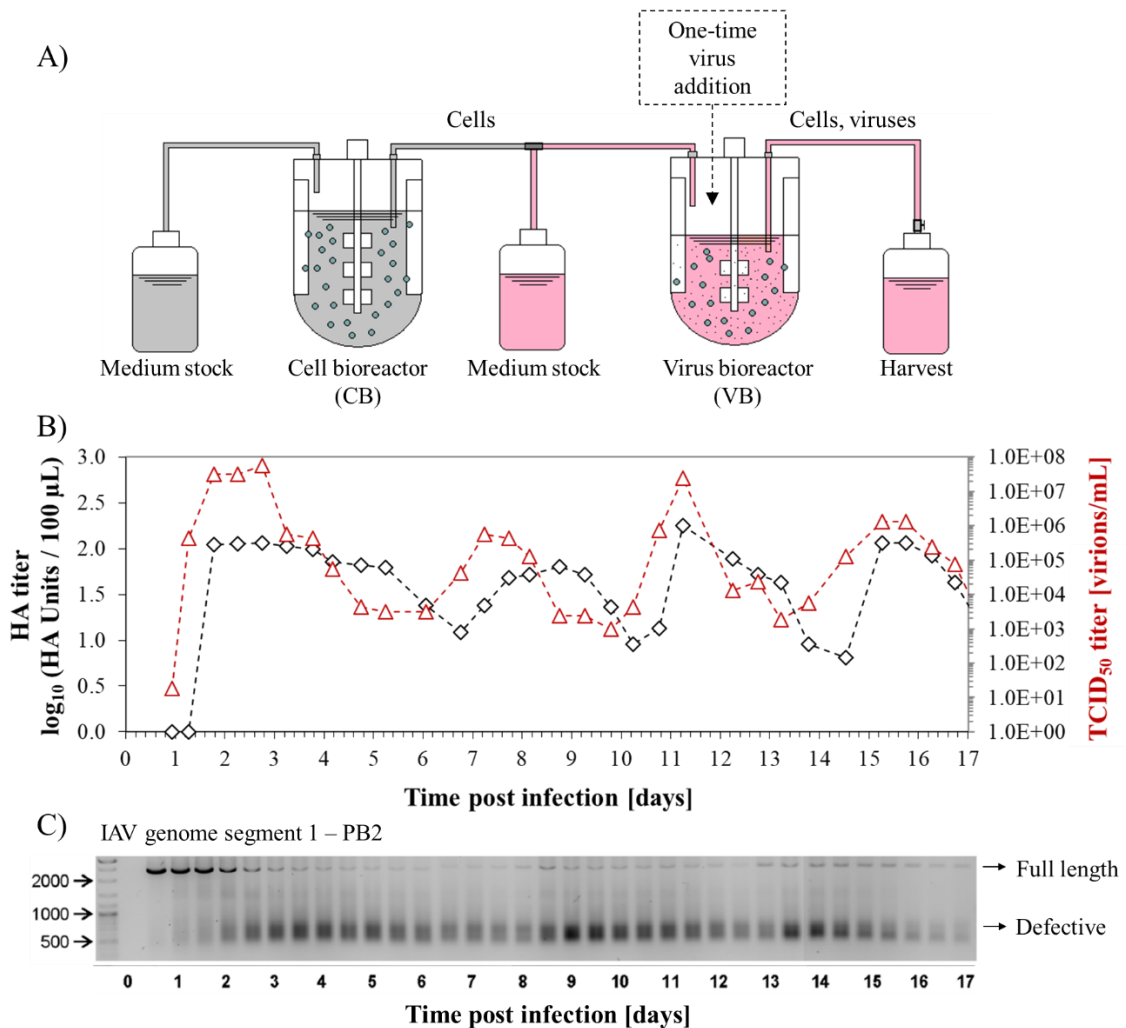


Figure 2.6. Continuous IAV production in a two-stage bioreactor (TSB) system. A) Diagram of the cascade of two continuous stirred tank bioreactors (CSTRs) referred to as TSB system. In this system, a CSTR is used for continuous cell production (cell bioreactor, CB). The cells are continuously transferred to a second CSTR where infection and virus propagation takes place (virus bioreactor, VB). A continuous harvest is obtained from this TSB system. Fresh medium is added to both CSTRs. Depending on the type of virus, compounds such as trypsin can be added to the fresh medium stock used to feed the virus bioreactor. B) Total virus particles (hemagglutinin, HA, black diamonds) and infectious virus particles (TCID₅₀, red triangles) of IAV propagated in the VB over 17 days by Frensing et al. [26]. C) Segment-specific polymerase chain reaction for the detection of full length (around 2000 base pairs (bp)) and defective genome segments (containing defective interfering particles, range between 500-700 bp) of IAV genome segment 1 that encodes the polymerase basic protein 2 (PB2). The size (in bp) of relevant marker bands is shown on the left. Figures B) and C) were modified with permission of Frensing & Heldt et al. [26].

The addition of more CSTR in series would allow several cultivation strategies, such as the reduction of back-mixing by maintaining a defined RT while increasing the number of vessels

(this, approaching a condition typical for tubular bioreactors), or increasing the RT of infectious virions and non-infected cells in the system, with virus burst in the subsequent vessels [30] [126]. However, series of CSTR systems involving the use of more than two vessels would probably not be accepted in large scale vaccine manufacturing due to the complexity of operation and the increasing risk of process failure.

Cascades of CSTRs have been used for propagation of bacteriophages [127] as well as for replication of viruses in human cells [30], insect cells [128], and avian cells [26]. Accordingly, in Table 2.1, examples for continuous production systems using cascades of CSTRs that were established at laboratory scale are considered.

Poliovirus and adenovirus production

In a pioneer work, poliovirus 1 and adenovirus were cultivated in two-stage and three-stage bioreactors in a HeLa S-3-1 and a HeLa-derived KB cell line, respectively [30]. The used bioreactor configuration was called “lysostat”. Poliovirus type 1 was grown with a yield of 421 TCID₅₀ per cell, and adenovirus type 14 with a yield of 116 TCID₅₀ per cell. This study showed that continuous virus production was possible and introduced a basic mathematical description of virus production in cascades of two and three CSTRs. This work also pointed out that thermolabile viruses need special considerations, when produced in continuous mode. In particular, such virus particles have to be removed from the CSTR with a dilution rate exceeding the specific virus inactivation rate. Moreover, it was suggested that, in general, infected cells must be kept in the bioreactor until lysed (or until virus release ceases in case of non-lytic viruses). Nevertheless, with a life cycle of 5 to 24 h as found for many viruses relevant in vaccine production, steady state conditions would be difficult to achieve and specific measures to keep virus yields at a high level might be required. Finally, cell concentrations at steady-state have to be selected carefully to avoid substrate limitations or the accumulation of inhibiting by-products of metabolism or viral compounds.

Baculovirus production

The research groups of Vlak and Tramper made a significant contribution to the field of continuous virus cultivation using cascades of CSTRs for production of baculovirus using insect cell cultures [128]. In a first publication, two cultivations using two-stage CSTR systems operated for 25 and 60 days, achieved steady-state production levels of polyhedra and non-occluded virus particles (NOVs) for up to 25 days. It was observed that a drop in virus titers was possible at advanced production times (35 days) in continuous mode, and it was suggested that this was due to a “passage effect” induced by DIPs [129]. Later, a first-order reaction mathematical model was

introduced to describe baculovirus production in two and three-stage cultivation systems [130]. The model was successful to predict the time courses of the viable cell and the non-infected cell concentrations in the virus production bioreactor, but failed to describe the passage effect. This latter aspect was covered in a follow-up publication with a structured model, where the effect of DIPs on virus titers of cascades of two and three CSTR was taken into account [131].

In another publication, a three-stage bioreactor set-up (using two CSTRs in series for virus propagation) was compared against a TSB system for baculovirus production [126] (using only one CSTR for infection). It was shown that the occurrence of viruses with a higher virus passage number was accelerated in a three stage bioreactor, which resulted in an earlier drop in virus yield (passage effect) compared to two-stage cultivations. Hence, three-stage bioreactor set-ups seem to be disadvantageous for baculovirus production compared to two-stage bioreactor systems. More studies were carried out by the same research group using a two-stage bioreactor system to produce a recombinant baculovirus containing the LacZ gene expressing β -galactosidase [132] [133]. A DNA analysis showed the existence of a predominant mutant baculovirus that lacked about 40% of the DNA genome, including the absence of the LacZ gene. This confirmed the presence of DIPs in baculovirus cultivations in continuous cascades and their impact in process productivity. In addition, it allowed to develop hypotheses regarding possible mechanisms of DIP formation [134].

In follow up study, genetically engineered baculoviruses were generated to maintain expression levels [135]. However, virus production still decreased after about 30 days of continuous passaging in bioreactors. Finally, semi-continuous infections were used to optimize virus production in the two-stage reactor system, in a process that used an inoculum of the previous infection as seed virus [136]. This mode of operation led to a better performance compared to continuously operated two-stage systems with regard to longer-term operation. In a more recent study [137], virus stability was increased by the utilization of extra homologous repeat regions, which are located throughout the baculovirus genome and are believed to act as origins of viral DNA replication. This approach resulted in prolonged expression of proteins and improved the stability of baculovirus expression vectors for the large-scale protein production in insect cell bioreactors.

Table 2. 1. List of viruses cultivated in continuous bioreactors since 1965.

Virus	Bioreactor Configuration ¹	Cell line	Origin	Duration (d p.i) ²	Max. virus titer (x10 ⁷ TCID ₅₀ /mL)	Mathematical Model	Passage effect observed?	Comments	Reference
Poliovirus 1	Cascade of two CSTRs	Hela S-3-1	Human	11	8.3	Yes	No	First concepts and term "Lysostat" were introduced.	[30]
Adenovirus	Cascade of three CSTRs	Hela-derived KB cell line	Human	6.5	1.0	Yes	No		[30]
Baculovirus E2-strain	Cascades of two and three CSTRs	Sf-AE-21	Insect	30	1.0 ⁴	Yes	Yes	Earlier passage effect in three-stage with respect to two-stages	[137]
Recombinant Baculovirus - AcMNPV	Semi-continuous cascade of stirred tank bioreactors	Sf-9	Insect	80	10 ³	Yes	Yes	Passage effect was delayed with respect to continuous	[131] ; [136]
Recombinant Baculovirus - vIBD-7	CSTR in series with a tubular bioreactor	Sf-9	Insect	8	Not reported	No	Not analyzed	Baculovirus infection experiments for production of β-galactosidase	[138]
Recombinant Baculovirus with extra homologous regions (hrs)	Cascade of two CSTRs	Se301	Insect	27	100 ³	No	Yes	Insertion of an extra hr in the BAC vector led to prolonged protein expression	[139]
Influenza A/PR/8/34 (RKI)	Cascade of two CSTRs	AGE1.CR.pIX	Avian	18	700	Yes	Yes	Passage effect led to low yields	[26]

¹ CSTR: continuous stirred tank bioreactor

² d p.i.: days post infection

³ Titer of nonoccluded viruses (NOVs) in TCID₅₀ per mL

⁴ Units of polyhedra per cm³ of reactor

Influenza virus production

In a research work, influenza virus A/PR/8/34 from Robert Koch Institute (RKI) was continuously produced over 18 days with the avian cell line AGE1.CR in a TSB system [26]. A segregated mathematical model suggested that, if only STV particles are present in the virus population, constant IAV titers in a TSB system can be obtained over weeks of production. Total and infectious IAV titers similar to those of previous batch cultivations [18, 140] were observed during the first three days of culture with a TCID₅₀ titer of 5×10^7 virions/mL at 1.8 days p.i. and an HA titer of $2.0 \log_{10}$ (HA Units/ 100 μ L) (Figure 2.6 B). Interestingly, total and infectious virus titers fluctuated over several orders of magnitude during production time. The oscillations were due to the presence of DIPs, which was confirmed by a PCR assay for IAV genome segments 1, 2 and 3. The PCR result of only IAV segment 1 is shown in Figure 2.6 C. This PCR analysis showed FL genome segments of 2000 base pairs (bp) in size and defective IAV genomes (containing DIPs) between 500 and 700 bp that accumulated periodically over time. As mentioned above, DIPs have deletions in genes that are needed for replication. For that reason, they depend on co-infections with STV with FL genome for successful propagation [33]. At high DIP concentration, the replication of the STV is reduced, and the viruses are washed out of the TSB system. This generates oscillations in the virus titers which is known as “von Magnus effect” [34]. Since then, different approaches using the avian suspension cell line AGE1.CR.pIX [141] as a substrate for virus replication have been evaluated in this doctoral thesis to overcome this hurdle for continuous influenza virus vaccine production.

2.5.2 Tubular bioreactors

An alternative continuous production system could be the integration of a PFBR [35]. Tubular bioreactors have been used, for example, for waste water treatment [142], for production of bioethanol [143], and for production of algae [144]. Tubular bioreactors have unique properties such as a reduced back-mixing and a large surface-to-volume ratio that are useful for a variety of biotechnological applications. In contrast to CSTRs, reagents and products do not accumulate in the tubular bioreactor volume over process time [145]. The reduced back-mixing within the PFBR volume and the possible compartmentalization of the fluid via air bubbles ensure that DIPs produced within a compartment do not interact with recently infected cells at neighboring compartments. This combination can in theory reduce co-infection of cells compared to a normal batch or two-stage CSTR infection, and therefore significantly minimize the amount of DIPs produced compared to a CSTR of the same WV.

One option is the development of a cascade of CSTRs with recirculation. In this case, a tubular bioreactor is used in between both CSTRs, as depicted in Figure 2.7 A. This system has been

previously suggested for recombinant protein production using baculovirus technology [138]. Hypothetically, such a system can also be used for production of unstable viruses such as IAV. This approach would allow low MOI conditions in the entry of the PFBR by adjusting the recirculation flowrates. A low MOI condition at the point of infection (POI) would increase the chance of STV infection. Interestingly, a mathematical model developed by Laske et al. [146] has shown that if DIP infection occurs later than 3 h post infection (p.i.) and STV infection is already well advanced, defective interfering vRNA replication will either be less efficient or will not occur at all. Consequently, there will be a significant drop in progeny DIP number and STV yield can reach levels similar to DIP-free infections when DIP infection occurs too late. As mentioned above, ideal PFBRs have no back mixing, and therefore the co-infection in such bioreactor would be reduced. Hence, the chance that the event predicted by Laske et al. occurs is higher in the bioreactor of Figure 2.7 A compared to a cascade of CSTRs without recirculation, only if the RT of the PFBR is fixed to at least 3 h. Then, the amount of STV in VB would increase compared to a cascade of CSTRs without recirculation. As consequence, a reduction in the virus titer oscillations would be expected. This system, however, will provide a harvest with an increasing virus passage number and, due to the higher amount of STV particles, the virus mutation rate might increase compared to a virus propagated in a classical cascade of CSTRs. Because of that, such bioreactor can be an interesting development for virus evolution studies rather than vaccine production.

If the length of the tubing is adjusted to the MOI and the duration of the replication cycle, and a virus stock of defined virus passage number is used, a virus harvest with defined passage number can be collected continuously at the tube outlet (Figure 2.7 B). The MOI at POI is a function of the cell concentration in the chemostat, the infectious titer ($TCID_{50}$) in the virus stock, and the flow rates (see equation later in M&M). This system is the best approach for continuous production of unstable viruses for several reasons:

- 1) Elimination of the risk of viral antigenic variation as each cell that enters the tube is infected with a virus stock of defined passage number, and the number of additional virus passages inside the tube is limited.

- 2) Steady-state operation allowing harvesting of virus particles with defined quality attributes over extended time periods, such as glycosylation of viral antigens or DIP to STV ratio [85].

- 3) Suitable for production of viruses which show significant accumulation of DIPs and display high mutation rates, i.e. IAV [3,4,5]. If enough time for influenza virus replication inside the

PFBR is provided, the von Magnus effect would be avoided, and stable titers can be expected in the harvest.

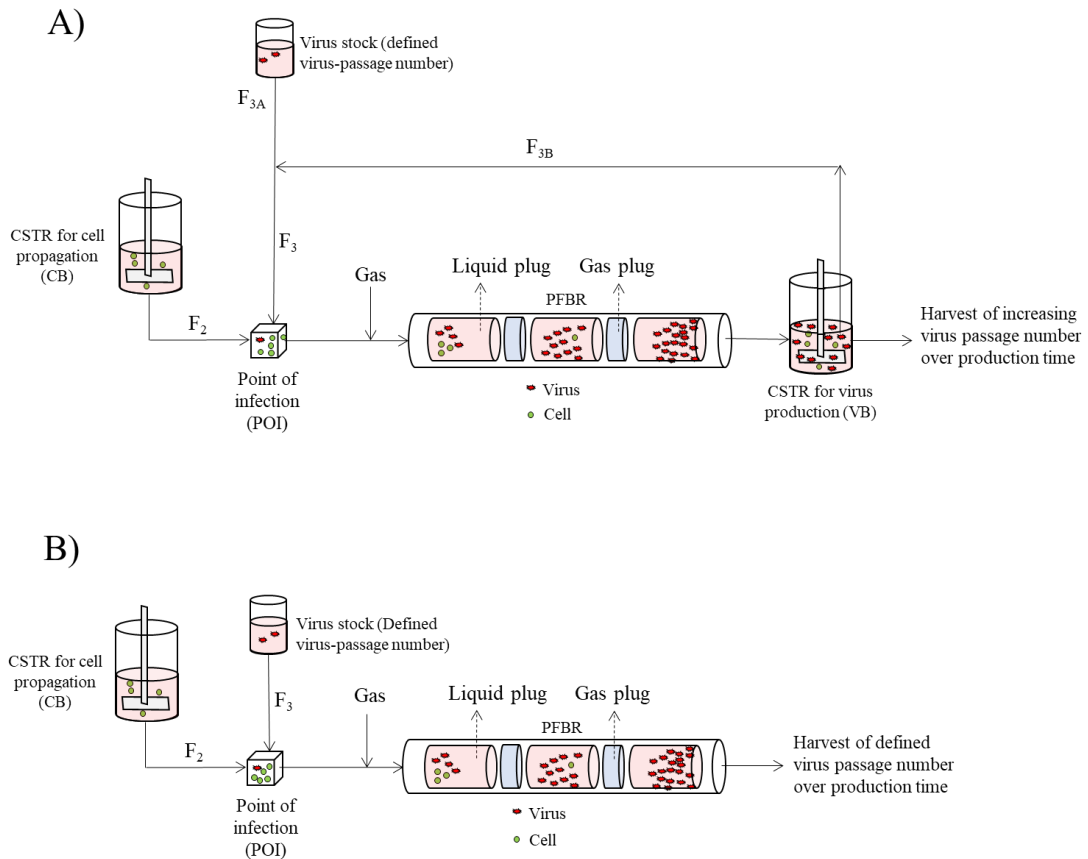


Figure 2. 7. Conceptual schemes of continuous virus production processes using a plug-flow tubular bioreactor (PFBR). A) A cascade of continuous stirred tank bioreactors (CSTRs) with recirculation into a PFBR. This system would enable a low MOI infection at the point of infection (POI) before entering in the virus production vessel (VB) by adjusting the flow rates F_2 and F_3 . In this system, the cells are produced in a CSTR operated as a chemostat (Cell bioreactor or CB) and viruses are stored either in a stock bottle (virus stock, F_{3A}) or are recirculated from the VB (F_{3B}). Cells and viruses are mixed at the POI before addition of air to generate bubble-separated compartments for cell breath. The fluid moves under a plug-flow regime along the PFBR and only virus propagation takes place within the PFBR. Finally, the fluid drops into the VB where virus replication is finalized. A continuous harvest with increasing virus passage number is obtained from VB. B) A chemostat followed by a PFBR. In this system full propagation of the virus within the PFBR takes place. The cells are produced in the CB and the virus is stored in a virus stock of defined passage number. Cells and viruses are mixed in the POI and full virus propagation occurs within the tube. A harvest of defined virus passage number (virus stock's passage number plus one) is produced over process time.

Finally, the following chapter describes the materials and methods used to achieve the production of MVA and influenza viruses in batch, semi-continuous and continuous mode. In particular, the following chapter describes a cascade of CSTRs (of 1 L scale) used to continuously produce MVA virus. Also, the development of a novel plug-flow tubular bioreactor to enable continuous production of influenza virus is described.

Chapter 3

Materials and Methods

3.1 Cell lines and culture media

The avian cell line AGE1.CR.pIX (ProBioGen AG, Germany) [147] was grown in the chemically defined medium CD-U3 (powder-based, PAA, Austria; liquid, Biochrom-Merck, Germany) supplemented with 2 mM of L-glutamine (Sigma-Aldrich, Germany), 2 mM L-alanine (Fluka Analytical, Sigma-Aldrich, Germany) and 10 ng/mL Long[®]R³IGF-I (SAFC Biosciences, USA). Cells were inoculated at a concentration of 0.8×10^6 cells/mL and passaged in shaker flasks at 37°C, 5% CO₂ in air, and 185 rpm.

The canine suspension cell line MDCK.SUS2 [148] (collaboration with Prof. Klaus Scharfenberg, University of Applied Sciences Emden-Leer, Germany) was maintained in a chemically defined medium Smif8 (Gibco, by contact through Prof. Klaus Scharfenberg, Germany) supplemented with 2 mM L-glutamine, and 2 mM pyruvate. Cells were cultivated in 125 or 250 mL shaker flasks using an inoculum of 0.5×10^6 cells/mL and passaged twice a week.

3.2 MVA and influenza viruses

The MVA virus isolate MVA-CR19 virus seed: 4.5×10^8 virions/mL, TCID₅₀ and MVA-CR19.GFP (MVA-CR.A3A9A34CR.GFP; virus seed: 1.0×10^9 virions/mL, FFU; 1·FFU ~ $0.7 \times \text{TCID}_{50}$) with a green-fluorescent protein insertion cassette were used (both isolates from ProBioGen AG, Germany). Before infection, virus seeds were sonicated in a water bath at room temperature for 1 min. An MOI of 0.05 was used in all cultivations.

The influenza virus isolate A/PR/8/34 from Robert Koch Institute (virus seed: 1.48×10^7 virions/mL, TCID₅₀; adapted in four passages in AGE1.CR.pIX cells) was used. An MOI of 0.025 was used in all cultivations [26].

3.3 Batch cultivations

3.3.1 Modified Vaccinia Ankara production in batch mode

AGE1.CR.pIX cells were cultured in 50 mL WV shaker flasks (Corning, USA), for batch cultivations. With cell concentrations reaching about 5×10^6 cells/mL, a 1:1 dilution with fresh CD-U3 medium was performed. Then, virus infection was carried out and 4-5 mL samples at 0,

12, 24, 36, 48, 72 and 96 h p.i. were taken. Cell concentration, cell viability, metabolite concentrations, pH offline and virus titers were determined.

3.3.2 Influenza virus production in batch mode

A volume of 30 mL and 50 mL of AGE1.CR.pIX cells was taken from the cell bioreactor (CB) bioreactor of the PFBR system and infected in batch mode in shaker flasks (150 mL shakers, Corning, USA). With cell concentrations of about $5\text{-}6 \times 10^6$ cells/mL, a 100:58 dilution (culture volume: fresh medium) with fresh CD-U3 medium was performed to approach the infection conditions occurring at the POI in the PFBR system. The infection was carried out with an MOI of 0.025 and the influenza virus strain A/PR/8/34 was added in the fresh medium before the 100:58 dilution took place. Then, 4-5 mL samples at 0, 7, 18, 19, 20, 21 and 25 h p.i. were taken. Cell concentration, cell viability, metabolite concentrations, pH offline, virus titers, and DIP accumulation were determined.

3.4 Semi-continuous cultivations

A semi-continuous two-stage stirred tank cultivation system, or SSC, using two shaker flasks in series was established as a scale-down model to facilitate process optimization. The system consisted of a 120 mL WV shaker flask for cell production (Small cell bioreactor, SCB) linked to a 65-200 mL WV shaker flask for virus propagation (Small virus bioreactor, SVB), as shown in Figure 3.1. Shaker flasks without baffles were used due to the lower evaporation rate observed compared to shakers with baffles.

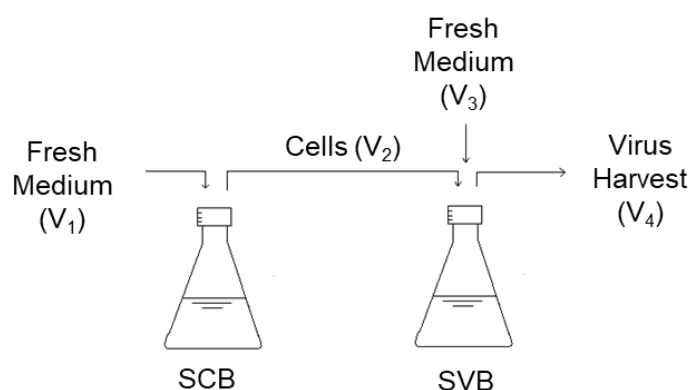


Figure 3. 1. Semi-continuous two stage cultivation. Diagram of the two-stage semi-continuous cultivation (SSC) system for small scale MVA virus and influenza A virus production using shaker flasks. Cells were produced in semi-continuous mode in the small cell bioreactor (SCB) and transferred to the small virus bioreactor (SVB) where virus infection and propagation took place. Twice a day, in chronological order, a harvest was taken (V₄), cells were transferred from SCB to SVB (V₂), and fresh medium was added to SCB and SVB (V₁ and V₃). The volumes of harvest, cell transfer and fresh medium were determined with the equations described in section 3.4.

The shakers were maintained in an orbital shaking incubator (Infors HT Multitron, Switzerland) at 37°C, 185 rpm and 5% CO₂ in air. Samples of 3-5 mL for measuring cell concentration, viability, pH, metabolites and STV titers and DIP accumulation in SCB and SVB were taken twice a day with a time range between 8-12 h.

After each sampling, medium exchanges were carried out in the following order: a) a volume from SVB was harvested, b) a culture volume from SCB to SVB was transferred, and c) fresh medium was added first to SCB and then to SVB. To avoid virus entering into SCB, steps a) and b) were carried out with 2 different single-use pipettes, and step c) with only 1 single-use pipette. The volumes of steps a), b) and c) were determined with the following equations:

$$V_{Harvest_n} = (t_n - t_{n-1}) \times (V_{SCB} + V_{SVB}) \times D_{SCB} \quad \text{Equation 1}$$

$$V_{SCB\ to\ SVB_n} = (t_n - t_{n-1}) \times V_{SCB} \times D_{SCB} \quad \text{Equation 2}$$

$$V_{FM\ to\ SCB_n} = (t_n - t_{n-1}) \times V_{SCB} \times D_{SCB} \quad \text{Equation 3}$$

$$V_{FM\ to\ SVB_n} = (t_n - t_{n-1}) \times ((V_{SCB} + V_{SVB}) \times D_{SCB} - D_{SCB} \times V_{SCB}) \quad \text{Equation 4}$$

Where n is the sample number, V is volume, t_n is the time at sampling “n”, t_{n-1} the time at sampling “n-1”, D_{SCB} is the dilution rate of SCB, and FM is fresh medium. The “apparent” or semi-continuous dilution rate of SCB (D_{SCB}) was the same of CB (D_{CB}) in all SSC experiments. In the rest of this work, the “apparent dilution rate” of the semi-continuous cultures is referred to, indistinctly, as “dilution rate”. These equations were obtained by performing a material balance, where the dilution rate of the system F₄/(V_{SCB} + V_{SVB}) is equal to the dilution rate of SCB [26].

3.4.1 Modified Vaccinia Ankara production in semi-continuous cultures

The MVA-CR19 and MVA-CR19.GFP virus strains were propagated using the SSC system. The first three cultivations were carried out taking an additional sampling of 3-5 mL after the medium exchanges. Afterwards, only one sample was taken before the medium exchanges.

3.4.2 Influenza virus production in semi-continuous cultures

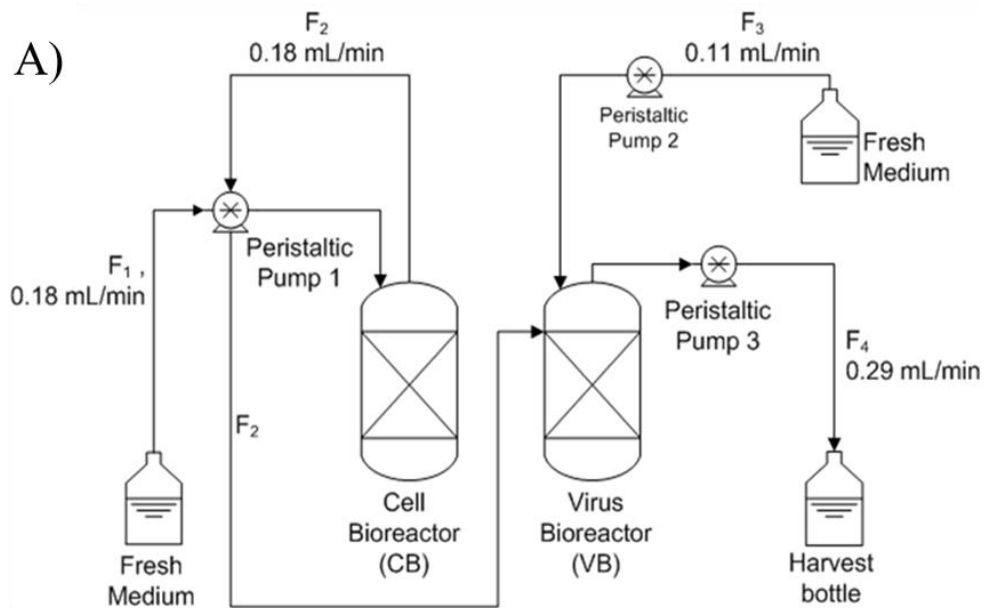
The influenza A/PR/8/34 virus strain, either adapted to MDCK or AGE1.CR.pIX cells, was propagated using the SSC system. Only one sample was taken before medium exchanges to determine pH, virus, cell and metabolites concentrations.

3.5 Continuous cultivations

3.5.1 Cascade of stirred tank bioreactors

A bioreactor system consisting of two 1 L stirred tank bioreactors (Biostat B Plus, Sartorius) was established (similar to Frensing et al. 2013 [26]), Figure 3.2. The first bioreactor (cell bioreactor, CB) was inoculated with AGE1.CR.pIX cells and operated at 37 °C, 120 rpm, 40% oxygen saturation and 850 mL WV. The medium used for the initial batch phase in CB was a 1:1 mixture of a powder-based CD-U3 medium (PAA), and a liquid CD-U3 medium (Biochrom). Due to cell agglomeration observed in previous experiments when 1 M NaOH and 1 M HCl were used, pH was not controlled during the batch phase, but monitored to avoid values below 6.9 (if necessary, medium exchanges were carried out instead of addition of acid and base).

When cell concentration in CB reached at least 5.0×10^6 cells/mL, 350 mL from CB were transferred to the second vessel (virus bioreactor, VB). Medium was immediately diluted 1:1 with fresh CD-U3 medium in each vessel, and the WVs were corrected to 850 mL and 440 mL in CB and VB, respectively. Continuous culture was initiated 2 h later and maintained without infection for 8 days. Only powder-based medium was used during continuous culture. Temperature of VB was controlled to 37 °C, oxygen concentration to 40-50% saturation, and its 440 mL WV was maintained with a dip tube. Before the infection, 1:1 dilution of VB was carried out, and 440 mL WV was set again. MVA-CR19 virus was added to VB at a MOI of 0.05 based on viable cell concentration and TCID₅₀ of the virus seed. The flow rates used are described in Figure 3.2, and the peristaltic pumps used were Ismatec Reglo-Digital MS2/8-160 (pump 1 and 2), and Watson Marlow 101U/R (pump 3). Samples of 5-6 mL were taken twice a day from both vessels with a time range of 8-12 h for measuring cell concentration, viability, off-line pH, metabolites and virus concentration.



B)

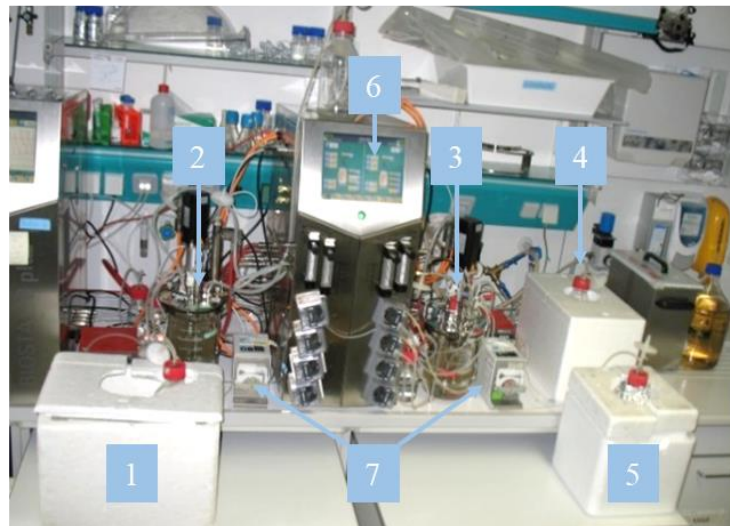


Figure 3. 2. Diagram of the two-stage cultivation systems used for continuous MVA virus production. A) Two-stage continuous stirred tank bioreactor (TSB) system using AGE1.CR.pIX cells with a production rate of 0.29 mL/min. Continuous cell production was maintained in the first bioreactor (cell bioreactor, CB; dilution rate 0.0127 h^{-1}). Cells were continuously transferred at a rate of 0.18 mL/min to a second vessel (virus bioreactor, VB; dilution rate 0.0390 h^{-1}), where MVA virus infection and propagation took place. The virus stock used to infect VB was inoculated only once (time 0 post infection), and the system was then left in batch mode for 12-24 hours to allow proper virus infection and propagation. Once the continuous cultured was started, fresh medium was added to CB and VB at a rate of 0.18 and 0.11 mL/min, respectively. B) Photograph of the TSB system showing the fresh medium stock of the CB (1), the CB (2), the VB (3), the fresh medium stock of the VB (4), the harvest (5), the process control screen (6), and pumps 1 and 2 (left and right, respectively) (7).

3.5.2 Cascade of stirred tank bioreactors with recirculation

A prototype of a cascade of CSTRs with recirculation was constructed, in particular the process with a recirculation of VB in Figure 2.7 A. The system consisted of a 1 L CSTR for cell propagation made of a glass bottle (Schott, Mainz, Germany; referred to as CB) followed by a tubular bioreactor (15 m silicone tube, 1.6 mm internal diameter; referred to as PFBR), connected to a CSTR for virus propagation (250 mL Schott bottle; referred to as VB), as depicted in Figure 3.3. Both bottles were modified with the incorporation of an outlet consisting of a glass-tube at the bottom, with 90° with respect to the wall, following recommendations of the CSTR constructed by Hu et al 1997 [138]. The temperature of both CSTR was measured with a thermometer and the heat was provided with a heating plate. The agitation was set to 150 RPM using a magnetic stirred incorporated in the heating plate. The fresh medium for the CB was maintained in a 1 L bottle (Schott, Mainz, Germany) cooled with ice in a styrofoam box. The PFBR was built inside a plastic container (PFBR-container) that was filled with water. The temperature of the water in the PFBR-container was maintained at 37°C using a digital-controlled water bath. The water of the PFBR-container was pumped to the water bath and then returned to the PFBR-container. The temperature set-point of the water bath was 44°C (Figure 3.3 D), which was found to provide a stable temperature of 37°C in the PFBR-container. The temperature of the PFBR-container was measured with a thermometer and the PFBR-container was covered with aluminum foil. One peristaltic pump was used for pumping fresh medium in and out of the CB vessel, and also for pumping the virus stock and gas to the tubular bioreactor (pump 1); a second pump was used for the recirculation of the bioreactors and for the gases introduced in the CB and VB (pump 2). A third peristaltic pump was used for collecting the harvest from VB (pump 3). A peristaltic Watson Marlow pump (pump 4, not described in Figure 3.3) was used for the temperature control system of the water bath.

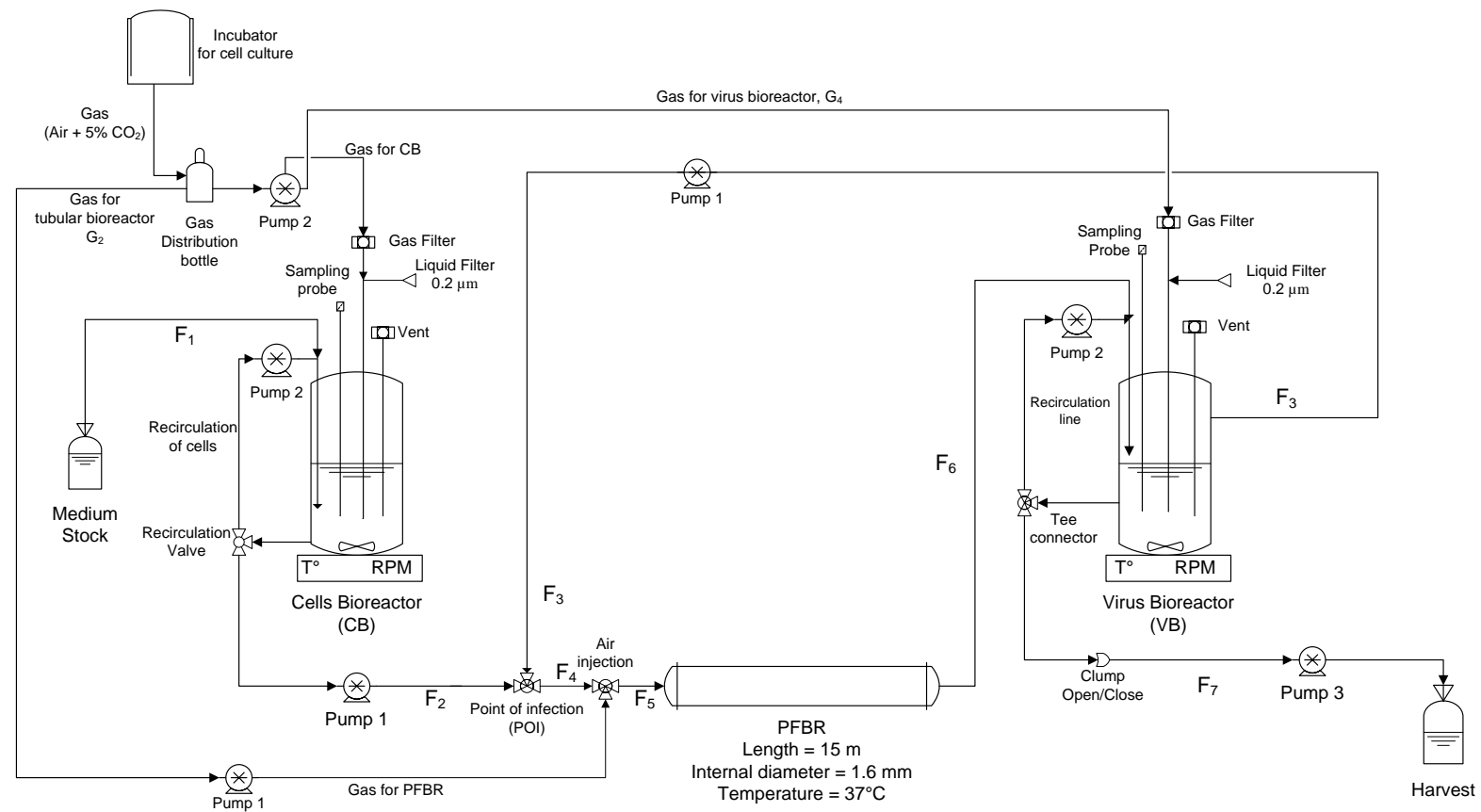


Figure 3.3. Process diagram of the prototype of a cascade of two CSTRs with recirculation. In this process continuous cell production takes place in the cell bioreactor (CB) by receiving a continuous supply of fresh medium (F₁). Cells are continuously harvested from CB (F₂), and infected with a recirculation line (F₃) from the virus bioreactor vessel (VB, right) in the point of infection (POI). The infected cells (F₅) travel through a tubular plug-flow bioreactor (middle, PFBR) with a residence time of up to 3 h before reaching the VB (F₆). Finally, a continuous harvest is taken from VB (F₇). The CB and VB bioreactor had 1 L and 0.250 L WV, respectively. The 15 m PFBR was built with silicone tubing and submerged in water at 37°C.



Figure 3. 3. Photograph of the cascade of two CSTRs with recirculation. A) Overview of the bioreactor: Water heating system (1), tubular bioreactor container or PFBR-container (2), stocks of fresh medium (3), cell bioreactor, CB (4), virus bioreactor, VB (5), harvest bottle (6), gas distribution bottle (7), pump 1 (8), pump 2 and 3 (9) . B) 1 L CB for cell growth and with recirculation line to avoid cell sedimentation, covered in alumina foil. C) 250 mL VB for virus propagation and recirculation line to the PFBR covered in alumina. D) Water bath (left) and PFBR-container. E) PFBR in water at 37°C with thermometer.

3.5.3 Continuous tubular bioreactor system

A PFBR system consisting of a 0.5 L scale CSTR (Dasgip, Germany) followed by a 211 mL PFBR was established, as shown in Figure 3.5. The PFBR system had a nominal production rate of 12 mL/h. The complete bioreactor system was constructed in a cultivation room with a controlled and stable temperature of 37°C. The first bioreactor (cell bioreactor, CB) was inoculated with AGE1.CR.pIX cells and operated at 37 °C, 150 rpm, pH of 7.0-7.3, and 350 mL WV. The oxygen to the CB was provided with a tube connected to two 0.2 µm air filters (Sartorius, Germany). The fresh CD-U3 medium bottle was maintained in a Styrofoam box with ice (which was replaced twice a day). When cell concentration reached at least 2.0×10^6 cells/mL the continuous cultivation was initiated but only PBS was pumped from the virus stock to prime the PFBR. After 48 h, the PBS in the virus stock bottle was replaced by fresh CD-U3 medium containing 42.8 Trypsin Units/mL (Gibco, Germany) and $2-3 \times 10^4$ virus/mL (based on TCID₅₀). The MOI at the POI was determined with the following equation:

$$\text{MOI} = \frac{F_3 \times [\text{virus concentration}]_{\text{Virus Stock}}}{F_2 \times [\text{cell concentration}]_{\text{Cell Bioreactor}}} \quad \text{Equation 5}$$

With F_3 , F_2 the flow rates of the virus stock and the CB, respectively. The virus stock was replaced every 48 h to avoid virus degradation, and the virus stock bottle was maintained together with the CB bottle in a styrofoam box with ice. The seven streams of the process and their flow rates used are described in Figure 3.5 and Table 3.1. Harvests were collected twice a day from the harvest bottle. Samples of 3-5 mL were taken once a day from CB, and twice a day from the harvest bottle for measuring cell concentration, viability, off-line pH, metabolites (glucose and lactate) and virus concentrations (HA titers and TCID₅₀).

The average RT in the tubular bioreactor was determined with the following equation:

$$\text{RT} = \frac{L}{V_T} \quad \text{Equation 6}$$

where the RT (h) is a function of the length (L, in m) of the PFBR and the linear velocity inside the tube (V_T , in m/h), respectively. The latter was calculated based on the flow at the tube outlet (m³/h) divided by the transversal area of the tube (m²). The flow rate at the tube outlet was determined by measuring the collected PFBR harvest volume twice a day.

Finally, the Reynolds number (Re) in the tubular bioreactor was calculated with the following equation:

$$\text{Re} = \frac{\rho \times V_T \times \phi}{\nu} \quad [-] \quad \text{Equation 7}$$

where ρ is the density of the fluid (993 kg/m³, water at 37°C), V_T is the mean velocity of the fluid (m/s), ϕ is the hydraulic diameter of the tube (m) and ν is the dynamic viscosity of the fluid (0.000691 kg/(m×s), water at 37°C).

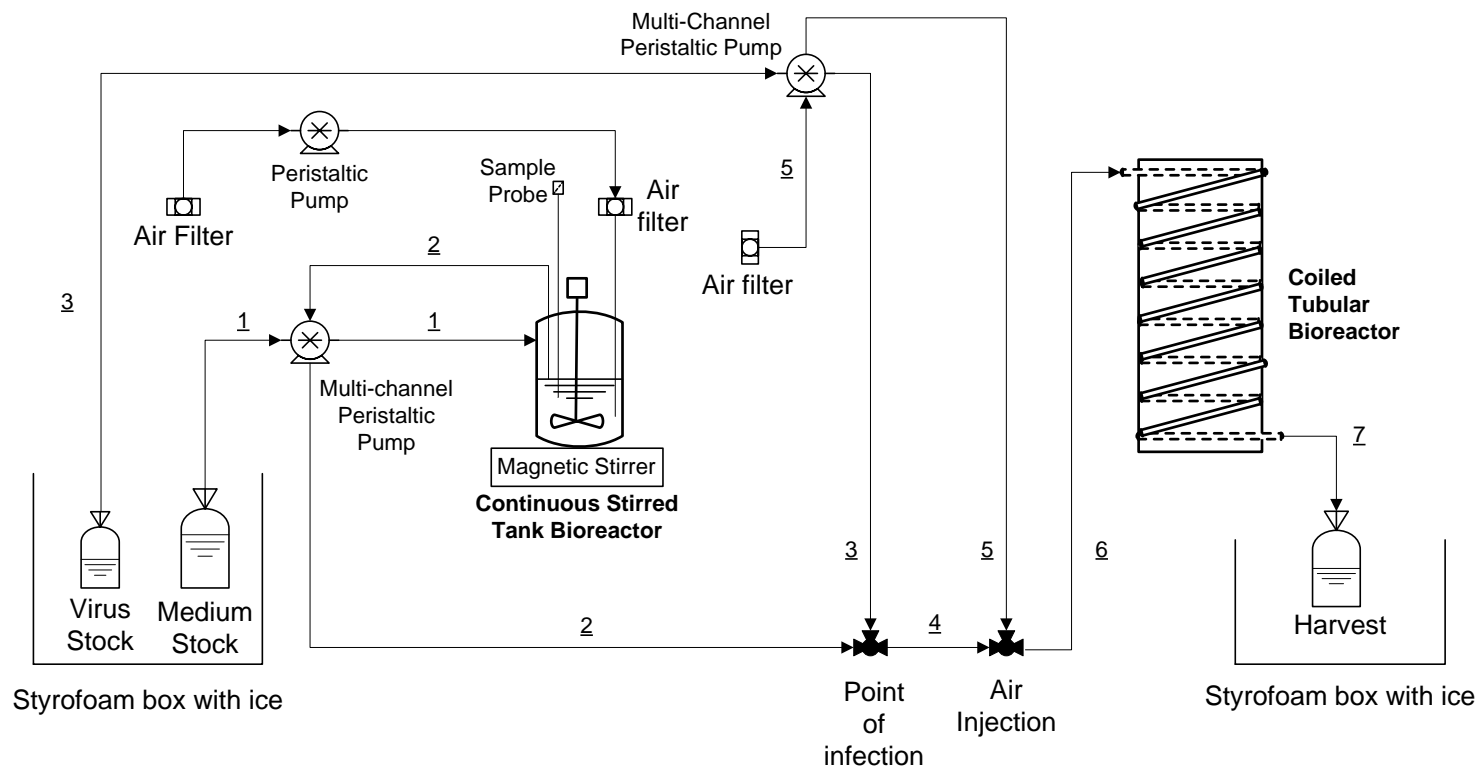


Figure 3. 4. Process flow diagram of the plug-flow tubular bioreactor system for continuous influenza virus production. The process consisted of a continuous stirred tank bioreactor, referred to as cell bioreactor (CB), followed by a coiled tubular plug-flow bioreactor (PFBR). The complete structure was built inside a 37°C cultivation room. The CB was operated as a chemostat with a dilution rate of approx. $0.9 \times \mu_{\max}$. The PFBR was constructed using a transparent silicone tube (1.6 mm internal diameter) that was coiled around a 20 cm internal diameter and 1 m high PLEXIGLAS® XT tube. Cells were produced continuously in the CB with continuous addition of fresh medium from the medium stock bottle (stream 1 or F₁). Cells were continuously transferred with the aid of a peristaltic pump to the point of infection (POI; F₂), where infection took place with influenza virus stored at 0°C in the virus stock (VS) bottle (F₃). The VS was replaced with fresh trypsin, virus and medium every 48 h. Air was taken from the room, filtered with at least one 0.2 μm air filter, and injected into the system for providing enough oxygen to the cells for survival until lysis (F₅). The mixture of cells, virus and bubbles (F₆) traveled through the PFBR with a nominal residence time of 20 h. Finally, the product (F₇) was collected in a harvest bottle and sampled twice a day for analysis.

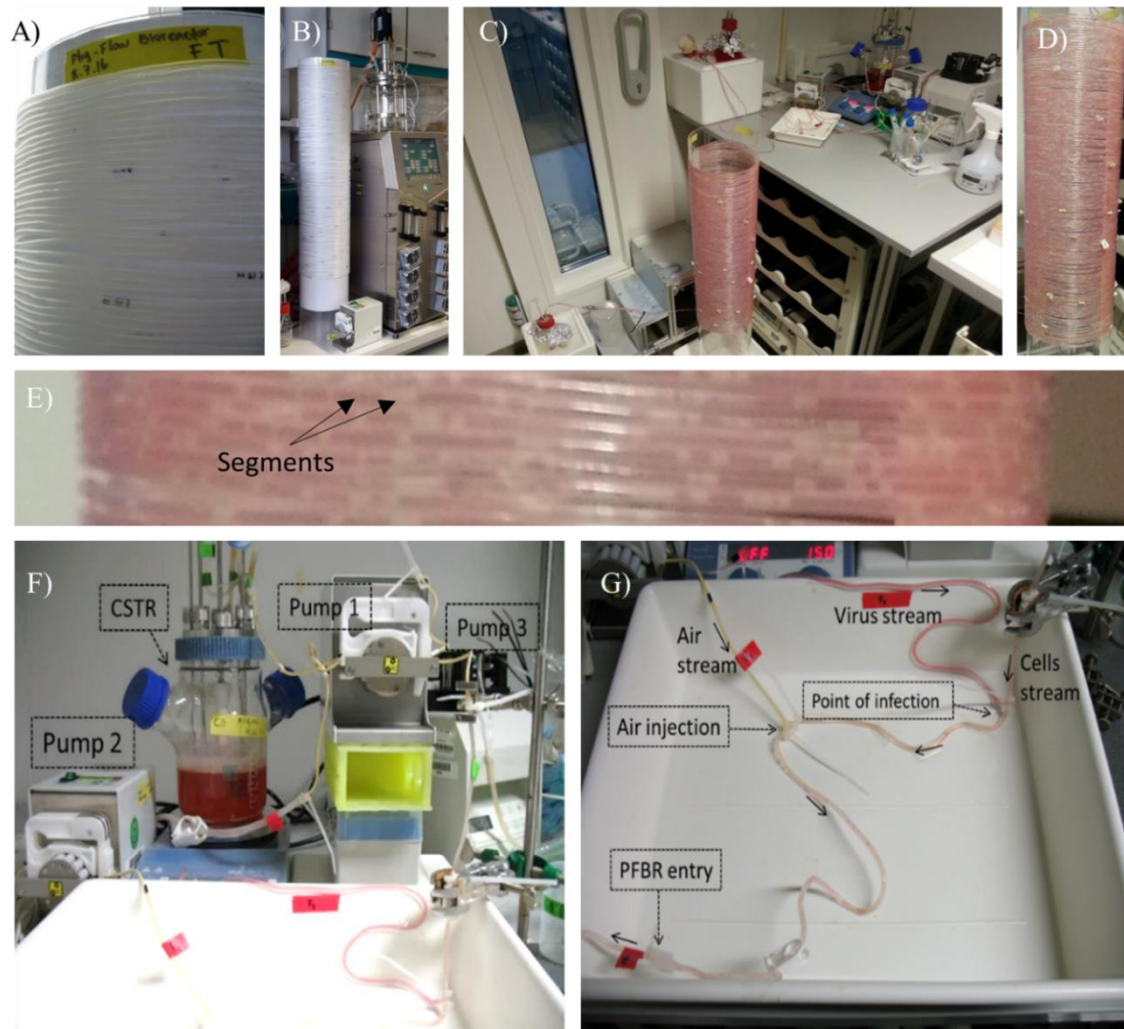


Figure 3. 5. Photographs of the continuous tubular bioreactor system. A) Coiled silicone tube around a scaffold consisting of a 20 cm internal diameter and 1 m high PLEXIGLAS® XT tube. B) Empty PFBR. The tube with a length of about 100 m was coiled from the top to the bottom of the PLEXIGLAS scaffold. C) First functional bioreactor prototype in operation in December 2015 with MDCK.SUS2 cells cultivated in Smif8 medium. D) Lateral picture of the PFBR with culture medium. Different distances along the tube where labeled (white papers). E) Segments of liquid and air inside the PFBR. F) This picture shows the 500 mL cell bioreactor (or CB) with all three pumps used in this prototype. G) Tubing system showing the point of infection, the point of air injection, and the entry point to the PFBR (female/male luer connector).

Table 3. 1. Description of the flow rates, linear velocity and components of each process stream.

Flow	Phase	Liquid Volumetric Flow rate [mL/min] ^a	Gas Volumetric Flow Rate [mL/min] ^a	Linear Velocity [cm/min] ^a	Components	Description
F ₁	liquid	0.15	0.00	ND	Fresh culture medium	Fresh medium transferred to the CSTR
F ₂	liquid	0.15	0.00	ND	Medium + cells	Cell culture taken from the CSTR
F ₃	liquid	0.05	0.00	ND	Medium + virus	Virus from the stock bottle for infection of the cells
F ₄	liquid	0.20	0.00	ND	Medium + cells + virus	Infected cells
F ₅	gas	0.00	0.10	ND	Air	Filtered-air needed for cellular respiration
F ₆	liquid + gas	0.20	0.10	10 ^a	Medium + cells + virus + air	Mixture of cells, virus and bubbles entering the PFBR
F ₇	liquid + gas	0.20	0.09 ^b	9 ^b	Medium + cells + virus + air	Final product after 20 h in the PFBR

ND = not determined; CSTR = continuous stirred tank bioreactor; PFBR = plug-flow tubular bioreactor

^a nominal value obtained from the design of the process.

^b this is an approximate value based on measurements of the time required by the bubbles to travel 10 centimeters at the entry and at the end of the tube. The linear velocity at the end of the tube (F₇) decreased approx. 5-10% with respect to the entry (F₆).

3.6 Process productivity estimations

The productivity of batch, semi-continuous and continuous cultivation systems was determined based on two parameters: time yield (TY, [virions/h]) and space-time yield (STY, [virions/(L×h)]). The following equations were used for all three cultivation modes:

$$TY_{t_n} = \frac{\sum_{t_0}^{t_n} (TCID_{50_{H,t_n}} \times V_{H,t_n})}{t_n} \quad \text{Equation 8}$$

$$STY_{t_n} = \frac{\sum_{t_0}^{t_n} (TCID_{50_{H,t_n}} \times V_{H,t_n})}{\sum_{t_0}^{t_n} (V_{H,t_n}) \times t_n} \quad \text{Equation 9}$$

Where t_n is the total operational time (initial batch phase plus virus production phase for semi-continuous and continuous), $TCID_{50_{H,t_n}}$ is the $TCID_{50}$ of a harvest at time t_n (if no harvest is taken at time t_n its value is zero), and V_{H,t_n} is the harvest volume collected at time t_n . Equations 8 and 9 were also used for estimating the productivity of a hypothetical batch process consisting of two parallel 645 mL bioreactors (8 days batch cycle), as described in section 4.4.1 and Table 4.1. This hypothetical system was chosen as a comparison to the TSB system, because it represents the alternative given up when the decision of operating both vessels in continuous mode is taken

(opportunity cost). Note: equations 8 and 9 are a summation, and can be used for batch, semi-continuous and continuous cultures. In a batch culture, the term V_{H,t_n} is zero except for the selected harvest time point, and the contribution of consecutive batch harvests are added up. In semi-continuous and continuous cultures, the term V_{H,t_n} has always a value (given by the harvest flow rate multiplied by $(t_n - t_{n-1})$).

3.7 Analytics

3.7.1 Influenza virus

Hemagglutinin assay

The total amount of influenza viruses produced was quantified by titration of viral hemagglutinin as described previously [149]. HA was converted to virions/mL, assuming the binding of one virus particle per red blood cell. Therefore, the concentration of red blood cells was set to 2×10^7 cells/mL. The maximum standard deviation for the reported HA values was $\pm 0.2 \log_{10}$ (HA Units/100 μ L) [150].

Tissue culture infectious dose 50 titration assays

The concentration of infectious influenza viruses was determined by tissue culture infectious dose fifty (TCID₅₀, virions/mL) as described by Genzel and Reichl [151]. The dilution error of the TCID₅₀ assay was $\pm 0.3 \log_{10}$ [150].

3.7.2 Modified Vaccinia Ankara virus

Tissue culture infectious dose 50 assay

The concentration of infectious virus particles was quantified by a TCID₅₀ assay as described previously [147]. The relative standard deviation of the assay was $0.4 \log_{10}$ [111].

Green fluorescent-derived TCID₅₀

In addition to the regular TCID₅₀ staining procedure, a GFP-derived TCID₅₀ titer was obtained by measuring cell fluorescence using a fluorescence microscope (λ 495 nm, Axio Observer A1, Zeiss, Germany). The assay was carried out immediately before performing the regular TCID₅₀ staining procedure. Fluorescent cells were identified until the last positive well, and the calculation was carried out using the same methodology as used for the regular TCID₅₀.

3.7.3 Cell concentration and viability

Concentration and viability of the avian cell line AGE1.CR.pIX and the canine cell line MDCK.SUS2 were determined with the ViCell™ XR cell viability analyzer (Beckman Coulter GmbH, Germany) with a standard deviation of 6% according to the manufacturer. The sample volume required by the device was in a range between 0.5-1.0 mL. The avian cell line grows as single cell suspensions and therefore direct measurement of a crude sample was possible. The MDCK.SUS2 cell grew as agglomerates, and therefore a “de-agglomeration step” was necessary before ViCell™ XR analysis. This step was carried out by collecting and centrifuging 1000 µL of culture at 1000 RPM for 30 s, then 950 µL of supernatant was removed, and 450 µL of 500 U/mL trypsin was added. The sample was stored at 37°C for 10 min. Finally, 500 µL of serum was added to stop trypsin activity.

3.7.4 Extracellular metabolites

Culture samples of 1 mL were taken to determine glucose, lactate, glutamine, glutamate, and ammonia concentrations using a BioProfile 100 Plus Nova analyzer (Nova Biomedical, United States). The relative standard deviations of the assays were 1.9% for glucose, and 10.5% for lactate. Ammonium, glutamate and glutamine were also measured are not considered in the following (values are available in the experimental data sheet).

3.7.5 Stability of Modified Vaccinia Ankara virus

The stability of MVA-CR19 virus was evaluated using the MVA-CR19.GFP recombinant strain using two criteria. The first criterion was that, if the recombinant virus is stable, then the ratio of the total infectious virus population (IVP) to the protein-expressing infectious virus population (PEIVP) should be constant during cultivation time. The PEIVP was measured by determining a GFP-derived TCID₅₀ by fluorescence microscopy (described in section 3.7.2). This ratio was determined with the following equation:

$$\text{Ratio}_{TCID50} = \frac{\text{IVP}}{\text{PEIVP}} \quad \text{Equation 10}$$

With IVP and PEIVP the mean of a technical triplicate. The second criterion used was a genetic analysis of the GFP insertion cassette using a polymerase chain reaction (PCR) protocol (described in detail in section 3.7.6). The samples analyzed with both criteria were taken from the first and last harvest of two SSC cultivations operated over 15.5 days, one with 25 h RT in the SVB and a second with 40 h RT in the SVB.

3.7.6 Polymerase chain reaction for evaluation of Modified Vaccinia Ankara virus stability

A polymerase chain reaction (PCR) assay for MVA virus was performed by ProBioGen (Berlin, Germany). The PCR was carried out by mixing the complete cell lysate (80 µL) with 20 µL of QuickExtract DNA Extraction Solution 1.0 (Epicentre, United States) and heated to 65°C for 10 min and to 98°C for 5 min. Of this preparation, 4 µL were subjected to PCR in a final volume of 20 µL with 0.15 µL Taq polymerase (Qiagen, Germany), 200 nM of each primer, and 125 µM of each nucleotide. The sequence of the primer pairs that span deletion sites 2, 3 and 4 of the viral genome have been published previously [9]. The expected sizes of the amplification products are 354, 447, and 502 bp for wildtype virus deletion sites 2 to 4, and 1285 for deletion site 3 in MVA-CR19.GFP. Thermocycling was initiated with 94°C for 80 s, followed by 35 cycles of 94°C for 20 s, 55°C for 20 s and 72°C for 90 s, and terminated with 72°C for 5 min. Amplicons were separated by electrophoreses in 1.5 % agarose gels.

3.7.7 Segment-specific PCR for determination of defective interfering influenza virus particles

A segment-specific PCR for qualitative determination of DIPs accumulation was carried out based on a method previously described [26]. The method used eight primer pairs. Crude culture samples were taken and stored at -80 °C. After thawing, the samples were centrifuged for 5 min at 1000 g. Viral RNA was purified from 150 µL supernatant using the extraction kit NucleoSpin RNA Virus (Macherey-Nagel, Düren, Germany). The method utilizes the Unit2 primer for performing reverse transcription [152]. The initial denaturation step was carried out at 98°C for 3 min followed by 25 cycles with 98°C for 25 s, 60°C (or 55°C for segment 6) for 45 s and 72 °C for 1-2 min. The final elongation was carried out at 72°C for 10 min. Gel electrophoresis was used to visualize the PCR products.

3.7.8 Software for data analysis

The results of this work were analyzed using Microsoft Excel. Graphs with numerical powers in base 10 are shown in Microsoft Excel format. For example, 1.0×10^8 is shown as 1E + 08 in a graph.

Chapter 4

Results & Discussion

Considering the different options for MVA virus and IAV production used in this work, the following chapter was divided in four parts starting with virus production in batch mode to finally present the results of the continuous production experiments. The first section describes batch production of MVA virus and IAV to identify maximum virus titers and yields. The chapter continues with the description of semi-continuous MVA virus and IAV production in shake flasks as a small-scale approach of cascades of two CSTRs (referred as TSB system). These systems helped to elucidate process performance for long term cultivations including the possible impact of DIP formation. The third section describes the two continuous production systems established in this work – a TSB system for continuous MVA virus production, and a PFBR system for continuous IAV production. Maximum viral titers yields and virus genetic stability over cultivation time are analyzed for each continuous production system. The last part summarizes the results obtained and compares the productivity of the various bioreactor systems.

The MVA virus results presented in this chapter have been already published in [23]. Also, most of the IAV results have been submitted for publication [153] and some results are available as a patent application [154].

4.1 Virus production in batch mode

Batch culture is the most common approach for production of cell culture-derived MVA virus and IAV. For this reason, batch cultures of MVA virus and IAV were carried out in order to elucidate cell and virus dynamics and to determine maximum virus titers. From a mathematical point of view, batch cultures are closed systems with zero dilution rate, which allows obtaining higher product concentrations compared to continuous cultures. Hence, the virus titers obtained from batch experiments serve as a reference to evaluate the performance of the continuous cultures established in this work. In the following, batch production of MVA virus and IAV using only the avian cell line AGE1.CR.pIX cell is presented. IAV production in suspension MDCK cells was not evaluated because literature with this cell line is already available [148].

4.1.1 Batch production of Modified Vaccinia Ankara virus in AGE1.CR.pIX cells

Cell concentration, pH and metabolites. Three batch cultures of MVA virus (BM-A, -B, and -C) at 50 mL scale were initiated with an approximate pH of 7.5 (Figure 4.1 A), and the pH dropped below 7.0 after 72 h of culture. Cells grew in batch mode up to 5.0×10^6 cells/mL, and a 50% dilution step led to a final cell concentration of 2.5×10^6 cells/mL at time of infection, as shown in Figure 4.1 B. A glucose and lactate concentrations near 27 and 10 mM, respectively, were obtained at the starting point of the infection phase (Figure 4.1 C). The lower lactate concentration of one of the cultures was due to a higher dilution step needed to adjust the cells to 2.5×10^6 cells/mL.

MVA virus production. MVA-CR19 virus strain was used for infection at MOI of 0.05 and maximum TCID₅₀ titers of 3.0×10^8 , 1.0×10^8 and 0.3×10^8 virions/mL were obtained at 72 h p.i., as shown in Figure 4.1. Interestingly, a maximum TCID₅₀ titer of 1.0×10^9 virions/mL was obtained 96 h p.i. in the BM-A experiment. This higher TCID₅₀ titer in BM-A was correlated with a greater number of viable cells in the culture, due to a higher dilution step with fresh medium carried out at the time of infection. MVA virus titers obtained in these batch experiments are similar to those previously described for MVA wild type replicated in AGE1.CR and AGE1.CR.pIX cells [18].

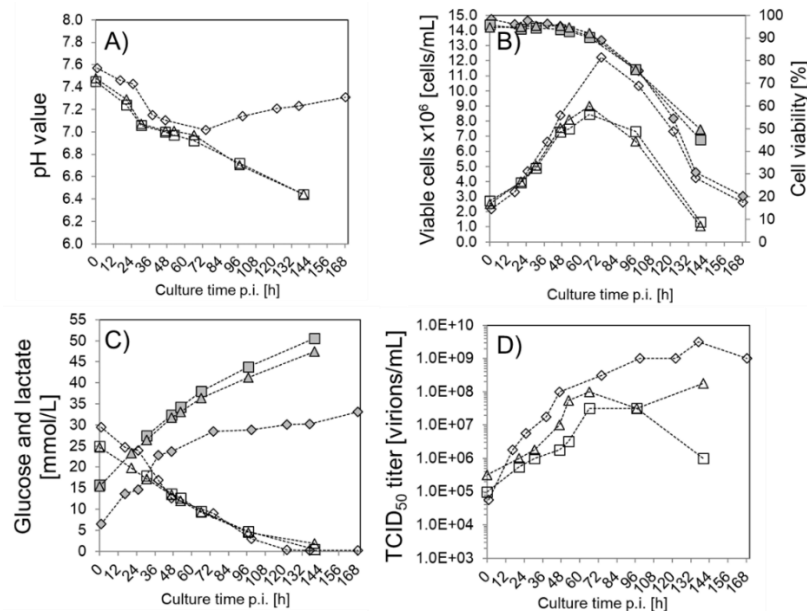


Figure 4. 1. MVA virus replication in batch cultures of AGE1.CR.pIX cells. Three batch experiments named BM-A (diamonds), BM-B (triangles) and BM-C (squares) were compared. A) pH values of the batch culture. B) Viable cell concentration (open symbols) and cell viability (closed symbols) of batch cultures. C) Glucose (open symbols) and lactate (closed symbols). D) Infectious virus titer TCID₅₀.

Questions such as the scalability of these batch results to larger bioreactor volumes might arise as all three experiments were performed in 50 mL shaker flasks. In this work, the new genotype MVA-CR19 virus, that can efficiently replicate in single-cells and does not require cell agglomeration at the time of infection, was used [9]. Also, the initial batch phase of the continuous experiment with cascades of CSTRs (Figure 4.5 D) demonstrated that cell growth in batch mode up to 5×10^6 cells/mL in 1 L bioreactors was possible. Hence, obtaining similar virus titers at larger volumes should be feasible.

4.1.2 Batch production of influenza A virus in AGE1.CR.pIX cells

Cell concentration, pH and metabolites. Two experiments at 50 mL scale (as for MVA virus) were carried out. The average pH at 0 h p.i. was 7.3 and the final pH value at 20 h p.i. was 7.1 (Figure 4.2 A). The viable cell concentration obtained at time of infection was 4.5×10^6 cells/mL with a viability of 94% (Figure 4.2 B), while 3.6×10^6 viable cells/mL with 73% viability were obtained at 20 h p.i. Glucose concentrations of 19.6 and 12.5 mmol/L were obtained between 0 and 20 h p.i., respectively, and lactate concentration between 10.4 and 19 mmol/L were obtained between 0 and 20 h p.i., respectively (Figure 4.2 C).

IAV virus production. HA titers between 2.1 and 2.3 \log_{10} (HA Units/100 μ L) were obtained between 19 and 25 h p.i. in both cultivations, as shown in Figure 4.2 D. Also, maximum TCID₅₀ titers between 1×10^8 and 3×10^9 virions/mL were obtained between 19 and 25 h p.i., as depicted in Figure 4.2 E. Such high TCID₅₀ titers compared to relatively low HA titers are typical for AGE1.CR.pIX cells [155]. Finally, the time course of MOI of the batch cultivation was also determined using the TCID₅₀ titers and viable cell densities. The average MOI at 0 h p.i. was 0.0056, while at 20 h p.i. was 224. Such high MOI conditions were observed by Frensing et al. [26] in continuous mode and were associated with the accumulation of DIPs.

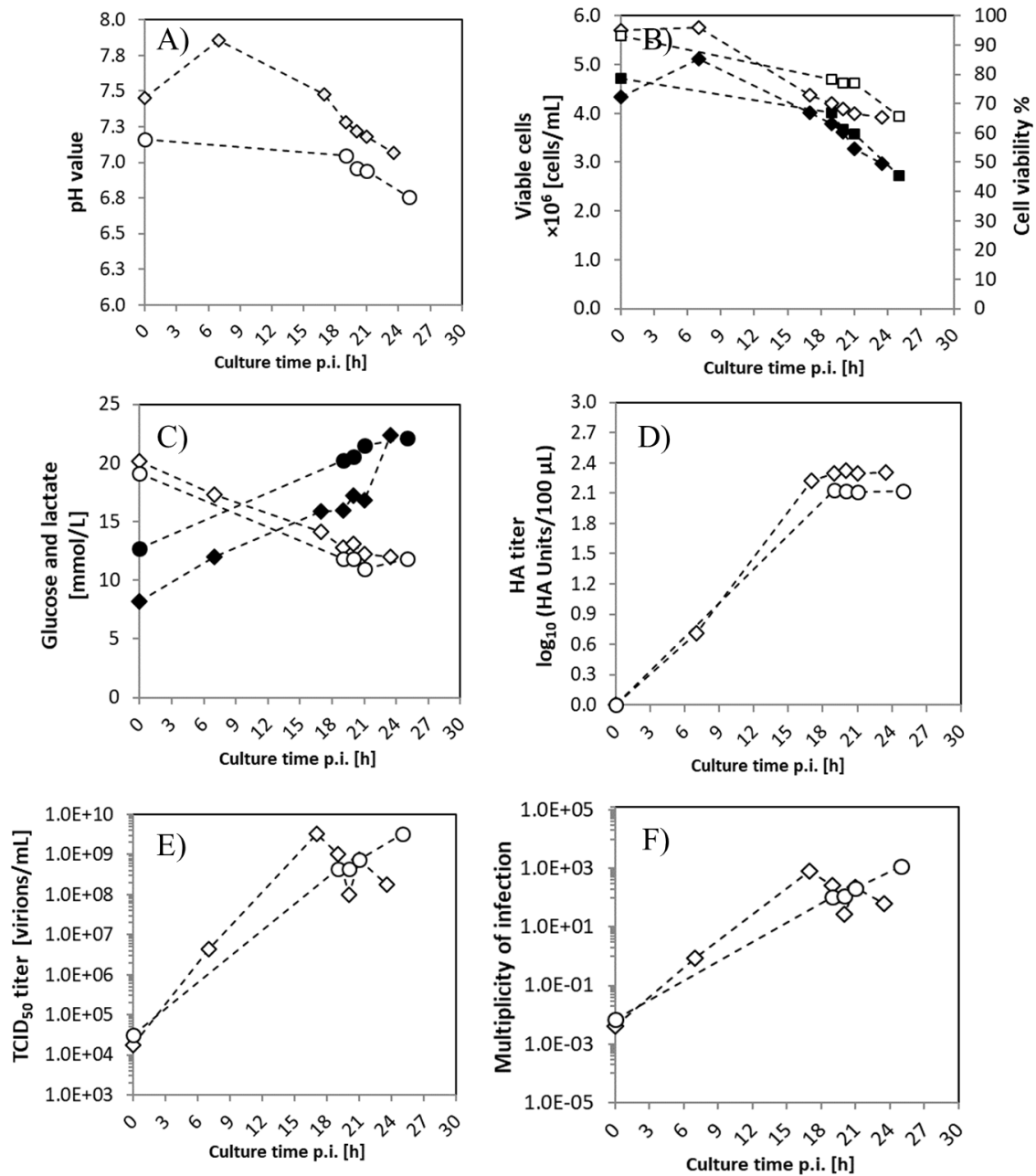


Figure 4. 2. Influenza virus replication in batch cultures of AGE1.CR.pIX cells. Two batch experiments named batch 1 (diamonds) and batch 2 (circles) were carried out. Samples at 0, 7, 17, 19, 20, 21, 22 and 24 h post infection (p.i.) were taken. A) pH value of batch 1 and batch 2. B) Viable cell concentration (black) and viability (white) of AGE1.CR.pIX cells. C) Glucose (white) and lactate (black) concentration in mmol/L. D) HA titer of batch 1 and 2. E) TCID₅₀ titers. F) Estimated MOI for batch conditions performed with corresponding viable cell concentration and TCID₅₀.

4.2 Virus production in semi-continuous mode

Semi-continuous cultures using shake flasks, or SSC system, were established as a small-scale approach of the cascade of the TSB system. The SSC system provided a fast setup for evaluation of several experiments in parallel. Cell and virus dynamics, maximum virus titers, presence of DIP-induced oscillations and genetic stability of viruses were determined with the SSC system. Therefore, the following section starts with the results of SSC experiments for production of MVA virus in avian AGE1.CR.pIX cells. MVA virus dynamics at different RT in the virus-infected vessel is evaluated. Then, IAV production was evaluated in avian AGE1.CR.pIX cells and in MDCK.SUS2 cells to determine viral titers.

The SSC system was also used to analyze genetic stability of a GFP-containing MVA virus strain and of IAV in long term cultures. However, to facilitate the comparison with long-term continuous cultures, these results are presented in section 4.3.2 and 4.3.7 for MVA virus and IAV, respectively.

4.2.1 Semi-continuous production of Modified Vaccinia Ankara virus in AGE1.CR.pIX cells

AGE1.CR.pIX cell growth. A SSC system in shaker flasks was established for propagation of AGE1.CR.pIX cells and MVA virus up to 15 days of cultivation. To start up the cultivation, AGE1.CR.pIX cells were seeded at a concentration of 0.8×10^6 cells/mL in SCB and SVB and maintained in batch mode for 3-4 days. The results of one representative cultivation (SM25-A of Table 4.1) is shown in Figure 4.3 A, B and C. After the initial batch phase, medium replacements at regular intervals were initiated and a semi-continuous steady state was successfully maintained during at least two weeks of cultivation. Viable cell concentrations in SCB fluctuated in a range of $8-12 \times 10^6$ cells/mL with viabilities above 90% (Figure 4.3 B). In SVB cell concentrations first also fluctuated in a similar range, but then fluctuations decreased as a consequence of virus replication. Cell viabilities of 90% or more were observed the first days but dropped after several days in semi-continuous mode. No limitation of glucose was observed during SSC cultivations and levels of lactate in steady state were diluted below the 30 mmol/L obtained at the 4th day of the initial batch phase.

Table 4. 1. Overview of MVA process parameters, virus titers and productivity obtained in batch, semi-continuous, and continuous experiments.

Experiment ^a	Cell Passage Number	Cell Conc. at toi [$\times 10^6$ cells/mL] ⁱ	Medium Manufacturer	Virus	Dilution rates; F_3 ^b	RT in SVB or VB [h] ^c	Volume SVB or VB [mL]	Days of Operation [d] ^d	Maximum Virus Titer [virions/mL]	Total Number of Virions Produced [virions] ^e	Total Harvest Volume [mL]	Time Yield [virions/h]	Space-time Yield [virions/(L h)]
BM-A	82	3.2	Biochrom	MVA-CR19	B	72	50	8.0	3E+08	2E+10	50	8.2E+07	1.6E+09
BM-B	41	2.5	Merck/Biochrom	MVA-CR19	B	72	50	8.0	1E+08	5E+09	50	2.6E+07	5.2E+08
BM-C	41	2.7	Merck/Biochrom	MVA-CR19	B	72	50	8.0	3E+07	2E+09	50	8.2E+06	1.6E+08
BM-average ^f	-	-	Merck/Biochrom	MVA-CR19	B	72	50	8.0	1E+08	7E+09	50	3.6E+07	7.3E+08
2 Parallel batches ^g	-	-	Merck/Biochrom	MVA-CR19	B	72	1290	17.0	1E+08	4E+11	2580	8.9E+08	3.4E+08
2 Parallel batches ^h	-	-	Merck/Biochrom	MVA-CR19	B	72	1290	26.0	1E+08	5E+11	3870	8.7E+08	2.2E+08
SM25-A	50	10.5	Biochrom	MVA-CR19	3-D ₁ = D ₂ ; F ₃ = F ₃	25	65	22.0	2E+09	2E+11	1136	3.7E+08	3.3E+08
SM25-B	90	12.9	Biochrom	MVA-CR19	3-D ₁ = D ₂ ; F ₃ = F ₃	25	65	22.0	2E+09	5E+11	1004	1.0E+09	1.0E+09
SM25-MOCK	82	-	Biochrom	MOCK	3-D ₁ = D ₂ ; F ₃ = F ₃	25	65	18.0	MOCK	MOCK	726	MOCK	MOCK
SM35-A	73	12.1	Biochrom	MVA-CR19	2-D ₁ = D ₂ ; F ₃ = F ₃	35	98	12.0	3E+08	2E+10	816	7.6E+07	9.3E+07
SM35-B	40	7.47	Merck/Biochrom	MVA-CR19	2-D ₁ = D ₂ ; F ₃ = F ₃	35	98	19.0	1E+09	2E+11	1157	4.1E+08	3.6E+08
SM35-C	40	4.42	Merck/Biochrom	MVA-CR19	2-D ₁ = D ₂ ; F ₃ = 0	35	65	18.0	3E+05	3E+07	649	7.4E+04	1.1E+05
SM64	73	11.8	Biochrom	MVA-CR19	1-D ₁ = D ₂ ; F ₃ = F ₃	64	198	12.0	6E+08	6E+10	1084	2.0E+08	1.8E+08
SG25	69	5.72	Merck/Biochrom	MVA-CR19.GFP	3-D ₁ = D ₂ ; F ₃ = F ₃	25	62	19.5	1E+08	3E+10	1148	6.0E+07	5.2E+07
SG40	69	6.01	Merck/Biochrom	MVA-CR19.GFP	2-D ₁ = D ₂ ; F ₃ = F ₃	40	120	19.5	6E+09	5E+11	1208	1.0E+09	8.7E+08
T25	50	9.19	PAA	MVA-CR19	3 D ₁ = D ₂ ; F ₃ = F ₃	25	440	21.7	6E+08	6E+11	7100	1.2E+09	1.7E+08

^a T= Two-stage continuous bioreactor; S=semi-continuous small scale cultivation; B=Batch; M=MVA-CR19 strain; G= MVA-CR19.GFP strain; XX = XX hours (25 h,35 h or 64 h) of residence time in the VB or the SVB.

^b $F_3 = D_1 (V_2 + V_1) - F_1$ with D_1 the dilution rate of CB or SCB, V , the volume of each vessel, and F , the flow rate.

^c RT = residence time; VB = Virus Bioreactor; the value shown for batch cultures corresponds to the harvest time (h p.i.).

^d considering a batch with 4 days of cell growth in all processes, 3 days of virus production and 1 day for cleaning and sterilization.

^e this value corresponds to the total number of virions produced after adding the virus collected from each harvests. This was calculated by multiplying the TCID₅₀ of each harvest by its volume.

^f the average TCID₅₀ titer of batch A, B and C was estimated to be 1×10^8 virions/mL

^g two parallel 645 mL batch bioreactors; calculations were carried out assuming 2 batch-cycles, because it approaches the operational time of the SSC cultivations (2 weeks). Note: the TY is valid only for a specific cultivation scale, while the STY is independent of the cultivation scale. The complete time course of such a process is shown in Figure 6.

^h two parallel 645 mL batch bioreactors; calculations were carried out assuming 3 cycles (26 d), because it approaches the operational time of the TSB experiment (T25; 3 weeks). The complete time course of such a process is shown in Figure 6.

ⁱ cell concentration at time of infection.

A semi-continuous steady-state production of AGE1.CR.pIX cells was successfully maintained over two weeks of cultivation. Hence, it was important to determine μ_{\max} during the batch phase (0.02 h^{-1}), which was slightly higher than in the batch phase of 1 L scale TSB cultivations (0.016 h^{-1}). Also, the sampling before and after the medium exchanges resulted in reductions of WV that made it difficult reaching a steady state. Accordingly, taking a sample only before the medium exchange was the preferred option in most of the experiments.

Also, a drop in cell viability in SVB was observed in all cultivations after some days p.i. This was a consequence of virus replication and, interestingly, was observed from day 10 p.i. in SM25-A experiment, and from day 4 p.i. in SM25-B (both experiments were operated at the same RT; cell viability data of SM25-B is not shown). Most likely, the reason for the delayed viability drop of SM25-A was a dilution of the virus concentration below 1×10^5 virions/mL after the first harvest.

MVA virus production in semi-continuous mode. SVB was infected with MVA virus after 3-4 days of batch cell growth and the semi-continuous mode with harvesting was started 12 h p.i. Virus titers showed 8-10 days of a transient phase followed by a stationary phase. TCID₅₀ values between $1 \cdot 10^7$ and 1×10^9 virions/mL, were obtained among all SSC experiments.

Virus titers obtained from the SSC showed a transient and a stationary phase. TCID₅₀ values between 1×10^7 and 1×10^9 virions/mL were obtained and were in accordance with those of batch cultivations, described in section 4.1.1, and also comparable to those of published data [18] [9]. Also, an important result that was first observed in this small-scale system was that virus titers in the stationary phase oscillated in order of magnitudes not larger than $2 \log_{10}$ which is clearly less than what was observed previously for IAV [26]. These oscillations were most likely produced by errors in the MVA virus titration assay and by variations in the cell concentration in SVB. This suggested that MVA virus can be produced in continuous mode without interference by defective particles.

Two experiments were operated at 25 h RT in SVB. Virus titers from SM25-A followed a similar pattern to the TSB system from day 4 p.i. onwards, reaching similar final titers. The second experiment, SM25-B (white squares, Figure 4.3 D), was more precisely operated and the virus titer dynamics was even closer to those obtained with the TSB system (operated also at 25 h RT in VB, as shown later in section 4.3.1). Therefore, these two experiments suggested that the SSC can serve as a scale down model of the TSB system. Previous works have demonstrated that semi-continuous cultivations can be very reliable to approximate continuous cultures [156]. More recently, mammalian cell kinetics in continuous systems was studied using semi-continuous

cultures in shake flasks [157]. Thus, the cell growth and MVA virus titer results showed that these concepts could be also applied for TSB systems using shaker flasks.

Impact of RT and addition of fresh medium in MVA virus titers. Three SSC experiments with 25, 35 and 64 h RT in SVB were carried out as shown in Figure 4.3 D. TCID₅₀ titers obtained with all RT experiments showed a common pattern consisting of an initial transient phase followed by a stationary phase. The MOI of 0.05, used in all experiments, led to initial virus concentrations close to 1.0×10^5 virions/mL. The fastest increase in virus titers was obtained with 25 h RT in SVB (experiment SM25-B) with approx. 1×10^8 virions/mL at 48 h p.i. Similar virus titers were obtained with 35 and 64 h RT in SVB but at 144-192 h p.i. (SM35-B and SM64 experiments, respectively).

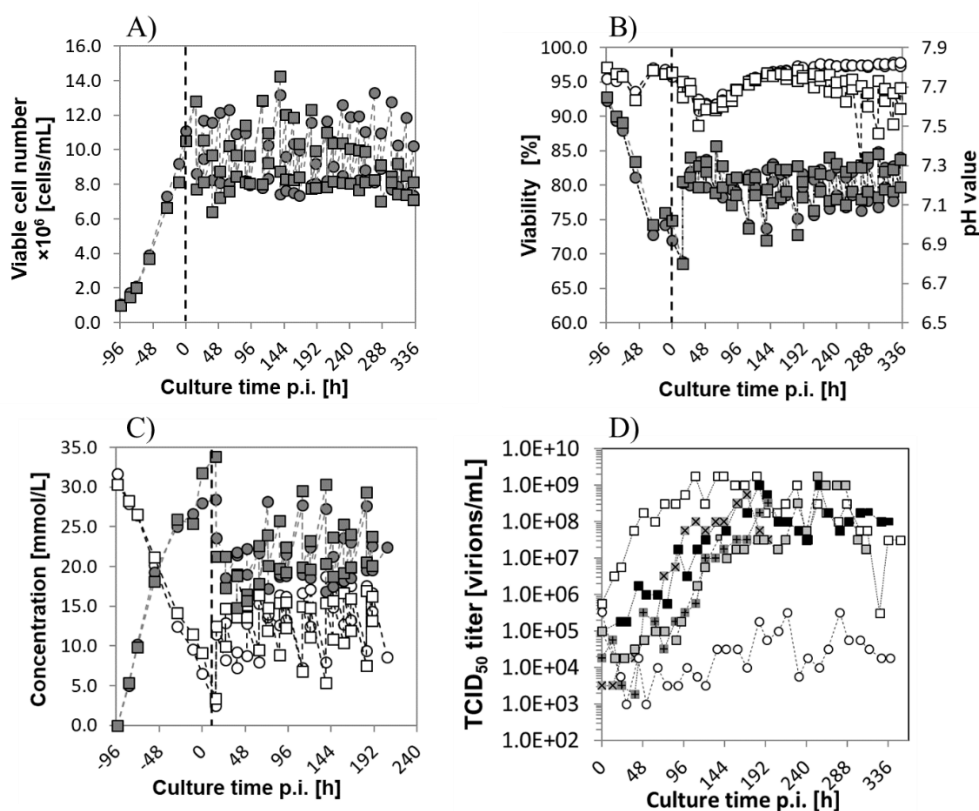


Figure 4. 3. Semi-continuous propagation of MVA-CR19 virus in a two-stage cultivation system using shaker flasks (SSC). The data of A), B) and C) belong to one representative SSC experiment of a total of nine experiments with variations in RT and medium addition in SVB (SM25-A, Table 4.2). A) Viable AGE1.CR.pIX cells concentration in SCB (circles) and SVB (squares). B) Viability (white) and pH value (grey) of SCB (circles) and SVB (squares). C) Concentration of glucose (white) and lactate (grey) in SCB (circles) and SVB (squares). D) MVA TCID₅₀ titers of the SSC experiments (squares) SM25-A (grey), SM25-B (white), SM35-A (grey with +), SM35-B (black), and SM64 (grey with X). One SSC experiment, SM35-C, was carried out without addition of fresh medium into SVB (white-circles). The dashed line represents the time of infection. The first harvest was carried out 8-12 h p.i..

In addition, one experiment was carried out to determine the impact of removing V_3 from SVB (SM35-C). As shown in Figure 4.3 D, this experiment resulted in the lowest virus titers among all experiments, with values not exceeding 1×10^5 virions/mL.

Although 35 and 64 h RT showed comparable titers, 64 h RT would not be a good option for scale-up as long RTs might end up in culture conditions with low levels of glucose and high lactate and ammonia that are clearly not beneficial for both cell and virus propagation. Interestingly, TCID₅₀ titers at steady state were very similar for different RT experiments and therefore, the TCID₅₀ seems to be independent of the RT.

Finally, one experiment was performed to investigate the impact of removing the addition (V_3) of fresh medium on the virus titers (SM35-C, Table 4.1; Figure 4.3 D). The idea of this experiment was to test if the productivity can be increased by keeping virus titers, while decreasing medium consumption. Surprisingly, the lowest TCID₅₀ titers were obtained from this experiment, with values between 1×10^3 and 1×10^5 virions/mL. Therefore, addition of fresh medium in the virus bioreactor is an important process variable to keep yields. This is in agreement with previous studies that showed that addition of fresh medium at time of infection is required for optimal virus propagation [158]. Adding fresh medium might play a role on diluting and faster washing-out of signaling molecules and metabolites that are not beneficial for cell growth, metabolism and, therefore, virus replication.

4.2.2 Semi-continuous production of influenza A virus in MDCK.SUS2 cells and in AGE1.CR.pIX cells

Influenza virus was propagated in semi-continuous mode using the MDCK.SUS2 and AGE1.CR.pIX cells. The shakers were maintained at 37°C and with agitation of 185 RPM for two or three weeks. The dilution rate used for both cell lines was $0.83 \times \mu_{\max}$, as described by Frensing et al. [26].

Cell growth. The MDCK.SUS2 cell line was maintained at stable concentrations over two weeks (Figure 4.4 A). Cells in the SCB shaker grew up to 4×10^6 cells/mL in batch mode and the average cell concentration in semi-continuous mode was 2×10^6 cell/mL. Similar concentrations were obtained in the SVB in batch and semi-continuous mode, with an oscillation in the cell concentration between 0.9×10^6 and 1.6×10^6 cells/mL that peaked at 192 and 336 h p.i. (days 8 and 14 p.i., respectively). The viability in SCB was maintained stable and above 95% over the cultivation period (Figure 4.4 B). Also, the viability in the SVB vessel oscillated between 87% and 95% with peaks at 192 and 336 h. HA titers with values up to $2.7 \log_{10}$ (HA Units/100 μ L)

were obtained with the MDCK.SUS2 cell line. HA titers oscillated between values of 0.0 and 2.7 \log_{10} (HA Units/100 μ L) with an oscillation period of about 240 h (10 days) approximately.

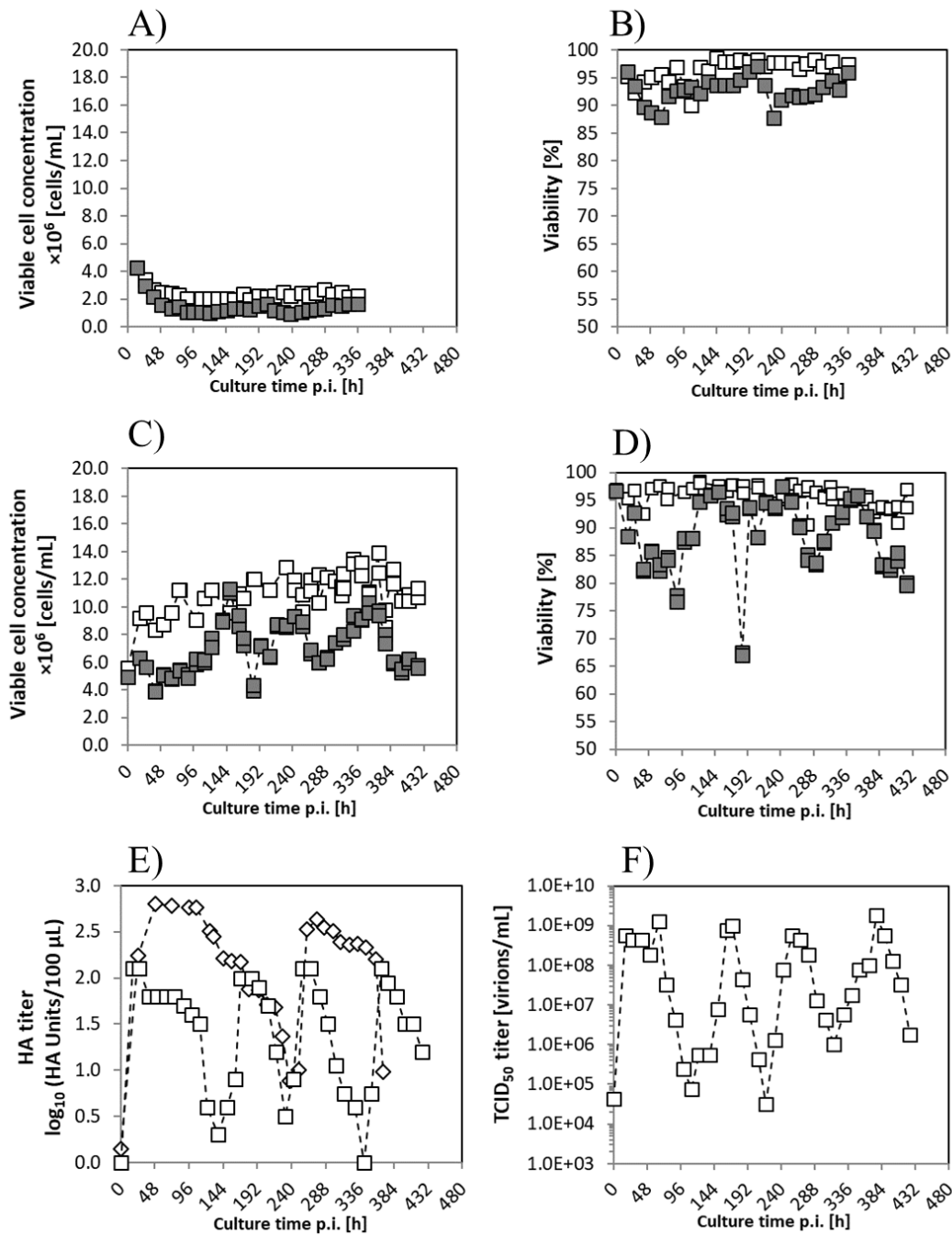


Figure 4. 4. Semi-continuous two-stage stirred cultivation of influenza virus using shaker flasks. Influenza virus was cultivated either in MDCK.SUS2 cells or AGE1.CR.pIX cells for two or three weeks, respectively. A) Viable MDCK.SUS2 cell concentration in the SCB shaker (white) and in the SVB shaker (grey). B) Viability of MDCK.SUS2 cells in the SCB shaker (white) and in the SVB shaker (grey). C) Viable AGE1.CR.pIX cell concentration in the SCB shaker (white) and in the SVB shaker (grey). D) Viability of AGE1.CR.pIX cells in the S-CB shaker (white) and in the S-VB shaker (grey). E) HA titers of the MDCK.SUS2 culture (diamonds) or AGE1.CR.pIX (squares). F) TCID₅₀ titers of the AGE1.CR.pIX culture. All cultures were infected with a MOI of 0.025.

The AGE1.CR.pIX cell line was grown in batch mode until 5.6×10^6 cells/mL before the infection in SVB (Figure 4.4 C). The first medium exchange was carried out 12 h p.i. and an average cell concentration of 11×10^6 cells/mL was obtained in the SCB vessel after three weeks of cultivation. Cell concentrations in the SVB oscillated between 4×10^6 and 11×10^6 cells/ml with peaks at 144, 264 and 360 h p.i.. The viability of AGE1.CR.pIX cells was maintained above 95% in the SCB and oscillated between 67% and 97% in SVB (Figure 4.4 D).

IAV production in semi-continuous mode. HA titers oscillated between a maximum HA value of $2.1 \log_{10}$ (HA Units/100 μ L) at 24 h p.i. and as low as $0.0 \log_{10}$ (HA Units/100 μ L) at 336 h p.i. (Figure 4.4 E), with peaks at 24, 168, 264 and 360 h p.i. TCID₅₀ oscillated in a similar dynamics as HA titers. Maximum TCID₅₀ titers of 1.3×10^9 virions/ml were obtained 72 h p.i., while a titer of 3.2×10^4 virions/mL was obtained at 216 h p.i. The TCID₅₀ peaks were identified at 24, 168, 264, and 360 h p.i.

4.3 Virus production in continuous mode

In this work a total of three continuous bioreactor setups were tested, however, only two of them showed successful results. One bioreactor system, the cascade of CSTRs with recirculation, failed in its operation and control and only preliminary results are presented. The other two systems – the TSB system and the PFBR – were successfully implemented and used to produce MVA virus and IAV, respectively.

Hence, the following section starts with continuous production of MVA virus in a TSB system. Cell growth, pH values, metabolite concentrations and virus titers are presented. Subsequently, the genetic stability of a GFP-containing MVA virus (referred to as MVA-CR19.GFP) is analyzed in long term cultures. The section continues with the preliminary results obtained for a cascade of CSTRs with recirculation that failed. The section concludes with continuous IAV production using a PFBR system and with two cell lines. The genetic stability of IAV produced with the PFBR system is evaluated using PCR and compared with IAV produced in batch and semi-continuous cultures.

4.3.1 Continuous production of Modified Vaccinia Ankara virus in AGE1.CR.pIX cells in a two-stage stirred tank bioreactor system

AGE1.CR.pIX cell growth. The TSB system was successfully operated for 720 h (30 days) in continuous mode, as shown in Figure 4.5 (abbreviated as T25 in Table 4.1). During the startup of the process, cell concentration in CB reached values of 5.0×10^6 cells/mL in batch operation with cell viabilities well above 85% (Figure 4.5 A and B). With the experimental data, a μ_{\max} of

0.0150 h⁻¹ was determined, in order to adjust the dilution rate to $0.83 \times \mu_{\max}$ as previously described for AGE1.CR cells. At this time, almost half of the volume of CB was transferred to the second vessel and a concentration of almost 2.5×10^6 cells/mL was reached in both vessels by diluting 1:1 with fresh medium. Two hours later, the pumps were started and the continuous process was maintained without infection of VB for the next 192 h (8 days), in order to observe the cell growth in the second vessel. Surprisingly, cells in VB continued to grow to 9.0×10^6 cells/mL, well above the envisaged 5.0×10^6 cells/mL of CB. During this time, the levels of glucose in VB reached values of 10 mmol/L (Figure 4.5 C), therefore a volume of VB was replaced by fresh medium and the vessel was subsequently infected with MVA-CR19 virus. Right after the infection, cell concentration and viability in VB decreased to 5.0×10^6 cells/mL and 70%, respectively, as to be expected with virus production. Unfortunately, cell concentration and viability in CB also decreased to 3.0×10^6 cells/mL and 85%, respectively, but those values remained constant until the end of the cultivation. A control of pH was almost not required during the whole process due to the addition of fresh medium.

Before starting the continuous experiment, cell viabilities not higher than 85% were observed in shaker flasks when using the CD-U3 powder medium (produced by PAA; available in large quantities) but not with the liquid CD-U3 medium (produced by Biochrom; only few liters available). For this reason, the initial batch phase of T25 experiment was planned with a 1:1 mixture of the powder-based and the liquid CD-U3 medium. This allowed to obtain 5.0×10^6 cells/mL in the initial batch phase with viabilities over 90%. This cell viability and concentration were in accordance with previous data [18]. Continuous culture was started after 72 h and AGE1.CR.pIX could be maintained for 648 h (27 days) in continuous culture (with addition of some cells at 360 h p.i. (15 days p.i.)). Once the continuous culture was started, cell viabilities in CB dropped to values around 85% as a consequence of using only powder medium. Despite of that, cells could be maintained stable at these viabilities for the rest of the experiment. These issues with cell growth and viability were solved after this experiment using the liquid CD-U3 medium (Biochrom) only. Therefore, growing AGE1.CR.pIX in the TSB system was feasible, and cell viabilities can be improved with the latest versions of liquid CD-U3 medium.

One interesting result was that cells in VB accumulated up to 9×10^6 cells/mL during the 192 h of continuous phase without infection (-168 to 0 h p.i., Figure 4.5 A). This cell concentration was higher than estimated based on a mathematical model described by Frensing & Heldt et al. 2013 [26] for a TSB system (not shown). In contrast, this model predicts that viable cell concentration in VB should not exceed that of the CB ($\sim 5 \times 10^6$ cells/mL) at steady-state in the absence of virus. One might speculate that in our TSB system without infection the AGE1.CR.pIX cells adapted to this specific medium. As a result, the μ_{\max} in VB was higher than CB (the model

assumed to have the same μ_{\max} in both bioreactors). In addition, the addition of fresh medium in VB could have resulted in an environment different from CB that stimulated an increase in μ_{\max} . If this was true, μ_{\max} in those 192 h was 9.6 times higher than μ_{\max} at normal growth conditions (cell concentrations increased from 4.6 to 8.5×10^6 cells/mL in 27 h, between -72 and -45.6 h p.i., Figure 4.5 A). A more plausible explanation is a phenomenon previously described by Batt et al. 1990 [159] for separation of death from viable hybridoma cells. In that case, the dip tube of VB, used to extract the harvest, might have acted as a settler with a relatively low flow rate and high internal diameter (0.26 mL/min and 4 mm, respectively). Clearly, to improve the understanding of the dynamics of a TSB system (with addition of fresh medium in the second vessel) for cultivation of animal cells would require further investigations [20, 125].

MVA virus production. MVA-CR19 virus was inoculated and an initial TCID₅₀ of almost 1.0×10^5 virions/mL was obtained (Figure 4.5 D). After 72 h of continuous culture, the TCID₅₀ reached values close to 1.0×10^8 virions/mL and MVA production was maintained stable for 432 h (18 days). A total of 6.0×10^{11} virions were collected from the harvest, with a total production volume of 7.1 L. This corresponds to an average TCID₅₀ of 9.0×10^7 virions/mL (calculated from T25 experiment data shown in Table 4.1). The STY and the TY were estimated to 1.8×10^8 virions/(L h) and 1.2×10^9 virions/h, respectively.

MVA production was over 432 h with TCID₅₀ titers up to 1×10^8 virions/mL, very similar to batch cultivations [18]. Most importantly, virus titers fluctuated in a range not larger than 1 log. Fluctuations in the virus levels and low virus yield as consequence of DIPs accumulation has been described for continuous and semi-continuous baculovirus cultivations [126, 136], and with up to 6 logs decrease in TCID₅₀ titers for continuous IAV production [26]. Previous studies have shown that defective viruses are also present within poxvirus populations [90, 89], but to our knowledge, interfering properties of these defective viruses have not been described. Therefore, the stable MVA virus titers observed, suggest that fluctuations might be due to variations in cell concentrations in VB over production time and the TCID₅₀-assay error. This is in line with previous experiments that showed stability of MVA virus titers for up to 20 serial passages [9]. Hence, DIPs accumulation seems not to be a limitation for continuous production of MVA virus for three weeks of continuous production.

In Figure 4.5 D, the TCID₅₀ of VB and the harvest is depicted. Note that, while the TCID₅₀ of VB represents the virus concentration in the vessel at a given time, the TCID₅₀ of the harvest represents the value that results from accumulating the production over a range of 8-12 h. During this period, MVA virus could be inactivated by host cell enzymes released to the supernatant, or might get diluted by fluctuations in the virus titer. Thus, the slightly lower TCID₅₀ titers obtained

in the harvest compared to VB might be closer to the real TCID₅₀ that will be obtained in a continuous process with a harvest vessel.

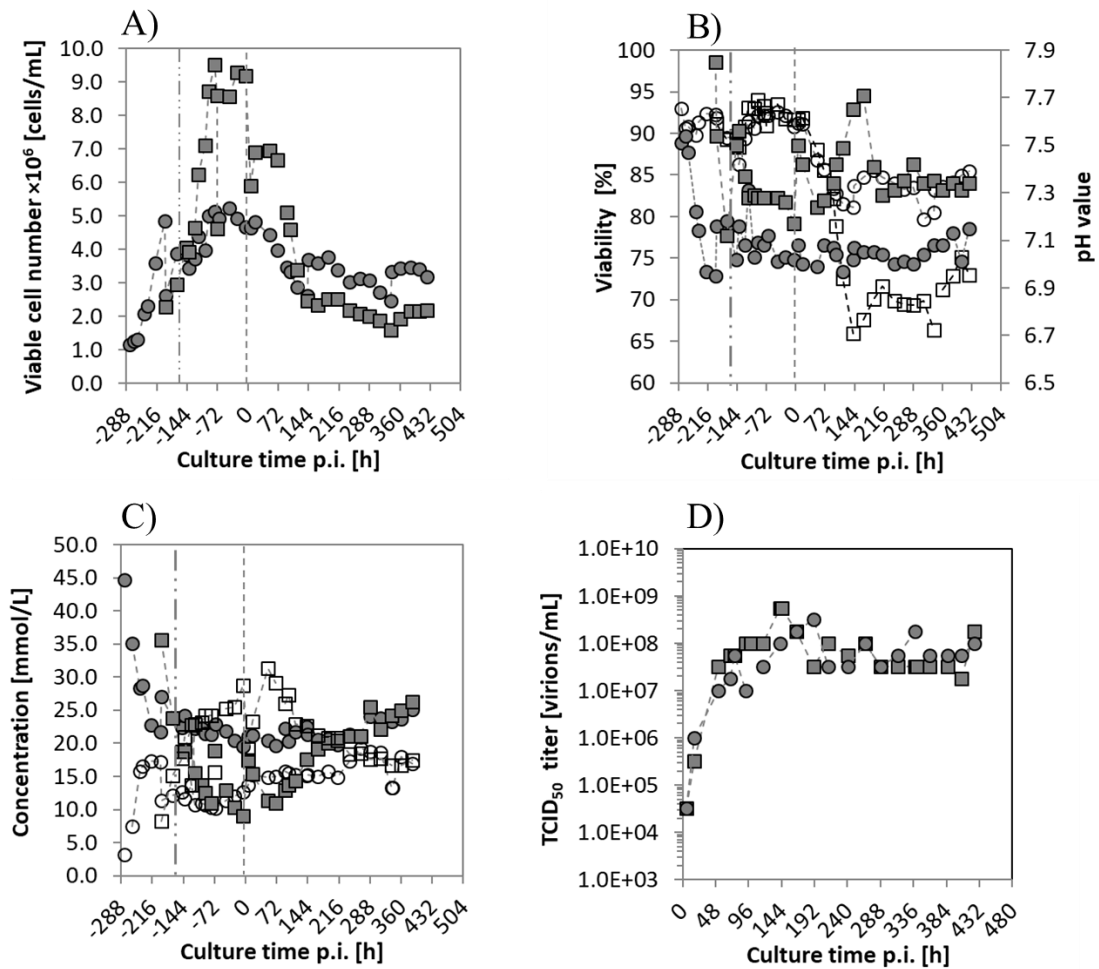


Figure 4.5. Continuous cultivation of MVA-CR19 virus in a two-stage stirred tank bioreactor system (TSB system). A) Viable cell concentration in CB (circles) and in VB (squares). B) Cell viability (white) and pH (grey) of CB (circles) and VB (squares). C) Concentration of glucose (grey) and lactate (white) in CB (circles) and VB (squares). D) TCID₅₀ titers of MVA-CR19 virus in VB (squares) and in the harvest (circles). The dotted-dashed vertical line at -168 h p.i. represents the start of the continuous culture in both vessels. The dashed line at 0 h p.i. represents the time of infection of VB.

4.3.2 Genetic stability of MVA virus in long-term cultures

The MVA-CR19.GFP virus strain was continuously passed over 360 h p.i. (15 days p.i.) in the SSC system. This recombinant virus holds a green fluorescent protein expression cassette whose level of expression can be evaluated over time. The GFP-derived TCID₅₀ was determined over cultivation time and plotted against the TCID₅₀, as depicted in Figure 4.6 A (25 h RT experiment, referred to as SG25) and Figure 4.6 D (40 h RT experiment, referred to as SG40). In both RT experiments, the GFP-derived TCID₅₀ titer (green) was similar to the TCID₅₀ titer (red) until the end of the cultivation time.

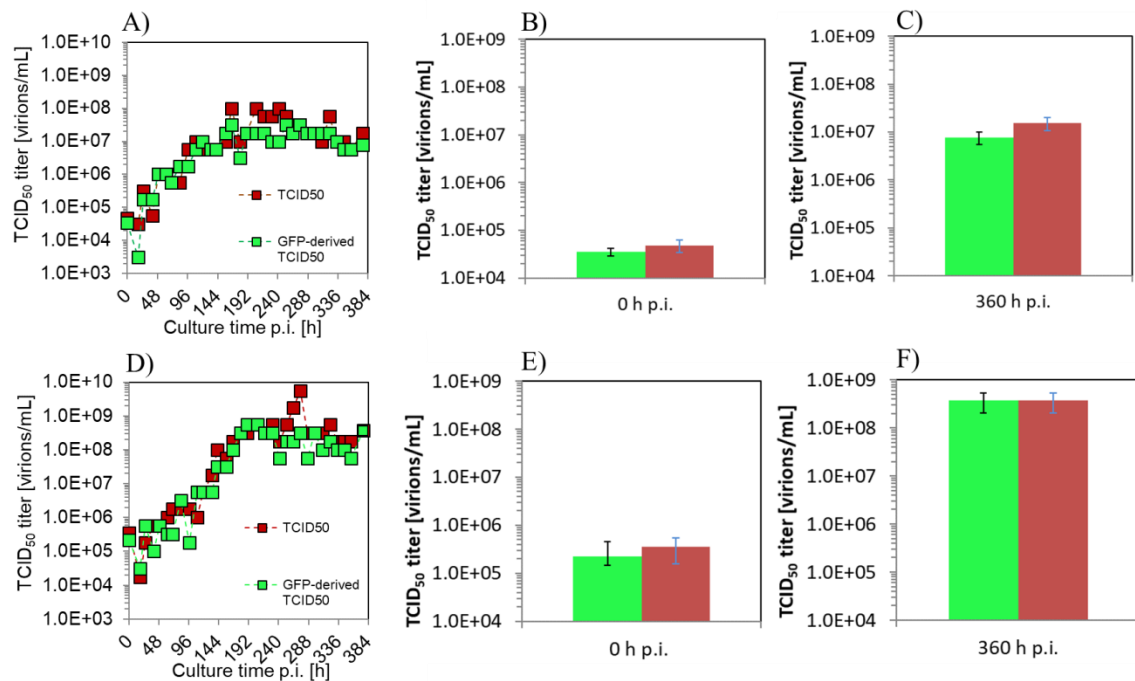


Figure 4. 6. Stability analysis of MVA-CR19.GFP virus in 360 h of semi-continuous cultivation. Two different RT in SVB were analyzed. Figures A, B and C correspond to experiment SG25 (25 h RT in SVB) and figures D, E, and F to experiment SG40 (40 h RT in SVB). A) TCID₅₀ (red) and GFP-derived TCID₅₀ (green). B) TCID₅₀ (red) and GFP-derived TCID₅₀ (green) at 0 h p.i. C) TCID₅₀ (red) and GFP-derived TCID₅₀ (green) at 360 h p.i. D) TCID₅₀ (red) and GFP-derived TCID₅₀ (green). E) TCID₅₀ (red) and GFP-derived TCID₅₀ (green) at 0 h p.i. F) TCID₅₀ (red) and GFP-derived TCID₅₀ (green) at 360 h p.i. G) PCR analysis of the deletion segments 2, 3, 4, 5 and 6 (Del 2-6) of MVA-CR19.GFP virus, and DNA ladder in the range of 100-2000 bp (M). The first and last harvest of experiments SG25 (two boxes on the left side) and SG40 (two boxes on the right side) were analyzed.

The TCID₅₀-ratio was calculated using Equation 10 and was used to analyze the first and last harvest sample. In the 25 h RT experiment, a TCID₅₀-ratio of 1.4 was obtained for the first harvest (Figure 4.6 B), while a ratio of 2.0 was calculated for the last harvest (Figure 4.6 C). Similarly, the ratio of the first and last harvest of the 40 h RT experiment were 1.6 and 1.0, respectively

(Figure 4.6 E and F). Therefore, based in the TCID₅₀-ratios and the overlapping standard deviations, the MVA-CR19.GFP virus was stable over 360 h of cultivation.

Furthermore, the almost 1 log higher TCID₅₀ titer obtained at 360 h p.i with the 40 h RT experiment, compared to the 25 h RT (Figure 4.6 C and F), suggest that the RT of choice to scale up an MVA-CR19.GFP production process would be 40 h and not 25 h. Interestingly, this significant difference in final virus titers and yields at different RTs was not observed using the MVA-CR19 virus (section 4.2.1). One explanation could be a reduction of the virus replication capacity after insertion of the GFP cassette.

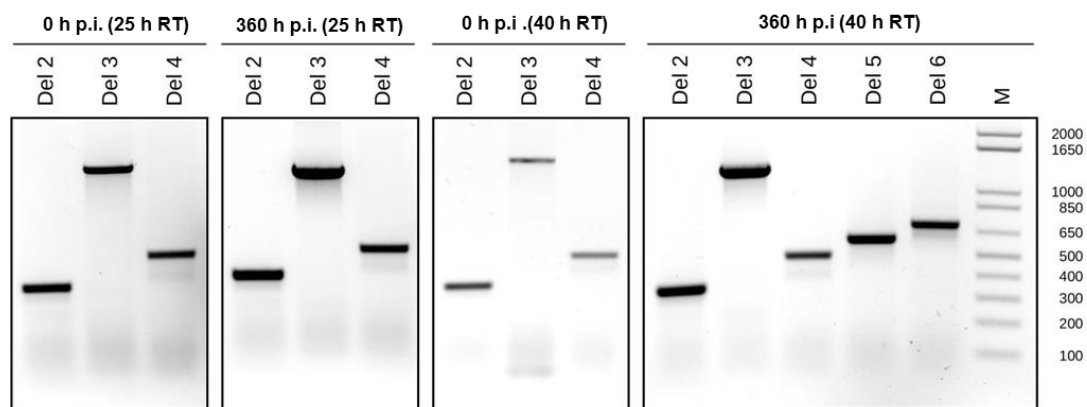


Figure 4. 7. PCR stability analysis of MVA virus in 360 h of semi-continuous cultivation with two different RT in SVB. The figure shows the PCR analysis of the deletion segments 2, 3, 4, 5 and 6 (Del 2-6) of MVA-CR19.GFP virus, and DNA ladder in the range of 100-2000 bp (M). The first and last harvest of experiments SG25 (two boxes on the left side, 25 h RT in SVB) and SG40 (two boxes on the right side, 40 h RT in VB) were analyzed.

The stability of the MVA-CR19.GFP recombinant virus was also analyzed using PCR for the first and last harvest of both SSC cultivations. For both RT experiments, the GFP insertion cassette amplified by this method was visible in the deletion segment 3 (Del 3) of the first (0 h p.i.) and last harvest (360 h p.i.) with a size of 1428 kbp (Figure 4.7). This result indicated that MVA virus was stable over two weeks at least in the GFP insertion cassette.

Note that deletion segment 3 of the wild type MVA virus (without a GFP insertion) has a size of 447 bp (Figure 4.7). For both RT experiments, a 1285 bp band was visible in the first and last harvests (0 and 360 h p.i, respectively). This segment was generated by adding the GFP insertion cassette over the 447 bp of deletion segment 3. Hence, the presence of this band in the first and last harvest was an indication of MVA stability. Moreover, smaller-size bands are not observed in deletion segment 3 (Del 3) after 360 h of culture, which suggests that, over cultivation time, reversion of segment 3 into its original size (447 bp) was not performed by the virus. These results support the hypothesis that MVA virus is stable at least in the GFP insertion cassette over 360 h

of cultivation. Important is to note that this result does not answer how stable the virus is in other sections of the genome, but at least the selected insertion region seems to be stable and is therefore a good candidate for generation of other recombinant MVA virus strains.

4.3.3 Continuous production of influenza A virus in AGE1.CR.pIX cells in a cascade of CSTRs with recirculation

A total of five cultivations were carried out to test the hypothesis that a cascade of CSTRs with recirculation would result in stable influenza virus titers. The experiment were named Tubular 1 until Tubular 5). To do that, a small-scale bioreactor system was constructed.

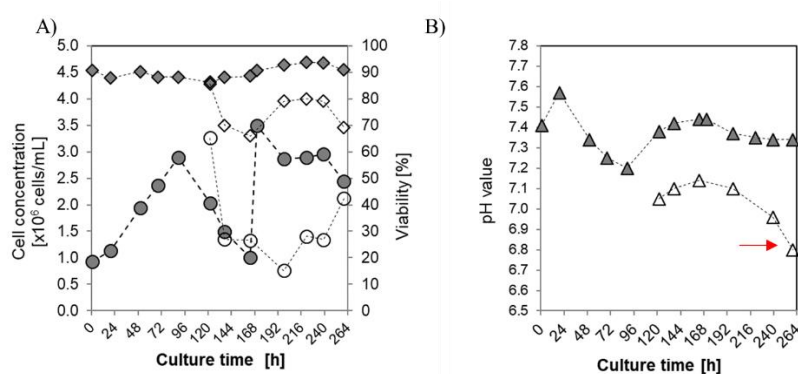


Figure 4. 8. Results of one representative cascade of CSTRs with recirculation (Tubular 5). A) Cell growth (circles) and viability (diamonds) of CB (closed symbols) and VB (open symbols). B) pH value of CB (closed) and VB (open). The red arrow indicates a drop of pH to values below 6.8.

AGE1.CR.pIX cells were seeded into CB at 1×10^6 cells/ml and allowed to grow in batch mode before starting the continuous culture. Four bioreactor cultivations without infection were carried out until cells concentrations of about 4×10^6 cells/ml and viabilities above 90% were achieved. This was achieved in the initial batch phase and maintained once the continuous cultivation was started. However, cell sedimentation was a common problem that occurred at the glass-tube presumably due to poor mixing and a larger tube internal diameter compared to the PFBR. The sedimentation was partially solved by incorporating a recirculation into the bioreactor that sucked and transferred cells to the sedimentation point. This recirculation line is shown in Figure 3.4 B where it is isolated with alumina foil.

In experiment named Tubular 5, the VB bioreactor was infected at 120 h of culture. Cells grew to 3×10^6 cells/ml when a decrease in cell concentration was observed to 1×10^6 cells/ml, as shown in Figure 4.8 A at 168 h of culture. This drop was due to cell sedimentation in the glass-tube. However, recirculation at the sedimentation point was increased and the cell concentration in the CB was recovered to almost 3.5×10^6 cells/ml at 168 h of culture (few minutes after the previous

sample). Nevertheless, sedimentation did not influence cell viability in CB which was stable above 90%. Cell concentration in VB was started with 3.3×10^6 cells/ml and then decreased to 0.8×10^6 cells/ml at 198 h of culture. Cell viability in VB decreased to 66% 48 h p.i. as expected from virus propagation. Despite these promising results, the pH in VB decreased to values below 6.8 at 264 h of culture which is known to generate conformational changes in the HA protein that lead to virus inactivation [160]. For this reason, the bioreactor was stopped at 264 h of culture. Samples of the VB bioreactor for HA and TCID₅₀ titration were taken but finally not analyzed.

Despite the construction of this prototype and the good cell growth observed, the approach was abandoned after Tubular 5four due to the impossibility to manually control pH in the virus bioreactor. The option of constructing this bioreactor in a 1 L benchtop bioreactor could have easily solved the issues here described. However, this was not done during this doctoral thesis because the efforts regarding continuous IAV production were concentrated in the development of a tubular reactor with complete propagation of IAV along the tube.

Finally, a promising first result regarding cascades of CSTRs with recirculation was obtained from a mathematical model developed by Markus Rammhold in his master thesis [161]. That model showed that, for certain process conditions, the HA titer of a cascade of CSTRs with recirculation can be maintained stable over weeks. Therefore, a cascade of CSTRs with recirculation is still a potential bioreactor platform that could be used for continuous propagation of influenza virus and to perform virus evolution studies. However, the doubts concerning viral stability and increasing viral passage numbers over cultivation time that cannot be avoided with such bioreactor systems are limitations for using this technology for human vaccine production.

4.3.4 Development of a continuous tubular bioreactor system for influenza A virus production

The following experiments consisted of a CSTR followed by a PFBR in series and is referred to as PFBR system. The main characteristic of this system is that complete virus propagation can occur in the PFBR. The major doubt regarding the feasibility of this system compared to a cascade of CSTR with recirculation was the prolonged RT that cells would need inside the PFBR, the need of oxygen supply at different points of the bioreactor for allowing cell respiration, and the need of a very long tube that could result in a high pressure drop and the risk of cell sedimentation. For these reasons, before the bioreactor was constructed, the oxygen consumption of cells was estimated. For this reason, data available in literature for specific oxygen uptake rates (OUR) was found and considered to be in the range of 3.05×10^{-14} and 6.9×10^{-13} mol/(cell×h) [162] [141] [155]. It is known that the dynamics of a well-mixed PFBR from the input to the output can be represented as a batch process (with the RT of the PFBR equal to the batch operation time) [163].

With this assumption was possible to estimate that in a batch culture with 100% initial oxygen saturation, with a cell concentration of 1×10^6 cells/mL and no oxygen supply, the cells would consume oxygen down to 1% saturation in a time between 0.3 and 6.8 h (data in the supplement). This result suggested that the PFBR would present difficulties in providing oxygen to the cells during a 20 h RT process. However, silicone tubes are used in biotechnology for oxygen exchange due to their porosity [164]. For this reason, and to counteract the lack of oxygen, the design of the PFBR considered using a silicone tube, in addition to incorporating an air injection at the entrance of the PFBR for cellular respiration. Moreover, a rough estimation of the pressure drop inside a 121 m silicone tube using the Darcy-Weisbach equation (laminar regime with $Re \sim 10$), resulted in a pressure drop of 6.8×10^{-6} bar, which indicated that a PFBR of that size is theoretically feasible.

The tubular bioreactor was then constructed and evaluated using water and air to determine fluxes and operational ranges. The peristaltic pump 1 was used to move the F_1 and F_2 (inlet and outlet of the CB, Figure 3.5), and pump 2 was used for the F_3 and F_4 (virus stock and air injection line, respectively). Based on experimental data of influenza HA titers in batch bioreactors [165, 166, 18], the main goal of this prototype was to reach 20 h RT in the tube, which should result in high HA virus titers. Therefore, a correlation between the RPM of pump 2 and the RT inside the PFBR was determined (Figure 4.9). Assuming a minimum linear velocity of 5 cm/min to avoid sedimentation in the tube, this graph shows that the PFBR system can operate in a RT range between 6.7 and 32 h of RT by modifying only the RPM of pump 2. Based in this test with water, such a process showed stable segments of air and water, as well as a linear velocity of 8.4 cm/min (determined by measuring the volume of water pumped out of the PFBR in a given time), which should be sufficient for avoiding sedimentation according to Hu *et al* [138]. Finally, all PFBR experiments were designed with nominal values of RT, MOI, flow, and Re, however, the actual values over time are also reported.

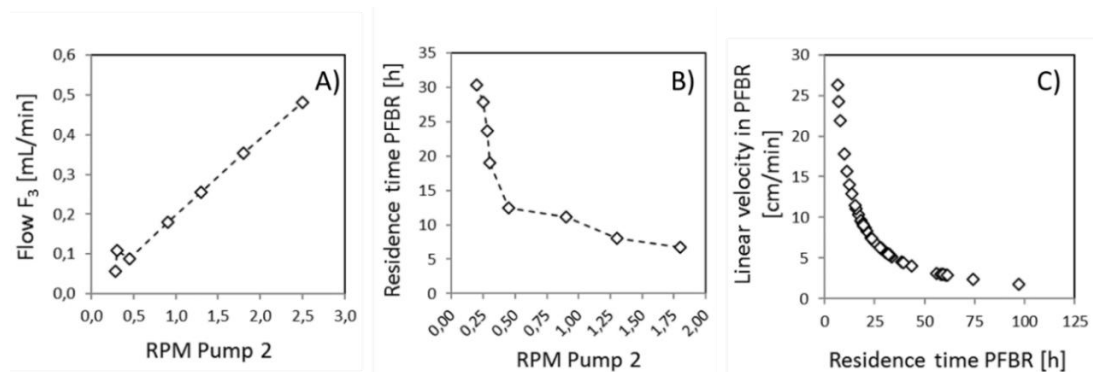


Figure 4. 9. Characterization of the residence time and linear velocity in the PFBR. A) correlation between the RPM of pump 2 and the flow rate of the virus stock (flow F_3). B) Correlation between the RPM of pump 2 and the residence time in the PFBR system.

4.3.5 Continuous production of influenza A virus in MDCK cells in a continuous tubular bioreactor system

MDCK cell growth, flow rates, pH value, Reynolds number and RT. The first functional cultivation with the PFBR system was performed for a total of 552 h (23 days), as shown in Figure 4.10. The bioreactor was primed with PBS and once the plugs in the tube were stable the bioreactor was seeded and infection was started immediately.

Cells were seeded in the bioreactor at 1×10^6 cells/mL, as shown in Figure 4.10 A. The continuous culture was initiated immediately at day 0 of culture, however, cells continued to grow inside the CB. This was due to a lower dilution rate than the previously estimated, despite the pump calibrations performed before starting the culture. The most possible explanation to this behavior is that the flow rate of the CB outlet is lower than the obtained during the calibration because the high back pressure coming from the tubular bioreactor that builds up with the bubbles and the liquid. This error, however, it is a minor issue if cells reach a steady state at later times. Cells were observed leaving the PFBR harvest after 20 h, as expected from the RT. Also, cell viability in the CB was maintained stable above 90% while in the PFBR harvest was fluctuating between 30 and 60% during the cultivation time.

The flow rate and the RT of the tubular bioreactor was maintained stable over time (Figure 4.10 B). However, a small increase in the flow rate was done at 240 h of culture (10 days) that decreased the RT inside the tube. This increase in flow rate was required after a clogging event that happened inside the tube to clean the tube with cell sediments. When continuously monitored and high flow rates are applied, we have seen that the bioreactor can operate over two months without interruption.

Despite the small change in flow rate at 240 h, the Reynolds number was maintained at an average value of around seven during the whole cultivation time and the laminar regime was maintained stable.

Figure 4.10 D shows the virus concentration in the virus stock and also the nominal MOI at the POI. The virus stock concentration was fixed the first 240 h since it was intended to keep stable the infection conditions in the POI. However, and due to the clogging event combined with the fact that cells in the CB grew to higher concentrations than initially expected, the virus concentration in the stock was slightly increased to keep a nominal MOI of 0.02. As a result, the MOI decreased from 0.02 to values below 0.01 at 240 h, to then increase again to values near 0.02 as initially planned for this experiment.

An important aspect of this bioreactor was the pH values, which is shown in Figure 4.10 E. This figure shows that the pH in the virus stock (VS) and in the medium stock (MS) was decreased from values near 7.8 to 7.0 every second day. This was done in order to obtain a pH value close

to 7.1 at the POI. This was carried out because, during the first 96 h of culture, it was observed that the pH at the outlet of the bioreactor was very high with values above 8.0, as shown in Figure 4.10 F. It was believed that this was the reason for the low virus titers the first 144 h (6 days) of culture. Once the pH at the POI was decreased to values close to 7.1, the pH in the PFBR harvest started to decrease as well. This might explain the sudden increase in HA titers that was observed at day 6 of culture, which is discussed in the following (Fig 4.11).

IAV titer in the PFBR harvest. The first tubular bioreactor cultivation was operated during 552 h (23 days), and HA and TCID₅₀ titers were analyzed (Fig 4.11 A and B). During the first 144 h of culture, no HA titers were observed in the tubular bioreactor harvest, and the TCID₅₀ of the harvest was the same as in the virus stock. This indicated that the virus did not replicate inside the tube. Once the right conditions for virus propagation were reached (i.e., right pH value at the POI), an HA titer of approx. $1.6 \log_{10}$ (HA Units/100 μ L) and a TCID₅₀ of 4×10^5 virions/mL were obtained in the tube harvest, which indicated virus replication within the tube. The bioreactor operation was stable until 288 h of culture (12 days), when sedimentation and clogging occurred inside the tube. This was facilitated with the fact that MDCK.SUS2 grow in agglomerates, and later experiments with AGE1.CR.pIX cells (which grows in single cell suspensions [18]) were operated successfully without clogging for up to 8 weeks. Then, the flow rates were increased to washout the cell clump. This led to a RT of 18 h in the PFBR (Figure 4.10 B). To keep the nominal MOI of 0.02, the virus stock concentration was increased to 2×10^5 virions/mL. HA titers of approx. $2.5 \log_{10}$ (HA Units/100 μ L) and a TCID₅₀ up to 1×10^6 virions/mL were obtained in the tube harvest. From 504 h of culture (21 days), the pH of the manually-controlled CB bioreactor decreased from 7.2 to 6.6 (due to overnight failure of the aeration pump), and this led to a drop in the HA titers of the system. The experiment was stopped at this point.

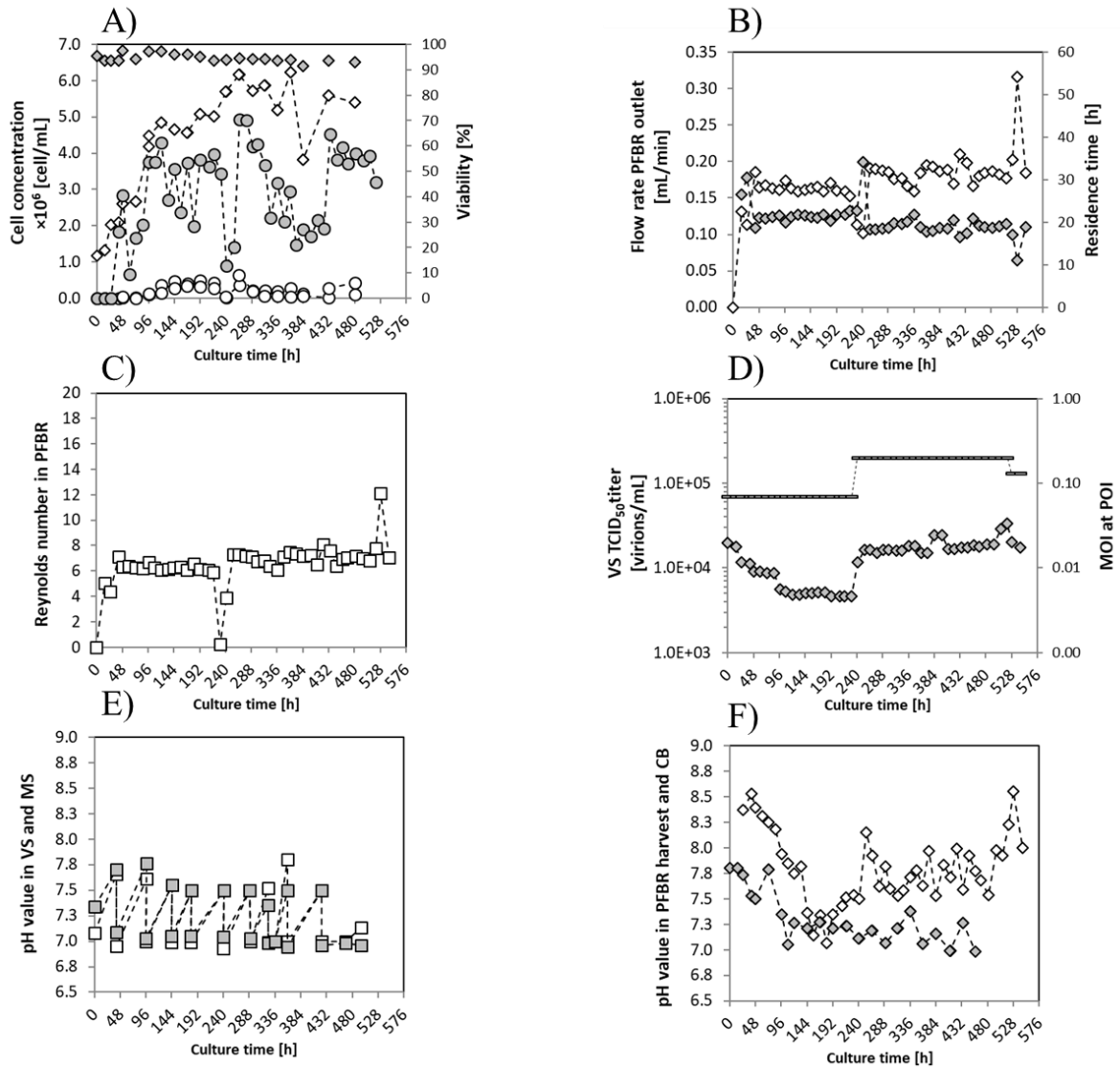


Figure 4. 10. Process variables of the continuous tubular plug-flow bioreactor (PFBR) system operated with suspension MDCK.SUS2 cells. A) Viable cell concentration (white) and viability (grey) in the cell bioreactor (CB) vessel (diamonds) and in the harvest (circles). B) Flow rate at the outlet of the PFBR system (white) and residence time in the PFBR (grey). C) Reynolds number of the fluid inside the PFBR. D) TCID₅₀ of the virus stock (VS, white) and multiplicity of infection (MOI) at the point of infection (POI) (black line). E) pH values in the VS (white) and in the medium stock (MS, grey). F) pH value in the PFBR harvest (white) and in the CB (grey).

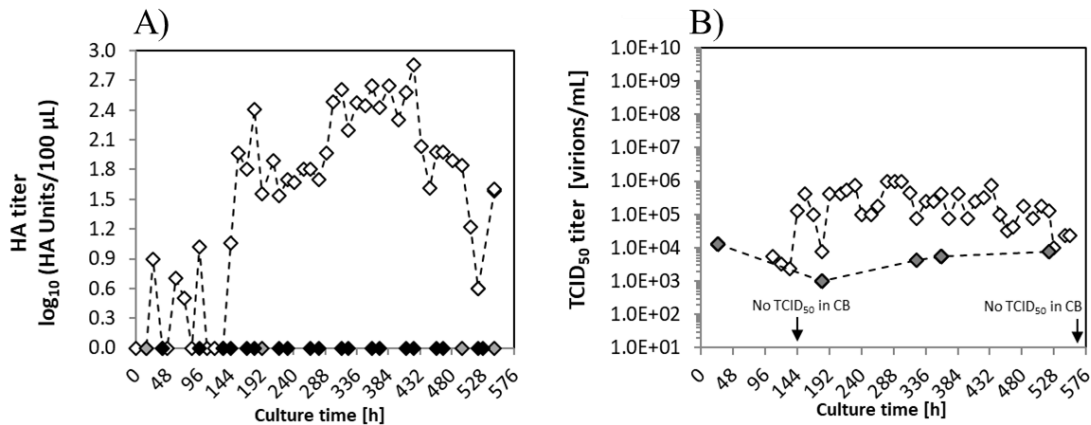


Figure 4. 11. Influenza virus replication in the plug-flow tubular bioreactor system using MDCK.SUS2 cells. A) Hemagglutinin (HA) titer in the harvest (white), in the virus stock (black) and in the cell bioreactor vessel (CB, grey). B) Infectious (TCID₅₀) titer in the harvest (white), in the virus stock (grey) and in the CB (zero value, indicated with arrows).

Impact of different MOIs on IAV production with MDCK.SUS2 cells. To test the hypothesis that higher MOIs in the PFBR system should lead to higher virus production, a three MOI conditions experiment was set. The RT of the PFBR was set to 18 h. MDCK.SUS2 cells were seeded into the CB at 5.0×10^6 cells/mL and cultivated with a dilution rate of $0.9 \times \mu_{\max}$ [154] (Figure 4.12 A). Cells were washed out from the bioreactor and reached a stable concentration of about 1.5×10^6 cells/mL after 120 h of culture. The real MOI at POI was calculated with Equation 5 and is shown plotted in Figure 4.12 A. Starting with low MOI (3×10^{-2}), the TCID₅₀ 0.2×10^6 virions/mL was increased stepwise from 0.7×10^6 virions/mL to 6.2×10^6 virions/mL to achieve MOIs of 0.1 and 3.0, respectively, for a period of 240 h.

Figure 4.12 B shows the HA titer in the harvest and in the virus stock, as well as the TCID₅₀ in the harvest. At low MOI conditions (first 70 h of culture), the HA titer in the PFBR harvest (closed circles) was similar to the HA titer in the virus stock (opened circles) with values around $0.9 \log_{10}$ (HA Units/100 µL). The HA increased up to $1.4 \log_{10}$ (HA Units/100 µL) in the harvest at medium MOI conditions (70 to 150 h of culture), while the HA titer in the virus stock was near $0.7 \log_{10}$ (HA Units/100 µL). The high MOI condition between 150 and 180 h of culture resulted in HA titers of $2.0 \log_{10}$ (HA Units/100 µL), while the virus stock had titers near $1.2 \log_{10}$ (HA Units/100 µL). At the end of the experiment, the MOI was decreased to 0.1 resulting in an HA titer as high as $2.4 \log_{10}$ (HA Units/100 µL) before decreasing to $1.6 \log_{10}$ (HA Units/100 µL).

The results obtained in this MOI experiment showed that the HA titers obtained at the PFBR harvest, under the laminar flow regime established, depend on the MOI in the POI. The concentration of MDCK.SUS2 cells produced by the PFBR system was close to 1.5×10^6 cells/mL, which was at least 2 fold smaller compared to the MDCK.SUS2 concentrations obtained in

previous batch cultivations [148] [167]. Therefore, comparing these results with HA titers of previous publications using MDCK.SUS2 cells would allow to have a reference for future optimizations. While a maximum HA titer of $2.4 \log_{10}$ (HA Units/100 μL) was obtained in the PFBR system at 216 h of culture and 18 h of RT, previous batch experiments have shown HA titers up to $3.0 \log_{10}$ (HA Units/100 μL) at 48 h p.i. [148]. HA titers of $3.7 \log_{10}$ (HA Units/100 μL) in high-cell-density hollow fiber bioreactors have been obtained with MDCK.SUS2 cells at around 72 h p.i., but at cell concentrations close to 4×10^7 cells/mL [119]. The HA titers available in literature for batch cultures are a helpful reference for further optimization of the PFBR system, but differences in infection conditions such as dilution steps at time of infection [167], higher cell concentrations [166], and time p.i. of batch versus RT of the PFBR, have to be considered carefully to avoid misinterpretations. Parameters such as cell-specific virus yields (CSVY), that are commonly used to compare different batch culture processes [16] [148], might have to be calculated differently for a continuous processes. Therefore, in addition to these experiments, a more precise comparison between a batch versus a continuous tubular bioreactor was made for AGE1.CR.pIX cells and will be presented in the following chapters.

The lowest MOI condition was 0.03 and resulted in only 16% of infected cells in the harvest (Figure 4.12 C). In contrast, the medium and high MOI (0.1 and 3.0, respectively) showed almost 100% of infected cells in the harvest. While the low MOI condition resulted only in an HA titer of $0.9 \log_{10}$ (HA Units/100 μL) in the harvest, the medium and high MOI conditions led to 1.5 and $2.0 \log_{10}$ (HA Units/100 μL), respectively. The HA titers obtained at high MOI conditions were similar to batch titers of control experiments (Figure 4.12 D). These experiments indicated that a batch culture at 18 h p.i. had 100% of infected cells with an HA titer of $2.2 \log_{10}$ (HA Units/100 μL). Interestingly, despite that the medium and high MOI conditions had both 100% of infected cells, the medium MOI resulted in a lower HA titer. This suggests that the medium MOI conditions may need more RT in the tube to reach a higher titer. Hence, an infection process carried out in the PFBR system under the actual laminar regime (Reynolds number of 10-50 for this experiment) can infect all the cells at MOIs near 0.1. To reach batch-like titers at MOI of 0.1, however, the RT needs to be increased for at least 5 h to provide more time for virus propagation. For MOIs near 0.03 or less the mixing conditions inside the bioreactor have to be improved by e.g., introducing static-mixers or mechanical mixing (vibrations). Finally, a reduction of DIPs in the virus seed might improve virus propagation and lead to higher HA titers in the tubular bioreactor harvest [33]. Defective segments (possibly DIPs) were observed in the A/Puerto Rico/8/34 (RKI) virus seed used for this experiment and is presented later (Figure 4.16).

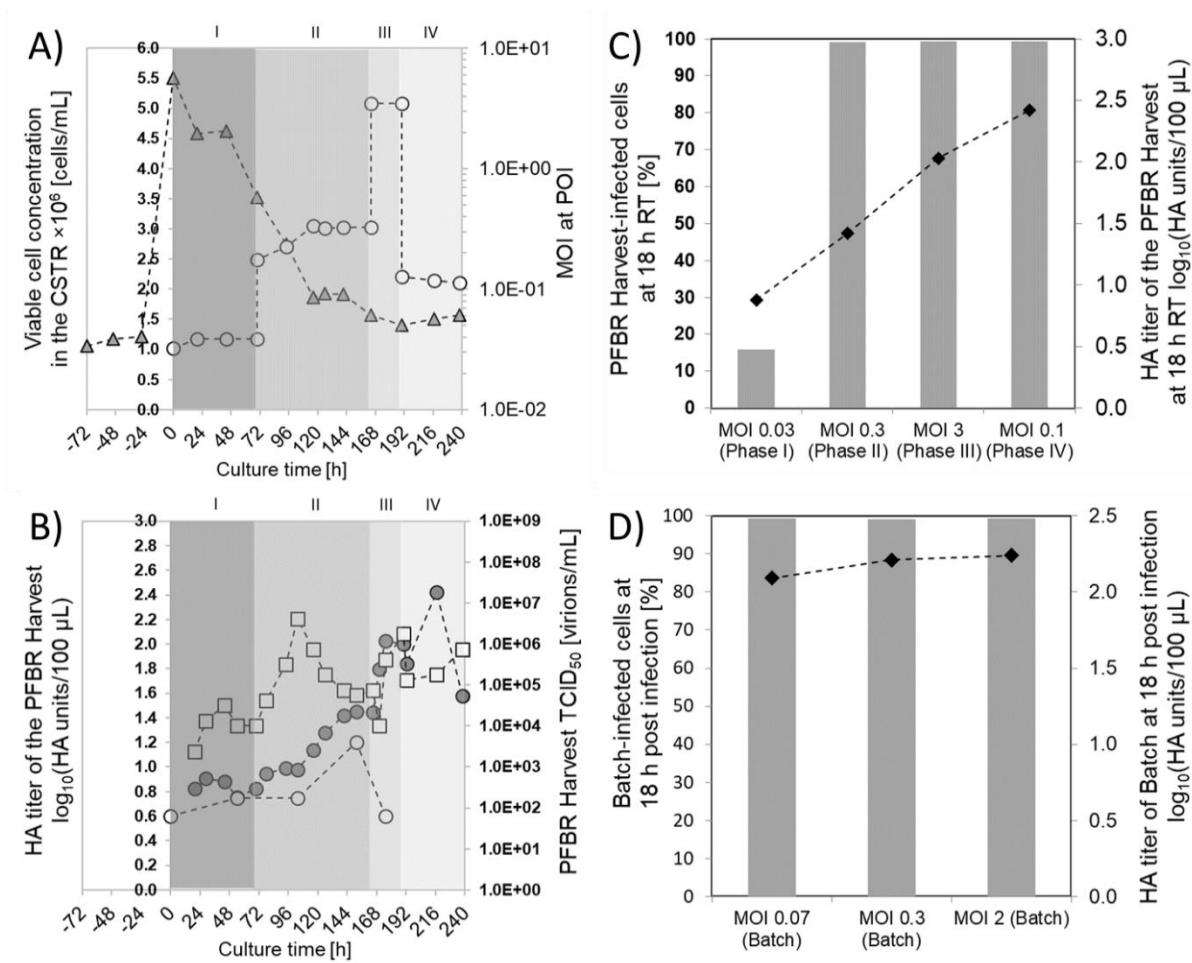


Figure 4. 12. Evaluation of different MOIs in the infection and propagation of influenza A virus (IAV) using MDCK.SUS2 cells in the tubular bioreactor system. The PFBR had a residence time of 18 h. A) Viable cells (triangles) in the CB and MOI at the POI (circles). The different background colors show the three MOI conditions selected which, in chronological order, are referred to as phases I, II, III and IV. The MOI was modified by changing the VS concentration from 0.2×10^6 virions/mL to 0.7×10^6 virions/mL and 6.2×10^6 virions/mL. B) Influenza HA titer in the tubular reactor harvest (closed circles) and in the virus stock (open circles). Also, TCID₅₀ titers in the reactor harvest (squares) are shown. C) Percentage of infected cells in the tubular bioreactor harvest at three different MOIs (columns) and maximum influenza HA titer in the tubular reactor harvest for each MOI condition (diamonds). D) Control experiment of IAV propagation at 18 h post infection (p.i.) in batch mode (shake flasks). The percentage of infected cells (columns) at three different MOIs, and HA titers (diamonds) at 18 h p.i. are shown. Suspension MDCK.SUS2 cells were used in the tubular reactor and control experiment. PFBR system experiment and shaker flasks cultivations performed by Wohlfarth, 2017 [168].

4.3.6 Continuous production of influenza A virus in AGE1.CR.pIX cells in a continuous tubular bioreactor system

AGE1.CR.pIX cell growth. Continuous cultivations in the CB were started immediately after seeding AGE1.CR.pIX cells at a concentration of 1.0×10^6 cells/mL. The two PFBR experiments were named Tubular cultivation A and B (Figure 4.13) and the nominal RT was set to 20 h. Maximum cell concentrations were achieved at 150 h and 200 h for Tubular cultivation A and B, respectively. In the PFBR harvest, first cells were visible after 20 h of culture for both cultivations, as expected for the nominal RT of 20 h. A lower cell concentration in the PFBR harvest compared to the CB was observed. This can be explained, in part, because of the dilution of F_2 by F_3 at the POI.

Cell viability in the CB was always above 90% for both cultivations. In the PFBR harvest, viabilities between 40 and 90% were obtained at the beginning of tubular cultivation A and stabilized between 80-90% after 110 h of culture (Figure 4.13 A). In tubular cultivation B, cell viabilities between 80-90% were measured in the PFBR harvest throughout the experiment (Figure 4.13 B). (Note: with a stable viability exceeding 90% in the CB, a backward contamination of the CB via F_2 can be excluded). In the PFBR harvest, lower cell viabilities compared to the CB were expected due to virus propagation inside the tube. However, additional experiments (not shown) indicated that reduced cell viabilities in the PFBR harvest can also be caused by problems with air-injection at the tube inlet (i.e. linked to failure of pump 2 and missing air supply via F_5). I.e. this may explain the low viabilities in the harvest of tubular cultivation A during the first 100 h (Figure 4.13 A), where long liquid segments with lower air-to-liquid ratios were observed. In contrast to MDCK.SUS2 cells, cell clumps in the PFBR, as consequence of cell sedimentation, were not observed for AGE1.CR.pIX cells.

Flow rate and RT in the PFBR. With the start of cultivations, the nominal RT of the PFBR was set to 20 h and calculated for each time point (Equation 6). Tubular cultivation A, however, showed a RT of 27 h for the first 24 h of culture, which later stabilized in the range of 20-21 h (Figure 4.13 C). Tubular cultivation B showed an oscillatory pattern of the RT that (after about 20 h) increased to 26 h RT and decreased again to 16 h RT at 225 h of culture (Figure 4.13 D). Afterwards, these oscillations in the RT decreased and approached the nominal RT of 20 h. Visual inspection of the velocity of liquid compartments in the transparent silicone tubes confirmed differences during these RT oscillations.

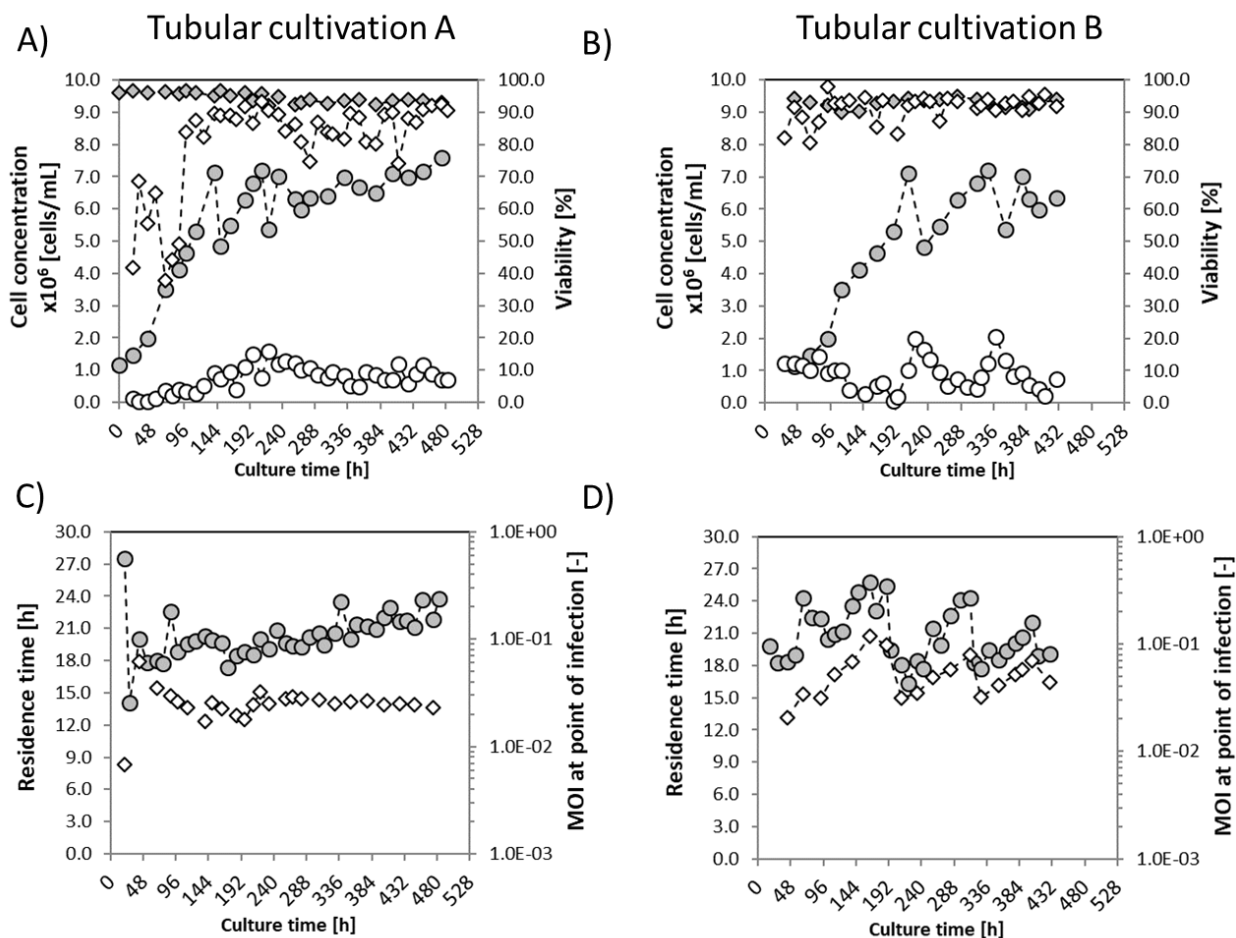


Figure 4.13. Cell concentration, viability, residence time and MOI of tubular cultivation A and B for production of influenza A virus in AGE1.CR.pIX suspension cells. A) and B), viable cell concentration (circles) and viability (diamonds) of the cell bioreactor (CB, grey symbols) and the PFBR harvests (open circles). C) and D) Residence time (circles) of the PFBRs and actual multiplicity of infection at the point of infection (diamonds). E) pH values in the virus stock (white) and in the medium stock (grey). F) pH value in the harvest (white) and in the CB (grey).

MOI in the PFBR. The nominal MOI of the tubular bioreactor system was set to 0.02 as chosen by Frensing et al. [26]. The actual MOI of tubular cultivation A (Figure 4.13 C), was, however, 6.8×10^{-3} for the first 24 h of culture; later it increased to 6.2×10^{-2} at 50 h of culture, and only then stabilized near 2.5×10^{-2} . Obtaining the nominal MOI at the POI was possible, because cells in the CB grew to the expected concentration. Thus, no re-adjustment of the infectious titer of the VS was required.

A different situation was obtained in tubular cultivation B, where the actual MOI oscillated between 2.1×10^{-2} and 1.2×10^{-1} during the first 200 h of culture. Afterwards (200-450 h), the MOI was reduced with values between 3.2×10^{-2} and 7.9×10^{-2} . This oscillation of the MOI was a result of changes in the cell concentration in the CB (Figure 4.13 B at 225 h of culture), which were due to manual corrections (removal of cells from the reactor and dilution with culture medium) in an

attempt to maintain the cell concentration near 6×10^6 cells/mL. Note that the MOI oscillation is not linked to the oscillations in the RT since eq. 1 and 2 show that MOI and RT are independent parameters. These oscillations in the MOI should be easy to avoid if the cell growth in CB can be maintained at steady state. These results showed that a continuous tubular bioreactor system, operated at steady-state, can be used for continuous production of influenza viruses with a defined MOI, which is not possible in cascades of CSTRs [26].

IAV titers and pH in the PFBR harvest. HA and TCID₅₀ virus titers were measured in the PFBR harvest twice a day. In tubular cultivation A (Figure 4.14 A), HA titers were below the detection limit for the first 60 h and gradually increased after 100 h of culture to values near $1.9 \log_{10}$ (HA Units/100 μ L) to finally stabilize at around $1.6 \log_{10}$ (HA units/100 μ L) for the rest of the experiment. In the tubular cultivation B (Figure 4.14 B), virus production was observed earlier and an HA value of $1.8 \log_{10}$ (HA Units/100 μ L) was measured at 50 h of culture. Afterwards, HA titers fluctuated between 0.9 and $1.5 \log_{10}$ (HA Units/100 μ mL) and reached a steady state after 200 h of culture at values near $1.1 \log_{10}$ (HA Units/ 100 μ L). This correlated with a decrease of oscillations in MOI and RT.

Infectious virus titers were measured in the PFBR harvest and in the VS bottle. The VS of tubular cultivation A was maintained at a TCID₅₀ between 0.9×10^4 and 1.8×10^5 virions/mL during the whole cultivation (Figure 4.14 C). The first TCID₅₀ value measured in the PFBR harvest was 1.8×10^4 virions/mL and increased to maximum 5×10^7 virions/mL at 150 h of culture. The TCID₅₀ at the PFBR harvest dropped at 150 h and finally stabilized near a value of 1.0×10^7 virions/mL. In tubular cultivation B, the VS was adjusted initially to a TCID₅₀ of 5×10^4 virions/mL (Figure 4.14 D) and maintained afterwards at 1×10^4 virions/mL. Surprisingly, the TCID₅₀ in the PFBR harvest was initially below the limit of quantification (1×10^3 virus/mL) for the first 48 h. Then, the TCID₅₀ increased to 1.0×10^7 virions/mL to finally stabilize near 1.0×10^6 virions/mL.

Overall, the HA titers in the PFBR harvest reached an average value of $1.6 \log_{10}$ (HA Units/100 μ L) and $1.1 \log_{10}$ (HA Units/100 μ L) in tubular cultivations A and B, respectively. Compared to virus titer values observed in batch mode with AGE1 cells (20 hp.i.), the HA of the PFBR harvests was clearly reduced and corresponded to batch titers expected between 10 and 15 h p.i. (Figure 4.2 A). Results indicate that virus propagation in the PFBR was not optimal. Besides virus diffusion limitations resulting in poor cell-to-cell spreading, other parameters such as the pH inside the tubes and drop in oxygen partial pressure in cell-containing compartments might be relevant. With a Reynolds number in the laminar regime ($Re \sim 40$ for this experiment), and the absence of mechanical mixing, mass transfer is expected to be diffusion limited. Hence, improving the PFBR harvest titers will require a further optimization of the infection conditions and the tube length. In addition, measures to improve mixing at the POI and along the tube, e.g.,

passive or static mixing, and incorporation of active mixing such as vibration or agitation platform should be investigated [169] [170].

The TCID₅₀ in the PFBR harvest was characterized by an initial drop, followed by an increase to values near 1.0×10^7 and 1.0×10^6 virions/mL for tubular cultivation A and B, respectively. At the beginning of cultivations, a similar TCID₅₀ in the harvest and in the VS was measured for up to 60 h. This was an indication of reduced virus replication inside the tube following the bioreactor start-up phase. Afterwards, a TCID₅₀ increase of up to three orders of magnitude was achieved compared to the TCID₅₀ in the VS. Compared to TCID₅₀ titers obtained in batch mode (Figure 4.2), the infectious titers obtained were at least two fold lower than those of batch at 20 h p.i.. This result, together with the lower HA titer with respect to batch, supports the hypothesis that virus propagation inside the PFBR was diffusion limited. Hence, further optimization of the PFBR system is needed to reach batch-like titers.

One process variable that could be key for virus replication was the pH value at the POI and in the PFBR harvest. Most likely, the high amount of oxygen contained in the bubbles of the PFBR is gassing out compounds like CO₂, leading to such increase in pH. High pH values were observed at the beginning of the tubular bioreactor experiment with MDCK cells and, in this experiment with avian cells, the goal was to obtain a better control of the pH in the entry of the tube to reach lower pH values in the harvest. This was realized by manually controlling the pH value of the virus stock and the medium stock every 48 h by replacing it by fresh medium with pH of 7.0, as depicted in Figure 4.15 A. This methodology, together with a pH value close to 7.0 in CB after 73 h of culture (Figure 4.15 B), resulted in pH values near 7.5 in the harvest for most of the cultivation time. These close-to-physiological pH values, although not optimal, were key for virus replication inside the PFBR and for stable production of influenza virus.

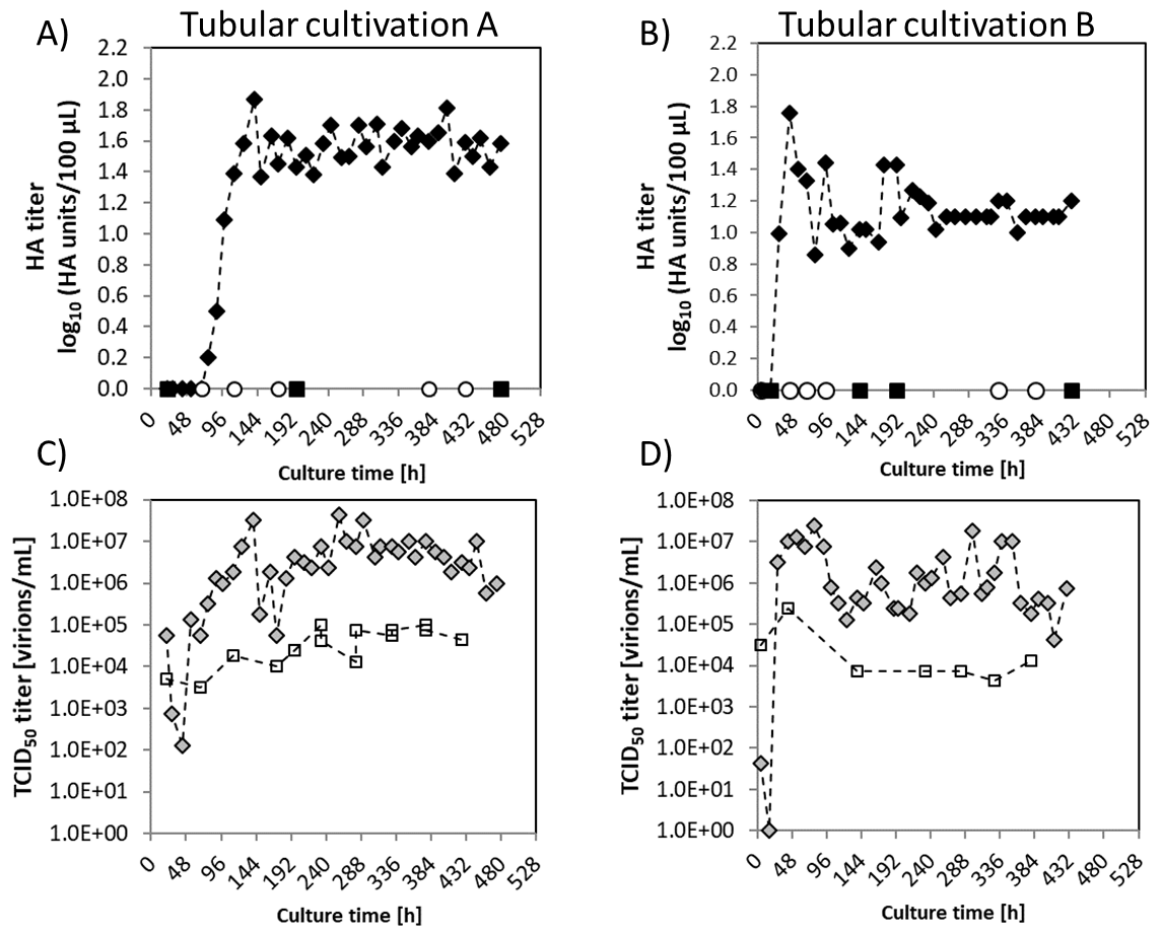


Figure 4. 14. Influenza A virus titers in AGE1.CR.pIX cells in the continuous tubular plug-flow bioreactor (PFBR) system. A) Influenza virus haemagglutinin (HA) titers in the PFBR harvest (closed diamonds), in the virus stock (VS, open circles) and in the cell bioreactor (CB, closed squares) of tubular cultivation A. B) Influenza HA virus titers in the PFBR harvest, VS and CB (same symbols than A) of tubular cultivation B. C) Influenza virus infectious (TCID₅₀) titers of the harvest (diamonds) and of the VS (squares) of tubular cultivation A. D) Influenza TCID₅₀ titers of the harvest and VS of tubular cultivation B (same symbols than C).

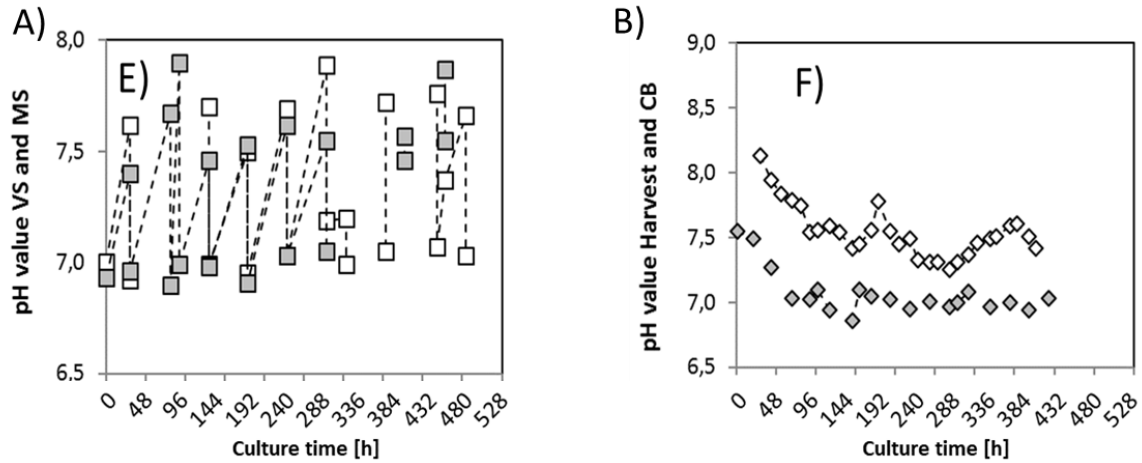


Figure 4. 15. pH values of one representative tubular plug-flow bioreactor system operated with AGE1.CR.pIX cells. A) pH values in the virus stock (VS, white) and in the medium stock (MS, grey). B) pH value in the harvest (white) and in the cell bioreactor (CB, grey).

4.3.7 Genetic stability of influenza A virus produced in long-term continuous tubular bioreactor cultures – comparison with batch and semi-continuous cultures

IAV DIPs accumulation in MDCK cells in the PFBR harvest. Non-quantitative PCR was used to analyze the influenza virus gene segments 1, 2, 3 and 5 of the virus seed (Fig 4.16) and the harvest obtained from the first functional tubular bioreactor run with MDCK.SUS2 cells (Figure 4.17). The MDCK-virus seed used for this experiment showed a high concentration of DS near 500 base pairs (bp), which provides advantages to DIP for its replication in the culture. The harvest analysis was done from 144 until 480 h of culture since HA and TCID₅₀ titers were detected in the harvest over these cultivation hours. The dashed line in Figure 4.17 shows the change in flow rates that was applied to the system at 264 h of culture, which changed the RT inside the PFBR and, therefore, the characteristics of the virus harvest. From 144 until 264 h of culture, with a RT of 20 h, segments 1, 2 and 5 showed a stable pattern, while segment 3 showed a double DIP band around 500 bp that then disappeared. After 264 h, the pattern of FL segments around 2000 bp is maintained stable for all segments while the DIP pattern around 500 bp changes from 348 h onwards as consequence of the increase in HA titers. This first result shows that it is possible to correlate changes in DIP population with changes in process parameters such as the RT in the PFBR. Moreover, a stable pattern of FL segment 1 for almost 240 h was not observed previously using cascades of CSTRs [26]. Hence, this first result suggested that obtaining a stable pattern of FL and DIPs is possible in a tubular bioreactor. Moreover, by changing the flow rates, it is possible to modify the product profile in terms of FL and DS content.

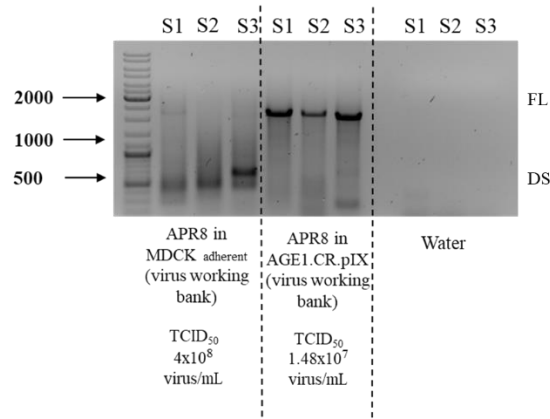


Figure 4. 16. Polymerase chain reaction analysis of influenza A virus seeds. Segment 1, 2 and 3 (S1, S2 and S3) of the influenza A/PR/8/34 virus seed from Robert Koch Institute (APR8), adapted either to adherent MDCK cells (MDCK_{adherent} left) or to avian AGE1.CR.pIX cells (middle), were analyzed. A water control was also included for each segment (right). The size in base pairs of relevant marker bands is shown on the left. Full length (FL) segments had a size of 2000 base pairs (bp) while defective segments (DS) between 700 and 500 bp.

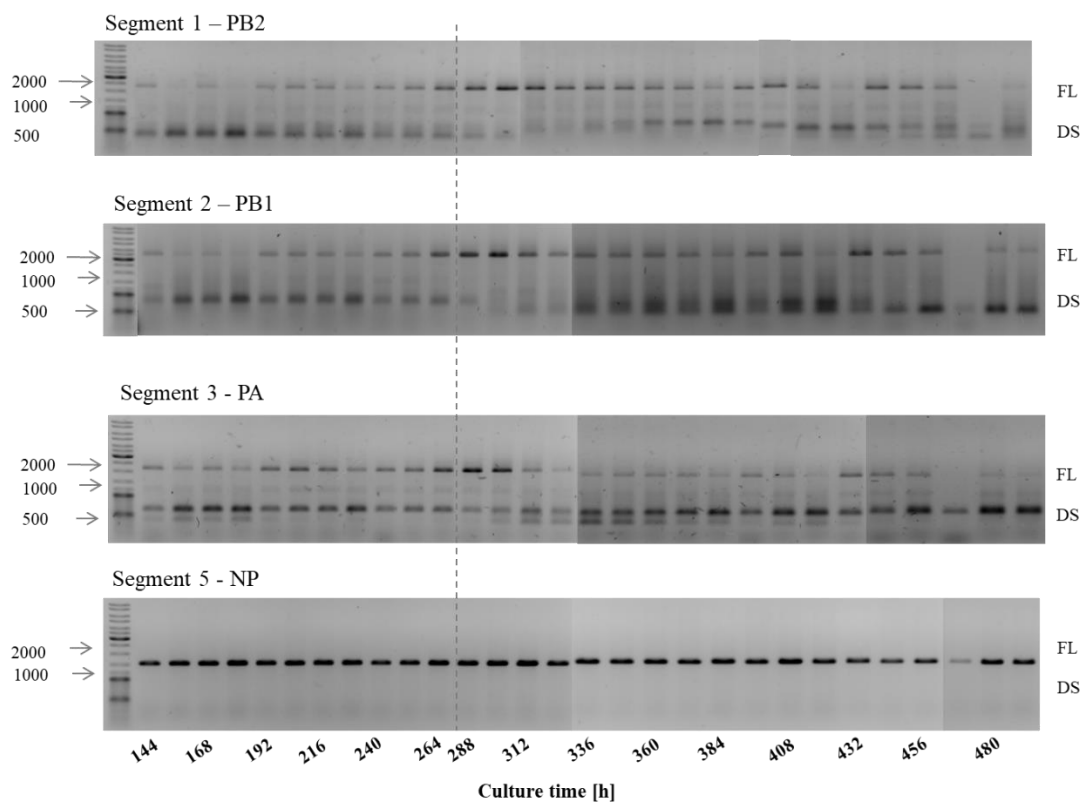


Figure 4. 17. Polymerase chain reaction analysis of influenza A virus produced with the tubular plug-flow bioreactor (PFBR) system in canine MDCK.SUS2 suspension cells. IAV RNA segments 1, 2, 3 and 5 were analyzed between 144 and 480 h of culture. Full length (FL) segments had a size of 2000 base pairs (bp) while defective segments (DS) between 700 and 500 bp. The dashed line indicates the time in which the virus stock concentration and the residence time (RT) in the PFBR were changed (RT from 20 to 18 h RT). Segment 1 encodes the polymerase basic protein 2 (PB2), segment 2 the polymerase basic protein 1 (PB1), segment 3 the polymerase acid protein (PA) and segment 5 the nucleocapsid protein (NP). The size in bp of relevant marker bands is shown on the left.

IAV DIP accumulation in AGE1.CR.pIX cells in the PFBR harvest. Non-quantitative PCR was used to analyze the virus seed (Figure 4.16) and the dynamics of replication of gene segments 1, 2 and 3 of IAV propagated in batch (Figure 4.18) and semi-continuous (Fig 4.19) cultures and the continuous tubular bioreactor system (Fig 4.20). The PCR assay for all figures shows bands of FL segments, and DS near 2000 bp and 500 bp, respectively.

The two IAV batch cultures reported before were analyzed by PCR. In both batch cultures (Figure 4.18), FL segments near 2000 bp were observed for all three genes between 0 and 24 h p.i.. Interestingly, DSs (less than 2000 bp) were observed at 0 h p.i. for segment 2. Later, at 7 h p.i., two bands were observed in the gel, and finally a FL segment with 2000 bp size only (20 h p.i.). In general, deletions near 500 bp were generated in all three segments in batch mode, with segment 2 most prone for deletions in the range of 500-2000 bp.

Semi-continuous cultures were maintained for a period of 450 h (Figure 4.19). This cultivation mode was selected as a small-scale approach mimicking a true continuous cascade of CSTRs [23]. A more pronounced periodic change in the ratio of FL to respective DS was observed when compared to the PCR measurements performed in batch cultures. The PCR signals for all three studied segments appear to oscillate in parallel, most likely due to the interference of FL genome replication by DIPs, and dependence of DIP replication on the presence of the FL segments. A similar replication dynamic was described previously [26] also for cascades of CSTR.

For segment 2 additional copies with a short deletion only (near 2000 bp) were observed at 0, 130, 220, and 320 h p.i. that coincide with the results obtained for batch cultures (0 and 7 h p.i., Fig 4.18). Whether the parallel oscillations of the various DS segments were due to co-packaging of minor deletions with one dominant genotype, or whether all segments with deletions each can interfere with standard virus replication is not clear yet.

All combined, the control experiments strongly suggest again that a drop in virus titers due to the “von Magnus effect” is a frequent observation in cascades of CSTR for the cell and IAV system analyzed here.

Segment-specific PCR analysis of the virus produced in the continuous tubular bioreactor system (PFBR harvest of tubular cultivation A) is depicted in Figure 4.20 for a production time of almost 500 h. For this cultivation regime a surprisingly constant pattern of FL bands was observed for all three segments over the whole duration of the experiment. This pattern differed substantially from the one observed for batch or semi-continuous cultures and suggests the absence of periodic DS dynamics.

Nevertheless, two bands were observed for segment 2 over the whole cultivation period, which was in line with the results observed at early time points p.i. in batch culture, as well as for various time points in semi-continuous cultures with TCID₅₀ titers lower than 1×10⁷ virions/mL. Assuming the theoretical scenario that a biological reaction in an ideal well-mixed PFBR follows a batch-like dynamic over the tube length [171], this result indicates that virus spreading and/or intracellular virus replication cycles were not fully completed in the PFBR. Such an effect would suggest that the PFBR is diffusion-limited and, therefore, optimization of MOI and RT (tube length) may be beneficial.

Nevertheless, the continuous tubular bioreactor system provides a virus harvest with a defined virus passage number (in this case, passage number of VS plus one if defined as culture-to-culture transfer) avoiding the accumulation of large numbers of virus segments with deletions, and possible interference with standard virus replication compared to cascades of CSTRs. This bioreactor system can be used to stably produce whole influenza virus for inactivated vaccine manufacturing, and can be also used to produce well-defined DIPs as antiviral agents against a wide range of influenza subtypes [85, 172].

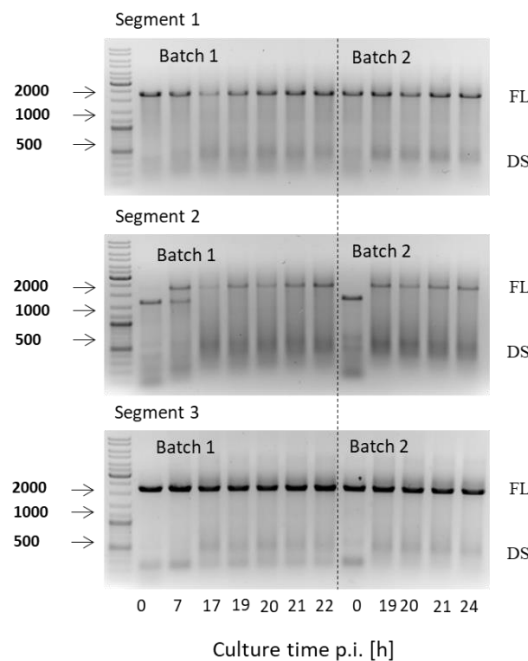


Figure 4. 18. Polymerase chain reaction analysis of the batch experiments in avian AGE1.CR.pIX cells. IAV genome segments 1, 2 and 3 were analyzed (Segment 1, 2 and 3). The experiment was carried out by taking cells from the cell bioreactor of the tubular plug-flow bioreactor system, and infecting them in a shaker flask in two experiments, called batch 1 and 2. Batch 1 is shown at the left of the dashed line, and batch 2 at the right of the dashed line. Samples were taken at 0, 7, 17, 19, 20, 21 and 22 h post infection (p.i.) in batch 1, and at 0, 19, 20, 21 and 24 h p.i. in batch 2. The size in base pairs of relevant marker bands is shown on the left. Full length (FL) segments had a size of 2000 base pairs (bp) while defective segments (DS) between 700 and 500 bp.

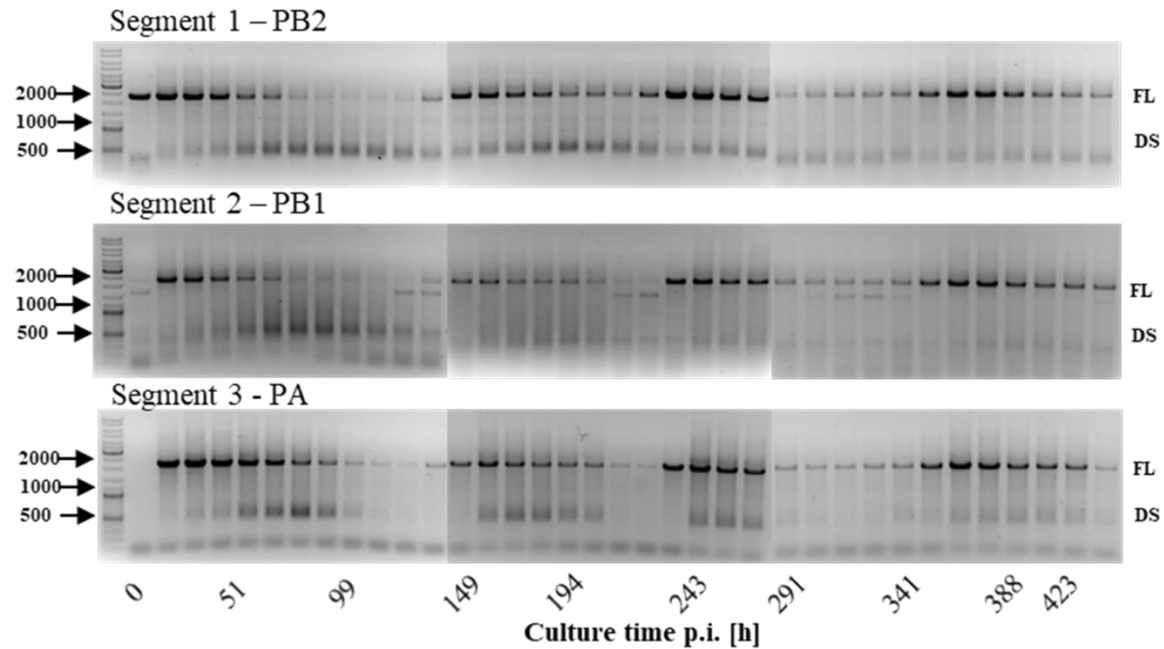


Figure 4. 19. Polymerase chain reaction analysis of influenza A virus produced with the semi-continuous cultivation in avian AGE1.CR.pIX cells. The semi-continuous cultivation was carried out using shaker flasks as described in materials and methods. Samples were taken twice a day and the cultivation was maintained for three weeks. Segment 1 encodes the polymerase basic protein 2 (PB2), segment 2 the polymerase basic protein 1 (PB1) and segment 3 the polymerase acid protein (PA). The size in base pairs of relevant marker bands is shown on the left. Full length (FL) segments had a size of 2000 base pairs (bp) while defective segments (DS) between 700 and 500 bp.

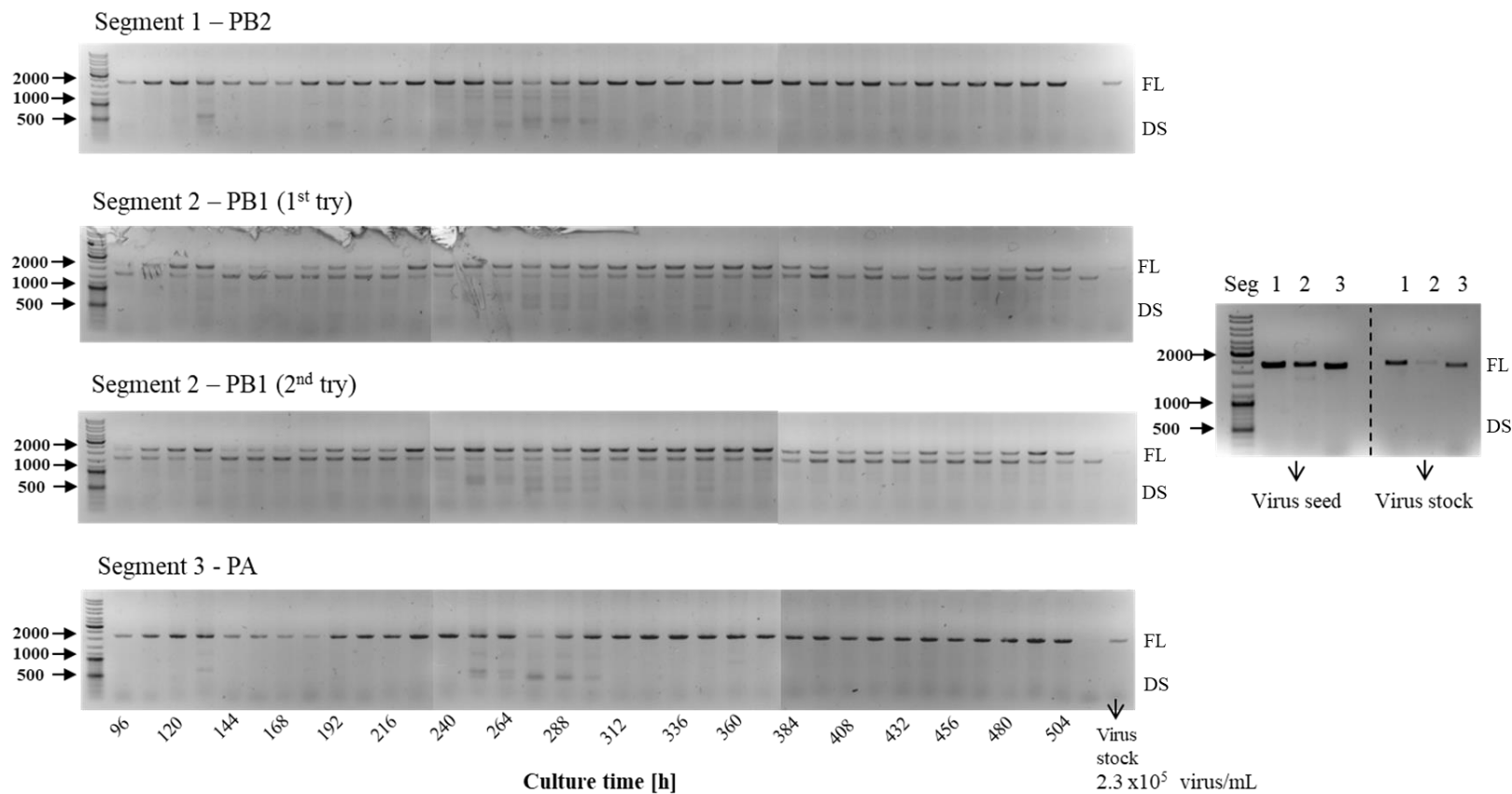


Figure 4. 20. Polymerase chain reaction (PCR) of influenza A virus produced with the PFBR system in avian AGE1.CR.pIX cells. IAV RNA segments (Seg) 1, 2 and 3 were analyzed between 96 and 504 h of culture. Full length (FL) segments had a size of 2000 base pairs (bp) while defective segments (DS) between 1000 and 500 bp. The PCR of segment 2 was done twice to confirm the presence of a second band near the FL segment. The PCR of the virus seed and from the virus stock (2.3×10^5 and 3.0×10^5 virions/mL, respectively; separated with a dashed line) were used as a control (right). Segment 1 encodes the polymerase basic protein 2 (PB2), segment 2 the polymerase basic protein 1 (PB1) and segment 3 the polymerase acid protein (PA). The size in base pairs of relevant marker bands is shown on the left.

4.4 Productivity of continuous processes versus batch cultivations

Continuous virus production is a promising approach for efficient viral vaccine production. However, determining the volumetric productivity (STY and TY) of the continuous bioreactors here analyzed is key for the technical and economic feasibility of such technologies in large scale manufacturing. Hence, in the following, the STY and TY of continuous MVA virus production in a TSB system is first evaluated and compared to a batch process. Then, the STY of continuous IAV production in this novel tubular bioreactor is compared to the alternative of using a TSB system and a batch process.

4.4.1 MVA virus productivity in a continuous two-stage bioreactor system

The productivity of the TSB system was compared against a batch and semi-continuous process. The TSB system has two bioreactors that can be operated differently, either as batch or as semi-continuous. Therefore, the comparison was carried out with the alternatives given up when the decision to use the two bioreactors in continuous mode was taken (defined as *opportunity cost* [173]). This meant that the batch productivity was determined for a system consisting of two batch bioreactors operated in parallel. The semi-continuous productivity was determined with the two bioreactors operated as in the SSC system. In the following, the STY and TY of batch and semi-continuous production processes are presented first, and then compared with the continuous TSB system.

In batch, a STY of 3.4×10^8 virions/(L h) and a TY of 8.9×10^8 virions/h were estimated for two parallel batch cultivations, using an average TCID₅₀ titer of 1.0×10^8 virions/mL (obtained from 100 mL scale batch cultures), and 17 days of operation (2 batch cycles).

Another productivity value for batch processes is obtained if the calculation includes 1 additional batch cycle (+8 days). An estimation for two parallel 1 L scale batch bioreactors resulted in a STY of 2.2×10^8 virions/(L h) and a TY of 8.7×10^8 virions/h, based on an average TCID₅₀ of 1.0×10^8 virions/mL and 26 days of operation (3 batch cycles).

The productivity of the semi-continuous process was determined using the data obtained from the SSC system. The best STY obtained was 1.0×10^9 virions/(L h) for the 25 h RT experiment (SM25-B, Table 4.1) followed by 3.6×10^8 virions/(L h) of the 35 h RT experiment (SM35-B, Table 4.1). These values were in the same order of magnitude of 1.0×10^9 virions/(L h) and 3.4×10^8 virions/(L h) that were calculated from the batch process operated 8 d (1 cycle) and 16 d (2 batch cycles), respectively. Therefore, a fair comparison suggests that the SSC system is equal or more efficient than the batch process, for production targets that require operational times of at least 16

days or more (2 batch cycles or more). However, the batch process is more efficient than SSC for production of MVA virus volumes equivalent to 1 batch cycle.

The STY estimations for the TSB system resulted in a value of 1.7×10^8 virions/(L h) for 24 days of operation. This was almost identical to the STY of the batch process operated for a similar period of time (3 cycles, 24 days, as shown in Table 4.1). Interestingly, the TY of the TSB system was estimated to 1.2×10^9 virions/h, which was larger than the 6.2×10^8 virions/h of the batch process (the TSB produced 6×10^{11} virions in 21 d, while the batch process would have produced 4×10^{11} virions in 24 d). In other words, the TSB system can be equal or more efficient than a batch production system, starting from an operational time equivalent to 3 or more batch-cycles.

For an installed production plant capacity, batch cultivation will be the option of choice for lower virus production targets, because the STY of a batch system operated over 8 d (1 cycle) or 16 d (2 cycles) was 5.2×10^8 and 2.6×10^8 virions/(L h), respectively (see Table 1). Nevertheless, this is only valid if TCID₅₀ titers of 1.0×10^8 virions/mL or more are obtained at time of harvest from batch cultivations, which is not always the case. Titers in the order of 1.0×10^7 virions/mL can also be obtained in batch cultivations (see titer of BM-C in Table 4.1). To address this, Figure 4.21 compares the STY and TY of the TSB system experiment (named T25 in Table 4.1) with the batch process evaluated at two TCID₅₀ conditions for STY and TY: 1.0×10^8 virions/mL (best-case, upper dashed line) and 1.0×10^7 virions/mL (worst-case, lower dashed line) over cultivation time. Figure 4.21 A shows that the STY of the continuous process is in the range of the batch process after 120 h p.i. and approaches the STY of the best-case batch process at late operational times. Interestingly, Figure 4.21 B shows that the TY of the TSB system overcomes the TY of the best-case batch process at 120 h p.i. and remains high over production time. From the data available, it was possible to estimate that, after three batch cycles, the TY of the TSB system is at least 37% greater than the batch process. Therefore, the efficiency of the batch process can be greater for production volumes less than three batch cycles. The TSB system is more efficient than batch for more than three batch cycles.

Other characteristics of the continuous system that were not taken into account in these yield calculations, such as the smaller bioreactor volumes required, lower investment costs, fewer seed-train steps to start production, and lower number of cleaning and sterilization steps, are clear advantages of the continuous system that would add to its productivity estimations.

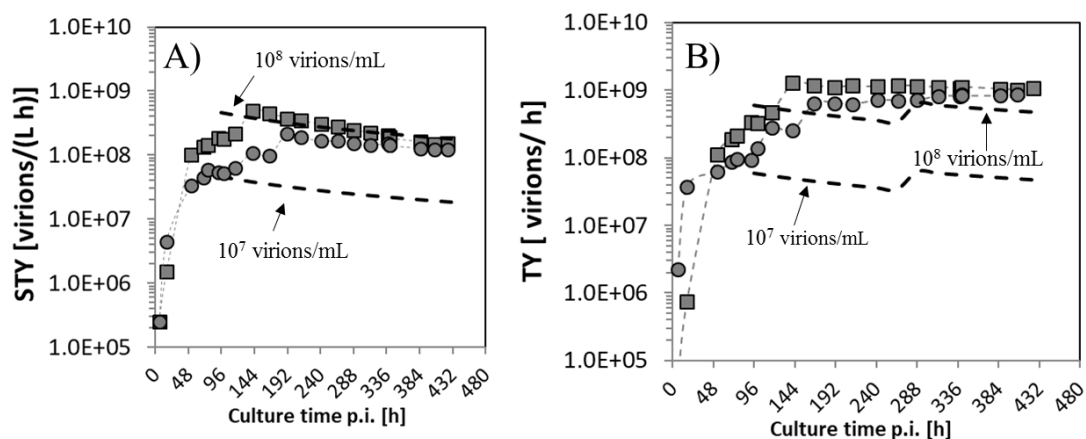


Figure 4.21 Productivity of the TSB system (1290 mL ww) compared with a batch process comprising two stirred tank bioreactors (645 mL each vessel, 1290 mL ww). Space-time-yield (STY) and time-yield (TY) were calculated using equations 7-10. A) STY of the continuous cultivation based on infectious (TCID₅₀) titer values of VB (squares) and the harvest (circles), versus STY of the batch process (dashed lines; upper and lower lines were estimated with a maximum TCID₅₀ at time of harvest of 1×10⁸ and 1×10⁷ virions/mL, respectively). B) TY of the continuous cultivation compared to the batch process (same symbols as in Fig A). The comparison assumed that the cell growth phase of the continuous and from the batch are identical and is not shown in the graphic (negative time values). Infection of both processes is carried out at time zero, and harvests of the batch process are taken at 72 and 288 h post infection (p.i.).

Finally, these results showed that continuous production of MVA virus in a TSB system was feasible as virus titers similar to batch processes were obtained, MVA virus was genetically stable at least over 15 days of cultivation, and the STY and TY indicated that its productivity can be equal or larger than a batch process for long operational times. Nevertheless, aspects such as replicating the virus not beyond five passages from the master seed, and also the risk of unwanted mutations that might arise during cultivation time have to be considered in establishing a TSB process, and will impact the final productivity of the process. These aspects and others requested by regulatory agencies will be very important to define a batch (or lot number) in a continuous virus production system. If this is realized, a continuous process can be established using a TSB system with two parallel virus bioreactor vessels, as shown in Figure 4.22. This system solves the problem of shutting down production during cleaning and sterilization of a TSB system with only one VB vessel. The process can be operated by infecting one virus bioreactor first, while the parallel virus bioreactor is infected with some delay. This system allows uninterrupted virus production with higher productivities compared to batch processes (Note: the idea of this bioreactor system was conceived during this PhD work but built once this work was finished for a project of the Defense Advanced Research Project Agency (DARPA) at the MPI Magdeburg. The paper that describes this bioreactor setup was published in parallel to the defense of this PhD thesis in November 2019 and is cited in [174]).

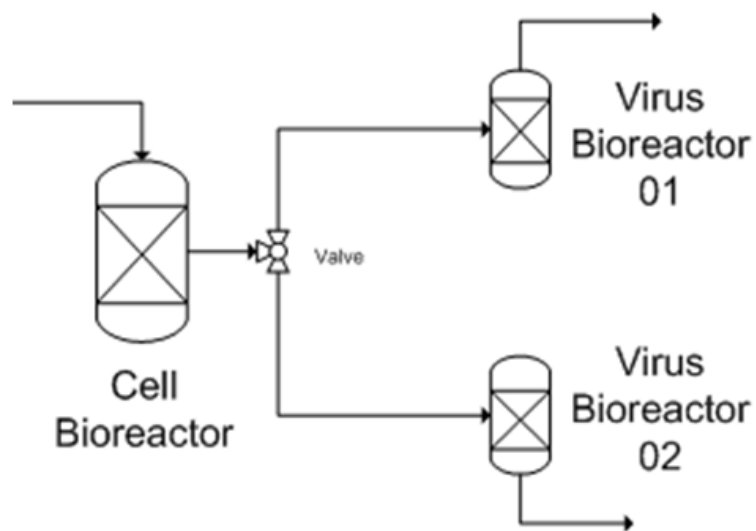


Figure 4. 22. Process layout of a hypothetical parallel two-stage continuous process for MVA virus production. The process consists of a first bioreactor (Cell Bioreactor) for continuous cell production, followed by two parallel bioreactors (Virus Bioreactor) for continuous virus propagation. Infection, production, cleaning and sterilization of both VB vessels occurs at different days, which allow uninterrupted virus production.

4.4.2 IAV productivity in the tubular bioreactor system

Based on the experimental data of IAV production obtained with MDCK.SUS2 cells, yield estimations were carried out and are summarized in Table 4.2 for three different bioreactor systems. A STY 1.5 times higher than batch cultivation and 2.5 times higher than the cascade of CSTRs was estimated for the PFBR system assuming a total production volume of 10 L and stable virus titers of $2.5 \log_{10}$ (HA Units/100 μ L) at steady-state operation (6 – 12 days). The large difference in the yield obtained from cascades of CSTRs is most likely due to the presence of virus titers oscillations induced by DIP accumulation in cascades of CSTRs. Without DIPs, influenza virus production in cascades of CSTRs might be as efficient as the tubular bioreactor because maximum virus titers are similar.

Table 4. 2. Virus yield comparison between the tubular plug-flow bioreactor (PFBR) system, the two-stage stirred tank bioreactor (TSB) system and the batch bioreactor (Two parallel batches) for production of 10 L of influenza A virus with MDCK.SUS2 cells (500 mL cell bioreactor volume).

	Total Bioreactor Volume [mL]	Volumetric Production Flow [mL/h]²	Average HA Titer \log_{10} (HA Units/100 μL)³	Average Virus Titer [virions/mL]⁴	Virus Production Flow [virions/h]	Volume Produced [L]	Time Required [h]	STY [virions/(L h)]⁵	STY [-]
PFBR system	711 (500 + 211)	12	2.55	7.20E+09	8.64E+10	10	833	8.07E+09	1.5
TSB system	1000	12	2.13	2.74E+09	3.29E+10	10	833	3.07E+09	0.6
Two parallel batches¹	1000	5.95	2.70	1.02E+10	6.07E+10	10	1680	5.52E+09	1.0

¹ 7 days batch cycle (3 days of cell growth, 3 days of virus propagation, 1 day of cleaning).

² the production flow [mL/h] of the PFBR system is the nominal used to design the experiment; for the TSB system, it is assumed to be the same than the PFBR system; for the Two Parallel Batches, the value was calculated assuming a production of 1000 mL in 7 days.

³ Average haemagglutinin (HA) titer refers to the value that would be obtained after collecting all harvests together. For the PFBR system the HA value was obtained by calculating an average of the HA titers between days 336 and 422 h of the experiment with MDCK.SUS2 cells; for TSB system the data was estimated from experimental data previously obtained in small scale-shaker experiments (data not shown); for batch, the HA value was obtained from an estimated HA titer at 72 h post infection as described by Lohr et al. Vaccine 2010 28: 6256-6264.

⁴ calculated assuming that 1 virus particle binds to 1 cell

⁵ the term liters (L) considers the volume of product produced and the volume of the bioreactor system.

The productivity values shown in Table 4.2 are valid not only for IAV production in MDCK.SUS2 cells but also in AGE1.CR.pIX cells. Independently of the cell line of choice, the presence of oscillations in virus levels is likely to be present if a cascade of CSTRs is used for virus propagation. Therefore, a speculation is that regardless of the cell line chosen to produce IAV, the productivity of the PFBR system should always be more efficient than the other two options for producing at least 10 times the bioreactor WV. Finally, the 50% STY improvement of the PFBR system with respect to a batch process is a first result that can be improved by further optimization of the system.

Chapter 5

Conclusions

The aim of this work was the establishment of continuous cultures for production of viruses in animal cells. Continuous cultivation systems can enable more efficient and cost-effective viral vaccine production compared to current batch manufacturing. However, characterization of such systems to elucidate virus genetic stability and impact of defective interfering particles were key aspects for the establishment of these processes. For that purpose, MVA virus and IAV were used. MVA virus can be used to develop recombinant vaccines against a variety of diseases, while influenza virus is used to prepare vaccines against the seasonal “flu” disease and pandemic outbreaks. Based on the available technology, a continuous MVA virus production system using cascades of CSTRs was proposed. In addition, further development was needed for continuous influenza virus production and, therefore, a new bioreactor technology that avoids the oscillations in virus titers, known as “von Magnus effect”, was developed. This new bioreactor technology, based on a plug-flow tubular bioreactor, represents a major step forward towards continuous production of cell culture-derived viruses.

Continuous MVA virus production. The first part of this thesis described MVA virus production in long-term passaging using continuous and semi-continuous cultures. The isolates MVA-CR19 and MVA-CR19.GFP virus that allow efficient replication in non-agglomerated AGE1.CR.pIX cells were used. A small scale semi-continuous approach, named SSC, resulted in stable production of cells over three weeks of cultivation, with virus titers that showed a transient phase followed by a stationary phase. The stable virus titers obtained with the SSC suggested the absence of the “von Magnus effect” over cultivation time. The SSC was also used to analyze the impact that RT of the virus bioreactor has on virus yields. Experiments with the MVA-CR19 virus isolate showed that the RT might influence the duration of the transient phase, but it has little impact in the final virus titers reached over the stationary phase. Furthermore, a stability analysis of a recombinant MVA virus expressing green fluorescent protein, by both a TCID₅₀-ratio and genetic stability criteria, showed that MVA virus is stable at least over 16 days of cultivation.

MVA virus production was then produced in a cascade of CSTRs or TSB system. This production system showed stable TCID₅₀ titers of about 9×10^7 virions/mL over 18 days of cultivation with similar space-time-yield compared to batch cultivation and with a time-yield about 40% greater than batch. Virus titers and replication dynamics predicted by scouting experiments performed in the SSC system were similar to those obtained with the TSB system

and no interference by DIPs was observed. Finally, cascades of CSTRs and semi-continuous cultures are promising platforms for production of of MVA virus-based recombinant vaccines and viral vectors.

Continuous influenza virus production. The second part of this thesis described a continuous production process of influenza A virus. For this purpose, a novel continuous tubular bioreactor system that avoids the “von Magnus effect” was established. The bioreactor system was composed of a CSTR (operated as a chemostat for cell production) with a plug flow tubular bioreactor in series. The whole system was referred to as PFBR system. The PFBR system had a total working volume of 711 mL, required 1 m² of surface area, and was built using a 105-120 m long tubular reactor. The culture format in the PFBR resembled successive bursts of defined single-passage batch processes, where each burst was compartmentalized by air bubbles. The bioreactor showed a robust operation over at least three weeks at a nominal flow rate of 0.2 mL/min. As a result, production of 12-times the bioreactor working volume with space-time-yields at least 50% greater than batch cultures would be possible within one month.

A first functional tubular bioreactor prototype was evaluated using suspension MDCK.SUS2 cells with different MOIs. HA and TCID₅₀ titers of up to 2.5 log₁₀ (HA Units/100 μL) and 1×10⁶ virus/mL were obtained, respectively. Then, influenza A/PR/8/34 (RKI) virus was produced with avian suspension AGE1.CR.pIX cells in two tubular bioreactor cultivations with 18 days of operation at a nominal MOI of 0.025. Stable HA titers of up to 1.6 log₁₀ (HA Units/100 μL) and TCID₅₀ titers of up to 1×10⁷ virus/mL were obtained. PCR analysis of influenza segments 1, 2 and 3 showed that accumulation of defective particles was not significant. These results demonstrated that the “von Magnus effect” can be avoided in such a PFBR system and stable influenza A virus production was possible.

Preliminary analysis of the PFBR harvest using flow cytometry and the suspension cell line MDCK.SUS2 showed that only 16% of the cell population was infected at an MOI of 0.03. At MOI above 0.1 almost all cells were infected and batch-like HA titers were obtained, suggesting that determination of optimal RT and improving mixing within the compartments are key factors to increase viral titers in the PFBR harvest. Future PFBR designs may improve process performance via passive and active mixing incorporating, e.g., static-mixers or mechanical agitation.

Overall, continuous production systems of MVA and influenza A virus using two types of bioreactors named TSB system and PFBR system were developed, respectively. The selection of the bioreactor strongly depends on the stability of the target virus. Stable DNA viruses such as MVA can be continuously propagated in a TSB system, while unstable RNA viruses such as

influenza A virus can only be propagated in the PFBR system. These systems also helped us to address the impact that defective interfering particles have in the propagation of MVA and influenza viruses. The establishment of continuous upstream processes for virus production in animal cells involves technical challenges that must be solved for each bioreactor and virus in particular. Aspects such as better automation in the measurement of cell and metabolite concentration are challenges that can be solved with technologies currently on the market. Other aspects such as online virus titration methods, or construction of an universal PFBR system (suitable for all types of viruses) might be more challenging. Previous approaches have only used cascades of CSTRs and, therefore, the tubular bioreactor built in this work opens new possibilities for continuous virus production. While such an approach might help now to efficiently produce influenza virus, it may become an important vaccine production platform in the future by allowing efficient production of other viruses that represent a major threat to human health worldwide.

Chapter 6

Outlook

Moving from batch to continuous production of cell culture-derived viruses in bioreactors could represent a substantial improvement in the production efficiency in current large-scale vaccine manufacturing. The establishment of such technologies, however, would involve the development of new bioreactors, automation and control technologies. In this work, two types of continuous bioreactors were explored depending on the type of virus: a cascade of CSTRs for production of a genetically stable virus such as MVA, and a combination of a CSTR and a PFBR for production of an unstable virus such as IAV. While the cascade of CSTRs is an existing technology that can be further optimized with available technologies, the tubular reactor represents a more disruptive innovation that may require the development of tailor-made technologies.

Continuous MVA virus production in a TSB system. From the point of view of virus production in cascades of CSTRs, future work could benefit from the incorporation of better monitoring systems and control of the process. The measurement and control of parameters such as cell concentration, and metabolites could be incorporated into the production process with existing technologies [175] [176]. This can complement the existing control for pH, oxygen and flow rates available in the market. The online measurement of viral titers, however, represents a major challenge. These technologies, together with the development of processes such as the one shown in Figure 4.22 could further increase the virus production efficiency.

Additionally, some molecular aspects can be also considered for further analysis. In this work, MVA virus production at different residence times and with different process conditions was studied. However, there are still open questions regarding the stability of the virus in continuous cultures of longer duration and under different conditions such as pH and dilution rates. Further studies can analyze stability not only from a protein (antigen) expression point of view, but also from the quality of glycosylation, if present [177, 178]. Also, the possibility of operating virus bioreactors at a lower temperature is an aspect that can be further considered since might increase virus yields [179].

Another aspect is the development of a cascade of CSTRs with recirculation loop. A small prototype of this reactor was built but failed in operation due to the lack of control systems. During the course of this thesis, a master's thesis was carried out for the development of a mathematical model of such a prototype [161]. The results showed that the incorporation of a recirculation loop can effectively improve viral titers and reduce oscillations in virus concentrations. This type of bioreactor could also be evaluated in the future for the production of IAV. Although its disadvantage is the increase in virus passage number and the possibility of mutations after long hours of operation, it could still be used over short operational times for efficient production of seed virus and virus evolution studies.

Continuous IAV virus production in a tubular bioreactor system. In this work a tubular bioreactor for the production of IAV was developed. For the first time, the problem of the "von Magnus effect" was solved with a reactor of this type. This opens the possibility of future innovations not only with IAV, but also with other viruses important for human health and vaccine development.

The design of a universal tubular bioreactor that can be used for any type of virus is challenging due to the different replication dynamics of viruses, diffusion limitations and pH and oxygen control in fluid compartments. Different length and diameters of tubular bioreactors and different points of oxygenation and pH control would be necessary. This can be solved with the incorporation of gas and liquid exchangers based on hollow fibers with more or less hydrophobicity depending on the fluid to be exchanged. However, once the problem of diffusion limitation is solved, the available parameters should allow the manipulation of many viruses.

In addition, the need to monitor and control process variables such as pH, oxygen and flow in the tubular bioreactor will need the development of measurement systems adaptable to the tube. At present, there are technologies designed for CSTRs and single use bags, as well as for measurement of culture parameters in well-plates, that could be adapted to a tube. Finally, the possibility of operating a tubular bioreactor at different conditions such as pH, oxygen and temperatures with respect to the rest of the process is an advantage that can be used to benefit any

engineering design with the aim of increasing productivity and producing a greater quantity of vaccine doses more efficiently.

List of Figures

Figure 2. 1. Electron photographs and scheme of vaccinia virus structure.....	6
Figure 2. 2. Reproductive cycle of vaccinia virus.....	8
Figure 2. 3. Electron micrograph and structure of influenza virus.....	9
Figure 2. 4. Replication cycle of influenza A virus (IAV).....	10
Figure 2. 5. Scheme of a batch process for production of modified vaccinia Ankara (MVA) virus.....	15
Figure 2. 6. Continuous IAV production in a two-stage bioreactor (TSB) system.	18
Figure 2. 7. Conceptual schemes of continuous virus production process using a plug-flow tubular bioreactor (PFBR).....	24
Figure 3. 1. Semi-continuous two stage cultivation..	26
Figure 3. 2. Diagram of the two-stage cultivation systems used for continuous MVA virus production.	29
Figure 3. 3. Photograph of the cascade of two CSTRs with recirculation.	32
Figure 3. 4. Process flow diagram of the plug-flow tubular bioreactor system for continuous influenza virus production.....	34
Figure 3. 5. Photographs of the continuous tubular bioreactor system.	35
Figure 4. 1. MVA virus replication in batch cultures of AGE1.CR.pIX cells.	41
Figure 4. 2. Influenza virus replication in batch cultures of AGE1.CR.pIX cells.....	43
Figure 4. 3. Semi-continuous propagation of MVA-CR19 virus in a two-stage cultivation system using shaker flasks (SSC).....	47
Figure 4. 4. Semi-continuous two-stage stirred cultivation of influenza virus using shaker flasks.	49
Figure 4. 5. Continuous cultivation of MVA-CR19 virus in a two-stage stirred tank bioreactor system (TSB system).....	53
Figure 4. 6. Stability analysis of MVA-CR19.GFP virus in 360 h of semi-continuous cultivation.	54
Figure 4. 7. PCR stability analysis of MVA virus in 360 h of semi-continuous cultivation with two different RT in SVB	55
Figure 4. 8. Results of one representative cascade of CSTRs with recirculation (Tubular 5).....	56
Figure 4. 9. Characterization of the residence time and linear velocity in the PFBR	58

Figure 4. 10. Process variables of the continuous tubular plug-flow bioreactor (PFBR) system operated with suspension MDCK.SUS2 cells.....	61
Figure 4. 11. Influenza virus replication in the plug-flow tubular bioreactor system using MDCK.SUS2 cells	62
Figure 4. 12. Evaluation of different MOIs in the infection and propagation of influenza A virus (IAV) using MDCK.SUS2 cells in the tubular bioreactor system.	64
Figure 4. 13. Cell concentration, viability, residence time and MOI of tubular cultivation A and B for production of influenza A virus in AGE1.CR.pIX suspension cells.....	66
Figure 4. 14. Influenza A virus titers in AGE1.CR.pIX cells in the continuous tubular plug-flow bioreactor (PFBR) system.	69
Figure 4. 15. pH values of one representative tubular plug-flow bioreactor system operated with AGE1.CR.pIX cells.....	70
Figure 4. 16. Polymerase chain reaction analysis of influenza A virus seed.	71
Figure 4. 17. Polymerase chain reaction analysis of influenza A virus produced with the tubular plug-flow bioreactor (PFBR) system in canine MDCK.SUS2 suspension cells.....	71
Figure 4. 18. Polymerase chain reaction analysis of the batch experiments in avian AGE1.CR.pIX cells.....	73
Figure 4. 19. Polymerase chain reaction analysis of influenza A virus produced with the semi-continuous cultivation in avian AGE1.CR.pIX cells.	74
Figure 4. 20. Polymerase chain reaction (PCR) of influenza A virus produced with the PFBR system in avian AGE1.CR.pIX cells.....	75
Figure 4. 21 Productivity of the TSB system (1290 mL wv) compared with a batch process comprising two stirred tank bioreactors (645 mL each vessel, 1290 mL wv)	78
Figure 4. 22. Process layout of a hypothetical parallel two-stage continuous process for MVA virus production	79
Figure 7. 1. Moody diagram to calculate the friction factor in the tubular plug-flow bioreactor.	108

List of Tables

Table 2. 1. List of viruses cultivated in continuous bioreactors since 1965.....	21
Table 3. 1. Description of the flow rates, linear velocity and components of each process stream	36
Table 4. 1. Overview of MVA process parameters, virus titers and productivity obtained in batch, semi-continuous, and continuous experiments.	45
Table 4. 2. Virus yield comparison between the tubular plug-flow reactor, the two-stage stirred tank and the batch bioreactor for production of 10 L of influenza A virus with MDCK.SUS2 cells (500 mL CSTR volume).	80
Table 7. 1. Estimation of time needed to drop oxygen saturation from 100% to 1% in an animal cell batch culture.	107
Table 7. 2. Estimation of the pressure drop using the Darcy-Weisbach equation in a 20 h residence time tube, 121 m in length, made of silicone tubing and with an internal diameter of 1.6 mm.....	109

List of Publications

This thesis contains results and ideas contributed by Felipe Tapia and that can be found in the following publications:

Publications

1. **Tapia F**, Wohlfart D, Jordan I., Sandig V, Genzel Y, Reichl U. Continuous influenza virus production in a tubular bioreactor system provides stable titers and avoids the “von Magnus effect”. PLoS ONE. 2019; 14(11): e0224317.

Contribution: Idea and conceptualization of the tubular bioreactor system, data curation, formal analysis, investigation, methodology development, project administration, validation, writing and manuscript edition.

2. **Tapia F**, Laske T, Wasik M., Rammhold M, Genzel Y, Reichl U. Production of defective interfering particles in parallel continuous cultures at two residence times - insight from qPCR measurements and viral dynamics modeling. Front Bioeng Biotechnol. 2019 Oct; 7:275. doi: 10.3389/fbioe.2019.00275.

Contribution: Conceptualization of the parallel bioreactor, data curation, formal analysis of experimental data, experimental investigation, methodology, validation of experimental results, writing and manuscript edition.

3. Rey-Jurado E, **Tapia F**, Muñoz-Durango N, Lay MK, Carreño LJ, Riedel CA, Bueno SM, Genzel Y, Kalergis AM. Assessing the Importance of Domestic Vaccine Manufacturing Centers: An Overview of Immunization Programs, Vaccine Manufacture, and Distribution. Front Immunol. 2018 Jan 18;9:26.

Contribution: literature investigation of cell culture-derived vaccine manufacturing platforms, writing and manuscript edition.

4. **Tapia F**, Jordan I, Genzel Y, Reichl U. Efficient and stable production of Modified Vaccinia Ankara virus in two-stage semi-continuous and in continuous stirred tank cultivation systems. PLoS One. 2017 Aug 24;12(8):e0182553. doi: 10.1371/journal.pone.0182553.

Contribution: Conceptualization of the cultivation setup, data curation, formal analysis, experimental investigation, methodology development, project administration, validation, writing and manuscript edition.

5. **Tapia F**, Vazquez-Ramirez D, Genzel Y, Reichl U. Bioreactors for high cell density and continuous multi-stage cultivations: options for process intensification in cell culture-based viral vaccine production. Appl Microbiol Biotechnol. 2016 Mar;100(5):2121-32. doi: 10.1007/s00253-015-7267-9.

Contribution: Conceptualization of the manuscript, investigation of continuous cultures, writing and manuscript edition.

Patents

1. **Tapia F**, Genzel Y., Reichl U. Plug flow tubular bioreactor, system containing the same and method for production of virus. WO/2017/190790.

Talks

1. **Tapia F**, Genzel Y, Sandig V, Reichl U. A continuous tubular bioreactor for stable production of influenza virus vaccines. European Society for Animal Cell Technology Conference (ESACT) 2017, Lausanne Conference Venue at EPFL campus, Lausanne, Switzerland.
2. **Tapia F**, Genzel Y, Sandig V, Reichl U. Intensificación de procesos en la elaboración de vacunas virales (Process intensification in viral vaccine manufacturing). Coloquios de Microbiología 2017, Jorge González-Förster seminar room, Pontificia Universidad Católica de Valparaíso, Valparaíso, Chile.
3. **Tapia F**, Genzel Y, Reichl U. Plug-flow tubular and stirred tank bioreactors for continuous vaccine production: virus stability and interference by defective interfering particles. Continuous biomanufacturing conference 2017, University of Oxford, Oxford, England.

Posters

1. **Tapia F**, Vogel T, Genzel Y, Gangemi JD, Hirschel M, Reichl U. Production of cell culture-based influenza A virus in hollow fiber bioreactors. European Society for Animal Cell Technology Conference (ESACT) 2013, Lille, France.
2. **Tapia F**, Vázquez D, Lohr V, Genzel Y, Jordan I, Reichl U. A flow cytometry-based assay for quantification of infectious influenza and vaccinia virions. Vaccine Technolovy Conference IV 2014, Playa del Carmen, Mexico.
3. **Tapia F**, Genzel Y, Jordan I, Sandig V, Reichl U. Continuous and semi-continuous production of MVA virus in two-stage bioreactor systems. European Society for Animal Cell Technology Conference (ESACT) 2015, Barcelona, Spain.
4. **Tapia F**, Genzel Y, Jordan I, Sandig V, Reichl U. Continuous production of viral vaccines with a two-stage bioreactor system. Integrated Continuous Biomanufacturing II Conference 2015, Berkeley, United States.
5. **Tapia F**, Marichal-Gallardo P, Pieler M, Genzel Y, Reichl U. Towards integrated continuous viral vaccines production using two-stage bioreactor systems. Cell Culture Engineering XV 2016, Palm Springs, United States.
6. **Tapia F**, Genzel Y, Jordan I, Sandig V, Reichl U. Propagation of influenza and MVA virus in cascades of continuous stirred tank bioreactors: challenging the “von Magnus effect”. Vaccine Technolovy Conference VI 2016, Albufeira, Portugal.
7. **Tapia F**, Genzel Y, Jordan I, Sandig V, Reichl U. Options for continuous virus vaccines production: tubular plug-flow bioreactor vs. cascades of CSTRs. Integrated Continuous Biomanufacturing III Cascais, Portugal.

Master thesis supervision

1. Wohlfarth, Daniel. Continuous production of influenza virus in a tubular bioreactor. 2017, Master Thesis in Biosystems Engineering at Otto-von-Guericke Universität Magdeburg.
2. Rödel, Paul. Long-term propagation of influenza A virus and defective interfering viral particles S1 (1). 2017, Master Thesis in Molecular Biosystems at Otto-von-Guericke Universität Magdeburg.

References

- [1] Who website. Smallpox article (accessed on 20th of June 2019). Available online: <https://www.who.int/biologicals/vaccines/smallpox/en/>.
- [2] Thèves C, Biagini P, Crubézy E. The rediscovery of smallpox. *Clin Microbiol Infect.* 2014;20(3):210-8.
- [3] Riedel S. Edward Jenner and the history of smallpox and vaccination. *Proc (Bayl Univ Med Cent).* 2005;18(1):21–5.
- [4] Barry, J.M. The site of origin of the 1918 influenza pandemic and its public health implications. *J Transl Med.* 2004; 2: 3.
- [5] Smith W, Andrewes C, Laidlaw P. A virus obtained from influenza patients. *Lancet.* 1933;225:66–8.
- [6] Mayr A, Stickl H, et al. The smallpox vaccination strain MVA: marker, genetic structure, experience gained with the parenteral vaccination and behavior in organisms with a debilitated defence mechanism. *Zentralbl Bakteriol B.* 1978;167(5-6):375-90.
- [7] Chahroudi, A. Differences and similarities in viral life cycle progression and host cell physiology after infection of human dendritic cells with modified vaccinia virus Ankara and vaccinia virus. *J Virol.* 2006;80(17):8469-81.
- [8] Jordan I, Northoff S, Thiele M, Hartmann S, Horn D, Howing K, et al. A chemically defined production process for highly attenuated poxviruses. *Biologicals.* 2011;39(1):50-8.
- [9] Jordan I, Horn D, John K, Sandig V. A genotype of modified vaccinia Ankara (MVA) that facilitates replication in suspension cultures in chemically defined medium. *Viruses.* 2013;5(1):321-39.
- [10] WHO website. Influenza (Seasonal) (accessed on 18th of June 2019). Available online: [https://www.who.int/news-room/fact-sheets/detail/influenza-\(seasonal\)](https://www.who.int/news-room/fact-sheets/detail/influenza-(seasonal)).
- [11] Iuliano AD, Roguski KM, Chang HH, Muscatello DJ, Palekar R, Tempia S. Estimates of global seasonal influenza-associated respiratory mortality: a modelling study. *Lancet.* 2018 Mar 31;391(10127):1285-1300.
- [12] Molinari NA, Ortega-Sanchez IR, Messonier ML, Thompson WW, Wortley PM, Weintraub E, et al. The annual impact of seasonal influenza in the US: measuring disease burden and costs. *Vaccine.* 2007; 25(27):5086-96.

- [13] Webster RG, Monto AS, Braciale TJ, Lamb RA. Textbook of Influenza. Second Edition. Wiley Blackwell: 2013. p. 3.
- [14] Perdue ML, Arnold F, Li S, Donabedian A, Cioce V, Warf T, Huebner R. The future of cell culture-based influenza vaccine production. *Expert Rev Vaccines*. 2011;10(8):1183-94.
- [15] McLean KA, Goldin S, Nannei C, Sparrow E, Torelli G. The 2015 global production capacity of seasonal and pandemic influenza vaccine. *Vaccine*. 2016;34(45):5410-3.
- [16] Genzel Y, Dietzsch C, Rapp E, Schwarzer J, Reichl U. MDCK and Vero cells for influenza virus vaccine production: a one-to-one comparison up to lab-scale bioreactor cultivation. *Appl Microbiol Biotechnol*. 2010;88(2):461-75.
- [17] Buckland B, Boulanger R, Fino M, Srivastava I, Holtz K, Khramtsov N, et al. Technology transfer and scale-up of the Flublok® recombinant hemagglutinin (HA) influenza vaccine manufacturing process. *Vaccine*. 2014 Sep 22;32(42):5496-502.
- [18] Lohr V, Rath A, Genzel Y, Jordan I, Sandig V, Reichl U. New avian suspension cell lines provide production of influenza virus and MVA in serum-free media: studies on growth, metabolism and virus propagation. *Vaccine*. 2009;27(36):4975-82.
- [19] Sun B, Yu X, Kong W, Sun S, Yang P, Zhu C, Zhang H, et al. Production of influenza H1N1 vaccine from MDCK cells using a novel disposable packed-bed bioreactor. *Appl Microbiol Biotechnol*. 2013;97(3):1063-70.
- [20] Tapia F, Vázquez-Ramírez D, Genzel Y, Reichl U. Bioreactors for high cell density and continuous multi-stage cultivations: options for process intensification in cell culture-based viral vaccine production. *Appl Microbiol Biotechnol*. 2016;100(5):2121-32.
- [21] Genzel Y, Fischer M, Reichl U. Serum-free influenza virus production avoiding washing steps and medium exchange in large-scale microcarrier culture. *Vaccine*. 2006;24(16):3261-72.
- [22] Wolf MW, Reichl U. Downstream processing of cell culture-derived virus particles. *Expert Rev Vaccines*. 2011;10(10):1451-75.
- [23] Tapia F, Jordan I, Genzel Y, Reichl U. Efficient and stable production of Modified Vaccinia Ankara virus in two-stage semi-continuous and in continuous stirred tank cultivation systems. *PLoS One*. 2017;12(8):e0182553.
- [24] Konstantinov KB, Cooney CL. White paper on continuous bioprocessing May 20-21, 2014 continuous manufacturing symposium. *J Pharm Sci*. 2015;104(3):813-20.
- [25] Novick A, Szilard L. Description of the chemostat. *Science*. 1950;112(2920):715-6.

- [26] Frensing T, Heldt FS, Pflugmacher A, Behrendt I, Jordan I, Flockerzi D, Genzel Y, Reichl U. Continuous influenza virus production in cell culture shows a periodic accumulation of defective interfering particles. *PLoS One*. 2013 Sep 5;8(9):e72288.
- [27] Ziv N, Brandt NJ, Gresham D. The use of chemostats in microbial systems biology. *J Vis Exp*. 2013;14;(80).
- [28] Gresham D, Hong J. The functional basis of adaptive evolution in chemostats. *FEMS Microbiol Rev*. 2015;39(1):2-16.
- [29] Málek I, Fencl Z. Theoretical and methodological basis of continuous culture of microorganisms (trans: Liebster J). Pub. House of the Czechoslovak Academy of Sciences; Academic Press, Prague and New York, 1966. p. 67-153.
- [30] Gori GB. Continuous cultivation of virus in cell suspensions by use of the lysostat. *Appl Microbiol*. 1965;13(6):909-17.
- [31] Roth F, Ullrich WM, Elizondo Herrera A, Seifert HS. Kontinuierliche Produktion von MKS-Virus in einem zweistufigen. *Berl Münch Tierärztl Wschr*. 1994;107(4):123-7.
- [32] Giri L, Feiss MG, Bonning BC, Murhammer DW. Production of baculovirus defective interfering particles during serial passage is delayed by removing transposon target sites in fp25k. *J Gen Virol*. 2012;93(2): 389–99.
- [33] Frensing T, Pflugmacher A, Bachmann M, Peschel B, Reichl U. Impact of defective interfering particles on virus replication and antiviral host response in cell culture-based influenza vaccine production. *Appl Microbiol Biotechnol*. 2014 ;98(21):8999-9008.
- [34] Von Magnus. Incomplete forms of influenza virus. 1954 *Adv. Virus. Res.* 2:59-78.
- [35] Šantek B, Ivancic M , Horvat P, S. Novak S, Maric V. Horizontal Tubular Bioreactors in Biotechnology. *Chem. Biochem. Eng. Q*; 2006;20(4):389–99.
- [36] Verheust C, Goossens M, Pauwels K, Breyer D. Biosafety aspects of modified vaccinia virus Ankara (MVA)-based vectors used for gene therapy or vaccination. *Vaccine*. 2012;30(16):2623-32.
- [37] Mayr A., Munz E. Changes in the vaccinia virus through continuing passages in chick embryo fibroblast cultures. *Zentralbl Bakteriolog Orig*. 1964;195(1):24-35.
- [38] Meyer H, Sutter G, Mayr A. Mapping of deletions in the genome of the highly attenuated vaccinia virus MVA and their influence on virulence. *J. Gen. Virol*. 1991;72(5):1031-8.

- [39] Malkin AJ, McPherson A, Gershon PD. Structure of Intracellular Mature Vaccinia Virus Visualized by In Situ Atomic Force Microscopy. *J Virol.* 2003; 77(11): 6332–40.
- [40] Jordan I, Lohr V, Genzel Y, Reichl U, Sandig V. Elements in the Development of a Production Process for Modified Vaccinia Virus Ankara. *Microorganisms.* 2013;1(1):100-21.
- [41] Smith GL, Moss B. Infectious poxvirus vectors have capacity for at least 25,000 base pairs of foreign DNA. *Gene.* 1983;25(1):21-8.
- [42] Peters D. Morphology of resting vaccinia virus. *Nature.* 1956;178(4548):1453-5.
- [43] Harrison SC. Discovery of antivirals against smallpox. *Proc Natl Acad Sci U S A.* 2004;101(31):11178-92.
- [44] Gilbert SC, Moorthy VS, Andrews L, Pathan AA, McConkey SJ, Vuola JM, Keating SM, Berthoud T, Webster D, McShane H, Hill AV. Synergistic DNA-MVA prime-boost vaccination regimes for malaria and tuberculosis. *Vaccine* 2006;24(21):4554-61.
- [45] Webster DP, Dunachie S, Vuola J, Berthoud T, Keating S, et al. Enhanced T cell-mediated protection against malaria in human challenges by using the recombinant poxviruses FP9 and modified vaccinia virus Ankara. *Proc Natl Acad Sci USA.* 2005;102(13):4836-41.
- [46] Coulibaly S, Brühl P, Mayrhofer J, Schmid K, Gerencer M, Falkner FG. The nonreplicating smallpox candidate vaccines defective vaccinia Lister (dVV-L) and modified vaccinia Ankara (MVA) elicit robust long-term protection. *Virology* 2005;341(1):91-101.
- [47] Cox HR. Active immunization against poliomyelitis. *Bull. N. Y. Acad. Med.* 1953;29(12):943-60.
- [48] Hess RD, Weber F, Watson K, Schmitt S. Regulatory, biosafety and safety challenges for novel cells as substrates for human vaccines. *Vaccine.* 2012;30(17):2715-27.
- [49] Kreijtz JH, Wiersma LC, De Gruyter HL, et al. A single immunization with modified vaccinia virus Ankara-based influenza virus H7 vaccine affords protection in the influenza A(H7N9) pneumonia ferret model. *J Infect Dis.* 2015;211(5):791-800.
- [50] Milligan ID, Gibani MM, Sewell R, Clutterbuck EA, Campbell D, Plested E, et al. Safety and Immunogenicity of Novel Adenovirus Type 26- and Modified Vaccinia Ankara-Vectored Ebola Vaccines: A Randomized Clinical Trial. *JAMA.* 2016;315(15):1610-23.
- [51] Ewer K, Rampling T, Venkatraman N, Bowyer G, Wright D, Lambe T, et al. A Monovalent Chimpanzee Adenovirus Ebola Vaccine Boosted with MVA. *N Engl J Med.* 2016;374(17):1635-46.

- [52] Vijayan A, Garcia-Arriaza J, Raman SC, Conesa JJ, Chichon FJ, Santiago C, et al. A Chimeric HIV-1 gp120 Fused with Vaccinia Virus 14K (A27) Protein as an HIV Immunogen. *PLoS One*. 2015;10(7):e0133595.
- [53] Leung-Theung-Long S, Gouanvic M, Coupet CA, et al. A Novel MVA-Based Multiphasic Vaccine for Prevention or Treatment of Tuberculosis Induces Broad and Multifunctional Cell-Mediated Immunity in Mice and Primates. *PLoS One*. 2015;10(11):e0143552.
- [54] Weber C, Buchner SM, Schnierle BS. A small antigenic determinant of the Chikungunya virus E2 protein is sufficient to induce neutralizing antibodies which are partially protective in mice. *PLoS Negl Trop Dis*. 2015;9(4):e0003684.
- [55] Zitzmann-Roth EM, von Sonnenburg F, de la Motte S, Arndtz-Wiedemann N, von Krempelhuber A, Uebler N, et al. Cardiac safety of Modified Vaccinia Ankara for vaccination against smallpox in a young, healthy study population. *PLoS One*. 2015;10(4):e0122653.
- [56] Green CA, Scarselli E, Sande CJ, Thompson AJ, de Lara CM, Taylor KS, et al. Chimpanzee adenovirus- and MVA-vectored respiratory syncytial virus vaccine is safe and immunogenic in adults. *Sci Transl Med*. 2015;7(300):300ra126.
- [57] Dunachie S, Berthoud T, Hill AV, Fletcher HA. Transcriptional changes induced by candidate malaria vaccines and correlation with protection against malaria in a human challenge model. *Vaccine*. 2015;33(40):5321-31.
- [58] Sebastian S, Gilbert SC. Recombinant modified vaccinia virus Ankara-based malaria vaccines. *Expert Rev Vaccines*. 2016;15(1):91-103.
- [59] Marin-Lopez A, Ortego J. Generation of Recombinant Modified Vaccinia Virus Ankara Encoding VP2, NS1, and VP7 Proteins of Bluetongue Virus. *Methods Mol Biol*. 2016;1349:137-50.
- [60] Volz A, Lim S, Kaserer M, Lulf A, Marr L, Jany S, et al. Immunogenicity and protective efficacy of recombinant Modified Vaccinia virus Ankara candidate vaccines delivering West Nile virus envelope antigens. *Vaccine*. 2016;34(16):1915-26.
- [61] Lamb RA, Krug RM. Orthomyxoviridae: the viruses and their replication. In: Knipe DM, Howley PM, Griffin DE, editors. *Fields Virology* 4th edn. Lippincott Williams & Wilkins; 2001, 2001.
- [62] Noda T. Native Morphology of Influenza Virions. *Front Microbiol*. 2011;2: 269.
- [63] Dadonaite B, Vijayakrishnan S, Fodor E, Bhella D, Hutchinson EC. Filamentous influenza viruses. *J Gen Virol*. 2016;97(8):1755-64.

- [64] Lange, W, Vogel, GE, Uphoff H. *Influenza: Virologie, Epidemiologie, Klinik, Therapie und Prophylaxe*. Berlin: Blackwell Wissenschafts-Verlag;1999.
- [65] CDC website. Influenza type A viruses (accessed on 20th of June 2019). Available online: <http://www.cdc.gov/flu/avianflu/influenza-a-virus-subtypes.htm>," [Online].
- [66] WHO website. Influenza virological updates. Influenza virus activity in the world 7 January 2013 (accessed on 20th of June 2019). Available online: www.who.int/influenza/gisrs_laboratory/updates/summaryreport_20130107/en.
- [67] Horimoto T, Kawaoka Y. Influenza: lessons from past pandemics, warnings from current incidents. *Nat Rev Microbiol* 2005;3(8): 591-600.
- [68] Von Itzstein M. The war against influenza: discovery and development of sialidase inhibitors. *Nat Rev Drug Discov*. 2007;6(12): 967-74," [Online].
- [69] Cady SD, Luo W, Hu F, Hong M. Structure and Function of the Influenza A M2 Proton Channel. *Biochemistry*. 2009; 48(31): 7356–64.
- [70] Webster R, Bean WJ, Gorman OT, Chambers TM, Kawaoka Y. Evolution and Ecology of Influenza A Viruses. *Microbiol. Rev.* 1992;56(1):152-79.
- [71] Samji T. Influenza A: Understanding the viral life cycle. *Yale J Biol Med*. 2009;82:153-9.
- [72] Shehel JJ, Wiley DC. Receptor binding and membrane fusion in virus entry: the influenza hemagglutinin. *Annu Rev Biochem* 2000;69:531-69.
- [73] Nature Education website. Genetics of the influenza virus by Suzanne Clancy (accessed on 20th of June 2019). Available online: <https://www.nature.com/scitable/topicpage/genetics-of-the-influenza-virus-716>.
- [74] Bangham CRM, Kirkwood TBL. Defective interfering particles and virus evolution. *Trend Microbiol* 1993;1(7): 260-64.
- [75] Kirkwood TBL, Bangham CRM. Cycles, chaos, and evolution in virus cultures: A model of defective interfering particles. *Proc Natl Acad Sci USA*. 1994;91:8685-89.
- [76] Epstein DA, Herman RC, Chien I, Lazzarini RA. Defective interfering particle generated by internal deletion of the vesicular stomatitis virus genome. *J Virol*. 1980;33(2): 818-29.
- [77] von Magnus P. Propagation of the PR8 strain of influenza A virus in chick embryos. II. The formation of incomplete virus following inoculation of large doses of seed virus. *Acta Pathol Microbiol Scand*. 1951;28(3):278-93.

- [78] Vasilijevic J, Zamarreño N, Oliveros JC, Rodriguez-Frandsen A, Gómez G, Rodriguez G. Reduced accumulation of defective viral genomes contributes to severe outcome in influenza virus infected patients. *PLoS Pathog.* 2017;13(10):e1006650.
- [79] Aaskov J, Buzacott K, Thu HM, Lowry K, Holmes EC. Long-term transmission of defective RNA viruses in humans and *Aedes* mosquitoes. *Science.* 2006;311(5758):236-8.
- [80] Noppornpanth S, Smits SL, Lien TX, Poovorawan Y, Osterhaus AD, Haagmans BL. Characterization of Hepatitis C Virus Deletion Mutants Circulating in Chronically Infected Patients. *J Virol.* 2007; 81(22):12496–503.
- [81] Rezelj VV, Levi LI, Vignuzzi M. The defective component of viral populations. *Curr Opin Virol.* 2018;33:74-80.
- [82] Frensing T. Defective interfering viruses and their impact on vaccines and viral vectors. *Biotechnol J.* 2015;10(5):681-9.
- [83] Von Laer DM, Mack D, Kruppa J. Delayed formation of defective interfering particles in vesicular stomatitis virus-infected cells: kinetic studies of viral protein and RNA synthesis during autointerference. *J Virol* 1988;62:1323-9.
- [84] Cave DR, Hendrickson FM, Huang AS. Defective interfering virus particles modulate virulence. *J Virol* 1985; 55(2): 366-73.
- [85] Dimmock NJ, Dove BK, Scott PD, Meng B, Taylor I, Cheung L, et al. Cloned Defective Interfering Influenza Virus Protects Ferrets from Pandemic 2009 Influenza A Virus and Allows Protective Immunity to Be Established. *PLoS One.* 2012;7(12): e49394.
- [86] Jacobson S, Charles P. Viral pathogenesis and resistance to defective interfering particles. *Nature.* 1980;283:311-13.
- [87] Frank SA. Within-host spatial dynamics of viruses and defective interfering particles. *J Theor Biol.* 2000;206:279-90.
- [88] Holowczak JA. Poxvirus DNA . In: Henle W, Hofschneider PH, et al., editors. *Current Topics in Microbiology and Immunology.* Springer; 1982. p. 27-70.
- [89] Moss B, Winters E, Cooper N. Instability and reiteration of DNA sequences within the vaccinia virus genome. *Proc Natl Acad Sci U S A.* 1981;78(3):1614-8.
- [90] Moyer RW, Rothe CT. The White Pock Mutants of Rabbit Poxvirus I . Spontaneous Host Range Mutants Contain Deletions. *Virology.* 1980;102(1):119-32.
- [91] Nayak DP. Defective interfering influenza viruses. *Ann. Rev. Microbiol.* 1980;34:619-44.

- [92] Genzel Y. Designing cell lines for viral vaccine production: Where do we stand?. *Biotechnol J.* 2015;10(5):728-40.
- [93] Wasik MA, Eichwald L, Genzel Y, Reichl U. Cell culture-based production of defective interfering particles for influenza antiviral therapy. *Appl Microbiol Biotechnol.* 2018;102(3):1167-77.
- [94] Bdeir N, Arora P, Gärtner S, Hoffmann M, Reichl U, Pöhlmann S, Winkler M. A system for production of defective interfering particles in the absence of infectious influenza A virus. *PLoS One.* 2019 Mar 1;14(3):e0212757.
- [95] Hutchinson EC. Genome packaging in influenza A virus. *J Gen Virol.* 2010;91(2):313-28.
- [96] Jennings PA, Finch JT, Winter G, Robertson JS. Does the higher order structure of the influenza virus ribonucleoprotein guide sequence rearrangements in influenza viral RNA? *Cell.* 1983. 34(2): 619–27.
- [97] Davis AR, Nayak DP. Sequence relationships among defective interfering influenza viral RNAs. *Proc Natl Acad Sci USA.* 1979; 6(7): 3092–96.
- [98] Nayak DP, Chambers TM, Akkina RK. Defective-Interfering (DI) RNAs of Influenza Viruses: Origin, Structure, Expression, and Interference. *Curr Top Microbiol Immunol.* 1985;114:103-51.
- [99] Rutkowski K, Ewan PW, Nasser SM. Administration of yellow fever vaccine in patients with egg allergy. *Int Arch Allergy Immunol.* 2013;161(3):274-8.
- [100] CDC website. How Influenza (Flu) Vaccines Are Made (accessed on 18th of June 2019); Available online: <https://www.cdc.gov/flu/protect/vaccine/how-fluvaccine-made.htm>.
- [101] Robertson JS, Nicolson C, Newman R, Major D, Dunleavy U, Wood JM. High growth reassortant influenza vaccine viruses: new approaches to their control. *Biologicals.* 1992;20(3):213-20.
- [102] NIBSC website. Pandemic influenza (accessed on 18th of June 2019). Available online: https://www.nibsc.org/science_and_research/virology/influenza_resource_/pandemic_influenza.aspx.
- [103] WHO website. Guidelines for the safe development and production of vaccines to human pandemic influenza viruses and viruses with pandemic potential (Accessed on 18th June 2019) https://www.who.int/biologicals/BS.2018.2349.Guidelines_Pandemic_2nd_PC_tz.pdf.

- [104] CDC website. Seasonal Influenza Vaccine Supply for the U.S. 2018-2019 Influenza Season (accessed on 20th of June 2019). Available online: <https://www.cdc.gov/flu/about/qa/vaxsupply.htm>.
- [105] DC website. Influenza vaccines — United States, 2018–19 influenza season (accessed on 18th of June 2019). Available online: <https://www.cdc.gov/flu/professionals/vaccines.htm>.
- [106] FDA website. FLUMIST® QUADRIVALENT (accessed on 18th of June 2019). Available online: <https://www.fda.gov/media/83072/download>.
- [107] Barr IG, Donis RO, Katz JM, McCauley JW, Odagiri T, Trusheim H, et al. Cell culture-derived influenza vaccines in the severe 2017-2018 epidemic season: a step towards improved influenza vaccine effectiveness. *NPJ Vaccines*. 2018;3:44.
- [108] FDA website. How Influenza (Flu) Vaccines Are Made (accessed on 18th of June 2019). Available online: <https://www.cdc.gov/flu/prevent/how-fluvaccine-made.htm>.
- [109] WHO website. Cell Culture Influenza Vaccines: The current status (Accessed on 18 June 2019) https://www.who.int/phi/DAY2_20_VanDenBosch_PM_Dubai2014.pdf.
- [110] Seqirus website. Seqirus announces next major advancement in influenza vaccine technology (accessed on 18th of June 2019). Available online: <https://www.seqirus.com/news/seqirus-announces-next-major-advancement-in-cell-based-influenza-vaccine-technology>.
- [111] Vázquez-Ramírez D, Jordan I, Sandig V, Genzel Y, Reichl U. High titer MVA and influenza A virus production using a hybrid fed-batch/perfusion strategy with an ATF system. *Appl Microbiol Biotechnol*. 2019;103(7):3025-3035.
- [112] Hegde NR. Cell culture-based influenza vaccines: A necessary and indispensable investment for the future. *Hum Vaccin Immunother*. 2015;11(5):1223-34.
- [113] Altenburg AF. Modified Vaccinia Virus Ankara (MVA) as Production Platform for Vaccines against Influenza and Other Viral Respiratory Diseases. *Viruses*. 2014; 6(7): 2735–61.
- [114] Cymerys J, Słońska A, Tucholska A, et al. Influence of long-term equine herpesvirus type 1 (EHV-1) infection on primary murine neurons-the possible effects of the multiple passages of EHV-1 on its neurovirulence. *Folia Microbiol (Praha)*. 2018;63(1):1-11.
- [115] Piret JM, Cooney CL. Mammalian cell and protein distributions in ultrafiltration hollow fiber bioreactors. *Biotechnol Bioeng*. 1990;36(9):902-10.

- [116] Piret JM, Cooney CL. Model of oxygen transport limitations in hollow fiber bioreactors. *Biotechnol Bioeng.* 1991;37(1):80-92.
- [117] Quinlan AV. A semicontinuous culture model that links cell growth to extracellular nutrient concentration. *Biotechnol Bioeng.* 1986;28(10):1455-61.
- [118] Shen BQ, Clarke MF, Palsson BO. Kinetics of retroviral production from the amphotropic Ψ CRIP murine producer cell line. *Cytotechnology.* 1996;22(1-3):185-95.
- [119] Tapia F, Vogel T, Genzel Y, Behrendt I, Hirschel M, Gangemi JD, Reichl U. Production of high-titer human influenza A virus with adherent and suspension MDCK cells cultured in a single-use hollow fiber bioreactor. *Vaccine.* 2014;32(8):1003-11.
- [120] Roumillat LF, Feorino PM, Lukert PD. Persistent infection of a human lymphoblastoid cell line with equine herpesvirus 1. *Infect Immun.* 1979; 24(2): 539–44.
- [121] Roumillat LF, Feorino PM, Caplan DD, Lukert PD. Analysis and Characterization of Herpes Simplex Virus After Its Persistence in a Lymphoblastoid Cell Line for 15 Months. *Infect Immun.* 1980; 29(2): 671–7.
- [122] Hoskisson PA, Hobbs G. Continuous culture--making a comeback? *Microbiology.* 2005;151(10):3153-9.
- [123] Warikoo V, Godawat R, Brower K, Jain S, Cummings D, Simons E, et al. Integrated continuous production of recombinant therapeutic proteins. *Biotechnol Bioeng.* 2012;109(12):3018-29.
- [124] Fencel Z, Ricica J, Kodesova J. The use of the multi-stage chemostat for microbial product formation. *J Appl Chem Biotechnol.* 1972;22(3):405-16.
- [125] de Gooijer CD, Bakker WAM, Beeftink HH, Tramper J. Bioreactors in series: An overview of design procedures and practical applications. *Enzyme Microb Technol.* 1996;18(3):202-19.
- [126] van Lier FL, van den End EJ, de Gooijer CD, Vlak JM, Tramper J. Continuous production of baculovirus in a cascade of insect-cell bioreactors. *Appl Microbiol Biotechnol.* 1990 Apr;33(1):43-7.
- [127] Jacobson H, Jacobson LS. Virustat, a device for continuous production of viruses. *Appl Microbiol.* 1966;14(6):940-52.
- [128] Kompier R, Tramper J, Vlak J. A continuous process for the production of baculovirus using insect-cell cultures. *Biotechnol Lett.* 1988;10(12):849-54.
- [129] Krell PJ. Passage effect of virus infection in insect cells. *Cytotechnology.* 1996;20(1-3):125-37.

- [130] de Gooijer CD, van Lier FLJ, van den End EJ, Vlak JM, Tramper J. A model for baculovirus production with continuous insect cell cultures. *Appl Microbiol Biotechnol* 30(5):497-501.
- [131] de Gooijer CD, Koken RH, Van Lier FL, Kool M, Vlak JM, Tramper J. A structured dynamic model for the baculovirus infection process in insect-cell reactor configurations. *Biotechnol Bioeng.* 1992;40(4):537-48.
- [132] Lier FLJ, Kool M, End FJ, Gooijer CD, Usmany M, Vlak JM, Tramper J. Production of baculovirus or recombinant derivatives in continuous insect-cell bioreactors. *Annals N Y Acad Sci.* 1990;613(1):183-90.
- [133] van Lier FL, van der Meijs WC, Grobben NG, Olie RA, Vlak JM, Tramper J. Continuous beta-galactosidase production with a recombinant baculovirus insect-cell system in bioreactors. *J Biotechnol.* 1992 Feb;22(3):291-8.
- [134] Kool M, Voncken JW, van Lier FL, Tramper J, Vlak JM. Detection and analysis of *Autographa californica* nuclear polyhedrosis virus mutants with defective interfering properties. *Virology.* 1991;183(2):739-46.
- [135] van Lier FL1, van Duijnhoven GC, de Vaan MM, Vlak JM, Tramper J. Continuous beta-galactosidase production in insect cells with a p10 gene based baculovirus vector in a two-stage bioreactor system. *Biotechnol Prog.* 1994 Jan-Feb;10(1):60-4.
- [136] van Lier FLJ, van den Hombergh JPTW, de Gooijer CD, den Boer MM, Vlak JM, Tramper J. Long-term semi-continuous production of recombinant baculovirus protein in a repeated (fed-)batch two-stage reactor system. *Enzyme Microb Technol.* 1996;18(6):460-6.
- [137] Pijlman GP, de Vrij J, van den End FJ, Vlak JM, Martens DE. Evaluation of baculovirus expression vectors with enhanced stability in continuous cascaded insect-cell bioreactors. *Biotechnol Bioeng.* 2004;87(6):743-53.
- [138] Hu YC, Wang MY, Bentley WE. A tubular segmented-flow bioreactor for the infection of insect cells with recombinant baculovirus. *Cytotechnology.* 1997;24(2):143-52.
- [139] Pijlman GP, de Vrij J, van den End FJ, Vlak JM, Martens DE. Evaluation of baculovirus expression vectors with enhanced stability in continuous cascaded insect-cell bioreactors. *Biotechnol Bioeng.* 2004 Sep 20;87(6):743-53.
- [140] Lohr V, Genzel Y, Jordan I, Katinger D, Mahr S, Sandig V, Reichl U. Live attenuated influenza viruses produced in a suspension process with avian AGE1.CR.pIX cells. *BMC Biotechnol.* 2012;12:79.

- [141] Lohr V, Hädicke O, Genzel Y, Jordan I, Büntemeyer H, Klamt S, Reichl U. The avian cell line AGE1.CR.pIX characterized by metabolic flux analysis. *BMC Biotechnol.* 2014;14:72.
- [142] Ersu CB, Ong SK. Treatment of wastewater containing phenol using a tubular ceramic membrane bioreactor. *Environ Technol.* 2008;29(2):225-34.
- [143] Moser. Tubular bioreactors: case study of bioreactor performance for industrial production and scientific research. *Biotechnol Bioeng.* 1991;37(11):1054-65.
- [144] Molina E, Fernández J, Ación FG, Chisti Y. Tubular photobioreactor design for algal cultures. *J Biotechnol.* 2001;92(2):113-31.
- [145] Levenspiel O. *Chemical reaction engineering.* 1st ed. John Wiley & Sons 1962, p. 99-124,139; Fogler S. *Elements of Chemical Reaction Engineering.* 3rd ed. Prentice-Hall International, Inc. 1999, p 10-25, 34-63, 809-69.
- [146] Laske T, Heldt FS, Hoffmann H, Frensing T, Reichl U. Modeling the intracellular replication of influenza A virus in the presence of defective interfering RNAs. *Virus Res.* 2016;213:90-9.
- [147] Jordan I, Vos A, Beilfuss S, Neubert A, Breul S, Sandig V. An avian cell line designed for production of highly attenuated viruses. *Vaccine.* 2009;27(5):748–56.
- [148] Lohr et al. A new MDCK suspension line cultivated in a fully defined medium in stirred-tank and wave bioreactor. *Vaccine.* 2010 Aug 31;28(38):6256-64.
- [149] Kalbfuss B, Knöchlein A, Kröber T, Reichl U. Monitoring influenza virus content in vaccine production: precise assays for the quantitation of hemagglutination and neuraminidase activity. *Biologicals.* 2008;36(3):145-61.
- [150] Genzel Y, Rödig J, Rapp E, Reichl, U. Vaccine production: Upstream processing with adherent or suspension cell lines. In R. Pörtner (Ed.), *Animal Cell Biotechnology: Methods and Protocols.* New York: Humana Press Inc. 2014. pp. 371-93.
- [151] Genzel Y, Reichl U. Vaccine production—state of the art and future needs in upstream processing. In: Poertner R, editor. *Animal cell biotechnology: methods and protocols.* Humana Press Inc.; 2007. p. 457–73.
- [152] Hoffmann E, Stech J, Guan Y, Webster RG, Perez DR. Universal primer set for the full-length amplification of all influenza A viruses. *Arch Virol.* 2001;146: 2275–89.
- [153] Tapia F, Wohlfarth D, Jordan I, Sandig V, Genzel Y, Reichl U. Continuous influenza virus production in a tubular bioreactor system provides stable titers and avoids the "von Magnus effect". *PLoS ONE.* 2019;14(11): e0224317.

- [154] Tapia F, Genzel Y, Reichl U. Plug flow tubular bioreactor, system containing the same and method for production of virus. 2016. Patent application WO2017190790A1 (pending).
- [155] Genzel Y, Vogel T, Buck J, Behrendt I, Ramirez DV, Schiedner G, Jordan I, Reichl U. High cell density cultivations by alternating tangential flow (ATF) perfusion for influenza A virus production using suspension cells. *Vaccine*. 2014;32(24):2770-81.
- [156] Westgate PJ, Emery AH. Approximation of continuous fermentation by semicontinuous cultures. *Biotechnol Bioeng*. 1990;35(5):437-53.
- [157] Henry O, Kwok E, Piret JM. Simpler Noninstrumented Batch and Semicontinuous Cultures Provide Mammalian Cell Kinetic Data Comparable to Continuous and Perfusion Cultures. *Biotechnol Prog*. 2008;24(4):921-31.
- [158] Genzel Y, Olmer RM, Schäfer B, Reichl U. Wave microcarrier cultivation of MDCK cells for influenza virus production in serum containing and serum-free media. *Vaccine*. 2006;24(35-36):6074-87.
- [159] Batt BC, Davis RH, Kompala DS. Inclined sedimentation for selective retention of viable hybridomas in a continuous suspension bioreactor. *Biotechnol Prog*. 1990;6(6):458-64.
- [160] Epand RM, Epand RF. Thermal denaturation of influenza virus and its relationship to membrane fusion. *Biochem J*. 2002; 365(3): 841–8.
- [161] Rammhold M. Model-Based optimization of continuous influenza vaccine production process. 2017. Master Thesis, Otto-von-Guericke University Magdeburg.
- [162] Fernandez-de-Cossio-Diaz J, Leon K, Mulet R. Characterizing steady states of genome-scale metabolic networks in continuous cell cultures. *PLoS Comput Biol*. 2017;13(11):e1005837.
- [163] Ingham J, Dunn IJ, Heinzle E, Prenosil JE, Snape JB, editors. *Chemical Engineering Dynamics, An Introduction to Modelling and Computer Simulation*. Wiley Germany; 2007. p. 189-90.
- [164] Moenne MI, Mouret JR, Sablayrolles JM, Agosin E, Farine V. Control of bubble-free oxygenation with silicone tubing during alcoholic fermentation. *Process Biochemistry* 2013;48(10):1453-61.
- [165] Genzel Y, Behrendt I, König S, Sann H, Reichl U. Metabolism of MDCK cells during cell growth and influenza virus production in large-scale microcarrier culture. *Vaccine*. 2004;22(17-18):2202-8.

- [166] Lohr V, Genzel Y, Behrendt I, Scharfenberg K, Reichl U. A new MDCK suspension line cultivated in a fully defined medium in stirred-tank and wave bioreactor. *Vaccine*. 2010;28(38):6256-64.
- [167] Peschel B, Frentzel S, Laske T, Genzel Y, Reichl U. Comparison of influenza virus yields and apoptosis-induction in an adherent and a suspension MDCK cell line. *Vaccine*. 2013;31(48):5693-9.
- [168] Wohlfarth, D. Continuous production of influenza virus in a tubular bioreactor. Master Thesis in Biosystems Engineering at Otto-von-Guericke Universität Magdeburg. 2017.
- [169] Stettler M, Zhang X, Hacker DL, De Jesus M, Wurm FM. Novel orbital shake bioreactors for transient production of CHO derived IgGs. *Biotechnol Prog*. 2007;23(6):1340-6.
- [170] Hessel V, Löwe h, Schönfeld F. Micromixers—a review on passive and active mixing principles. *Chem Eng Science*. 2005 60(8-9): 2479-2501.
- [171] J. Ingham, I.J. Dunn, E. Heinzle, J.E. Prenosil, J.B. Snape. *Chemical Engineering Dynamics, An Introduction to Modelling and Computer Simulation*. Wiley Germany, 2007. Page 189-190.
- [172] Kupke SY, Riedel D, Frensing T, Zmora P, Reichl U. A Novel Type of Influenza A Virus-Derived Defective Interfering Particle with Nucleotide Substitutions in Its Genome. *J Virol*. 2019;93(4):e01786-18.
- [173] Wikipedia, the free encyclopedia website. Opportunity cost (accessed on 17th of June 2019). Available online: https://en.wikipedia.org/wiki/Opportunity_cost.
- [174] Tapia F, Laske T, Wasik M., et al. Production of defective interfering particles in parallel continuous cultures at two residence times - insight from qPCR measurements and viral dynamics modeling. *Front Bioeng Biotechnol*. 2019. 18;7:275.
- [175] Nikolay A, Léon A, Schwamborn K, Genzel Y, Reichl U. Process intensification of EB66® cell cultivations leads to high-yield yellow fever and Zika virus production. *Appl Microbiol Biotechnol*. 2018;102(20):8725-37.
- [176] Weichert H, Becker M. Online glucose-lactate monitoring and control in cell culture and microbial fermentation bioprocesses. *BMC Proc*. 2013;7(6): P18.
- [177] Hessel A, Schwendinger M, Holzer GW, Orlinger KK, Coulibaly K, Savidis-Dacho H. Vectors Based on Modified Vaccinia Ankara Expressing Influenza H5N1 Hemagglutinin Induce Substantial Cross-Clade Protective Immunity. *PLoS One*. 2011; 6(1): e16247.
- [178] Kotwal GJ. Influence of glycosylation and oligomerization of vaccinia virus complement control protein on level and pattern of functional activity and immunogenicity. *Protein Cell*. 2010;1(12):1084–92.

- [179] Léon A, David AL, Madeline B, Guianvarc'h L, Dureau E, Champion-Arnaud P. The EB66® cell line as a valuable cell substrate for MVA-based vaccines production. *Vaccine*. 2016;34(48):5878-85.

Appendices

7.1 Oxygen consumption

One main hypothesis of this work is that the dissolved oxygen concentration profile inside a liquid segment traveling along the tubular bioreactor should resemble that of a batch culture with animal cells. Hence, the oxygen consumption rate of a generic animal cell line was estimated using literature data, for a batch culture of 1×10^6 cells/mL, with 100% saturation and without additional oxygen supply. The final goal was to determine the time needed until 1% oxygen saturation is obtained in such culture.

$$\text{Time [h]} = \frac{(100\% \text{ O}_{2\text{saturation}} [\text{mol/L}] - 1\% \text{ O}_{2\text{saturation}} [\text{mol/L}])}{(\text{Cell concentration} [\text{cells/L}] \times (\text{Oxygen Uptake Rate} [\text{mol}/(\text{cell} \times \text{h})])}$$

Table 7. 1. Estimation of time needed to drop oxygen saturation from 100% to 1% in an animal cell batch culture.

Parameter [units]	Value	Reference
Oxygen uptake rate 1 (OUR 1) [mol/cell*h]	3.05E-14	High cell density cultivations by alternating tangential flow (ATF) perfusion for influenza A virus production using suspension cells. Vaccine. 2014 May 19;32(24):2770-81
Oxygen uptake rate [mol/gDW*h]	2.E-04	Lohr V, Hädicke O, Genzel Y, Jordan I, Büntemeyer H, Klamt S, Reichl U. The avian cell line AGE1.CR.pIX characterized by metabolic flux analysis. BMC Biotechnology 2014;14:72
Mass of 1 cell [g]	3.0E-09	Fernandez-de-Cossio-Diaz J, Leon K, Mulet R. Characterizing steady states of genome-scale metabolic networks in continuous cell cultures. PLoS Comput Biol. 2017 Nov 13;13(11):e1005836
Oxygen uptake rate 2 (OUR 2) [mol/cell*h]	6.9E-13	Fernandez-de-Cossio-Diaz J, Leon K, Mulet R. Characterizing steady states of genome-scale metabolic networks in continuous cell cultures. PLoS Comput Biol. 2017 Nov 13;13(11):e1005837
Temperature °C	37	
Saturated Oxygen in H ₂ O [mg/L] at 37°C	6.70E+00	United States Geological Survey. Table of solubility of oxygen in water at various temperatures (Accessed on 19th of June 2019) https://water.usgs.gov/o/wq/FieldManual/Chapter6/table6.2_6.pdf
Saturated Oxygen in H ₂ O [mol/L] at 37°C	2.09E-04	
Oxygen Concentration at 40% saturation [mol/L]	8.38E-05	
Oxygen Concentration at 1% saturation [mol/L]	2.09E-06	
Volume reactor [mL]	1000	
Concentration cells per ml [cells/mL]	1.0.E+06	
Time to go from 100% to 1% O ₂ saturation [h] OUR 1	6.8	
Time to go from 100% to 1% O ₂ saturation [h] OUR 2	0.3	

Since Table 7.1. shows that a time between 0.3-6.8 h is needed to consume all oxygen in a liquid segment (depending on oxygen uptake values), this estimate suggest that additional oxygen supply may be needed along the tube.

7.2 Pressure drop in the tubular plug flow bioreactor

Since the construction of a tubular bioreactor of more than 100 meter of length and with few millimeters of diameter was not tested before, doubts about whether the pumps will be capable of moving such long liquid segments were raised first. Hence, the pressure drop was determined before such endeavor was initiated. Literature data was used for this purpose.

The pressure drop of a silicone tube with 121 m in length was calculated with the Darcy-Weisbach equation for a pipe:

$$\frac{\Delta p}{L} = f_D \cdot \frac{\rho}{2} \cdot \frac{\langle v \rangle^2}{D},$$

ρ = the density of the fluid (kg/m³);

D = the hydraulic diameter of the pipe (for a pipe of circular section, this equals the internal diameter of the tube)

$\langle v \rangle$ = the mean flow velocity, experimentally measured as the volumetric flow rate per unit cross-sectional wetted area (m/s);

f_D , the Darcy friction factor

To obtain the Darcy friction factor, the Moody diagram was used.

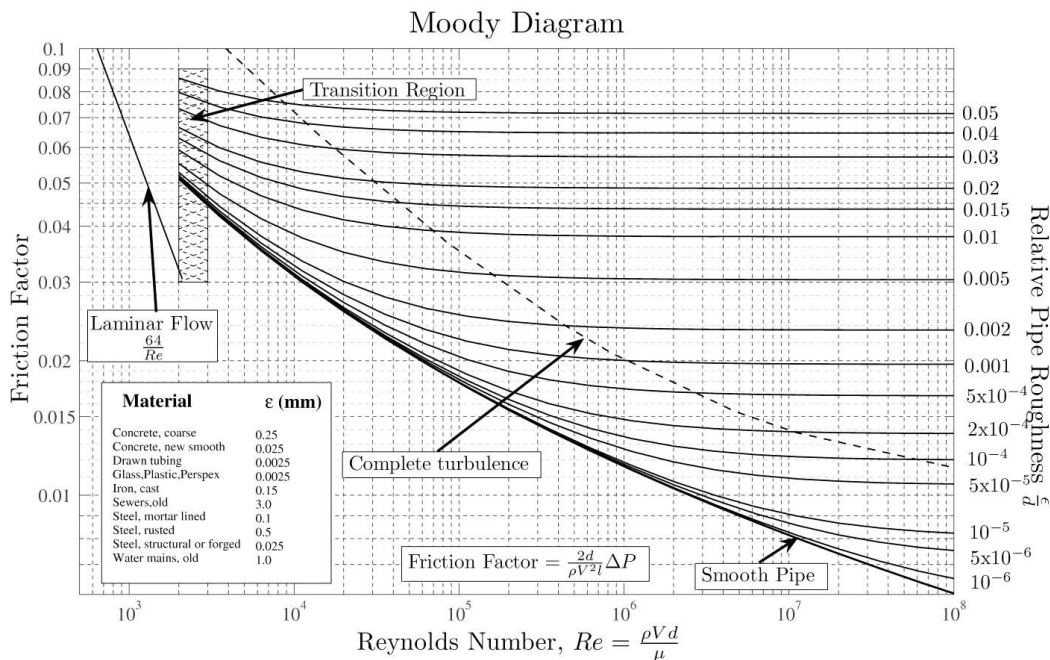


Figure 7. 1. Moody diagram to calculate the friction factor in the tubular plug-flow bioreactor.

The data of Table 7.2. shows that the Reynolds number was estimated to be around 10 for such tubular bioreactor, which implies a laminar regime.

For a laminar regime, the Darcy friction factor is $64/Re$, as depicted on the left-hand side of the Moody diagram (Fig. 7.1).

Table 7. 2. Estimation of the pressure drop using the Darcy-Weisbach equation in a 20 h residence time tube, 121 m in length, made of silicone tubing and with an internal diameter of 1.6 mm.

Process variable	Value
Flow rate [mL/min]	0.2
Flow rate [m ³ /s]	3.3E-09
Internal diameter [mm]	1.59
Velocity [cm/min]	10
Reynolds number [-]	10
Tube length [m]	121
f_c (Darcy factor) ¹	6
H_f [m] ²	7.0E-05
H_f [bar] ²	6.9E-06
ΔP [Pa]	0.7
ΔP [bar]	6.8E-06

¹ obtained from Moody diagram. For laminar flow $f_c = 64/Re$

² friction head losses in the tube. Darcy-Weisbach equation

Finally, a theoretical pressure drop of 6.8×10^{-6} [bar] in a 121 meter long silicone tube was small enough to try this bioreactor idea and build the first prototype.

References:

- DW Green, Perry RH. Perry's Chemical Engineers' Handbook. 8th Edition.
- The Darcy-Weisbach equation was taken from Wikipedia, the free encyclopedia (Accessed on 19th of June 2019). https://en.wikipedia.org/wiki/Darcy%E2%80%93Weisbach_equation
- Moody diagram taken from Wikipedia, the free encyclopedia (Accessed on 19th of June 2019). https://upload.wikimedia.org/wikipedia/commons/8/80/Moody_diagram.jpg

This page was intentionally left blank for the online version.